Regulation of glutamate dehydrogenase in C*orynebacterium glutamicum* and its impact on nitrogen control

Inaugural-Dissertation

zur

Erlangung des Doktorgrades

der Mathematisch-Naturwissenschaftlichen Fakultät

der Universität zu Köln

vorgelegt von

Tim Müller

aus Koblenz

Köln, Oktober 2005

Berichterstatter:

Prof. Dr. Andreas Burkovski
Prof. Dr. Reinhard Krämer

Tag der Disputation: 28.11.2005

Content

Abbreviations

Ap^R	resistant to ampicilin
bp	base pairs
CTAB	N-cetyl-N,N,N-trimethylammonium bromide
DMSO	dimethyl sulfoxide
EDTA	ethylendiaminetetraacetic acid
et al.	*et alii*
GDH	glutamate dehydrogenase
GOGAT	glutamate synthase
GS	glutamine synthetase
HPLC	high pressure liquid chromatography
kb	kilo base pairs
Km^R	resistant to kanamycin
MALDI-TOF	matrix-assisted laser despropotion/ionisation time of flight
MOPS	3-[N-morpholino]propansufonic acid
MSTFA	N-methyltrimethylsilyltrifluoroacetamide
Nx^R	resistant to nalidixic acid
OD_{600}	optical density at 600 nm
PAGE	polyacrylamide gel electrophoresis
RT	room temperature
RT-PCR	reverse transcription polymerase chain reaction
SDS	sodium dodecylsulphate
SOE-PCR	splicing by overlapping extension polymerase chain reaction
TEMED	N,N,N',N'-tetramethyl-ethylendiamine
Tris	2-amino-hydroxymethylpropane-1,3-diol

Abstract

Global regulatory networks are essential for the adaptation to changing environmental conditions and allow bacteria to survive conditions of stress and starvation. Nitrogen control is one of these networks. It regulates the uptake and assimilation of nitrogen containing compounds in dependence on their availability. In *Corynebacterium glutamicum*, a gram-positive soil bacterium of important biotechnological relevance, glutamate dehydrogenase (GDH) seems to play an important but so far less investigated role in nitrogen control. In this work, the regulation of glutamate dehydrogenase and its impact on nitrogen control in *C. glutamicum* were investigated.

Transcription of *gdh* is induced under nitrogen limitation. By DNA affinity purification with magnetic beads, four transcriptional regulators were isolated, which bind specifically to a fragment of the *gdh* promoter region that is responsible for the nitrogen-dependent transcription control. These are the putative transcriptional regulators FarR, WhiH, and OxyR, and the well-characterized transcriptional regulator AmtR, which is a major player of nitrogen control *C. glutamicum*. The exact binding sites of AmtR and FarR were mapped and a principle capacity of FarR to repress *gdh*-promoter-driven transcription was demonstrated. Surprisingly, neither single deletions nor a quadruple deletion of *amtR*, *farR*, *whiH*, and *oxyR* in *C. glutamicum* have any effect on nitrogen-dependent transcription of *gdh*. Consequently, these regulators are not essential for the nitrogen-dependent regulation of *gdh* transcription. Nevertheless, they might regulate *gdh* transcription in response to other stress conditions. A broad range of stress conditions were identified that influence *gdh* transcription. In addition, a putative role of FarR in the regulation of fatty acid biosynthesis and/or glutamate overproduction was revealed.

In the second part of this work, the role of GDH in nitrogen control of *C. glutamicum* was investigated. A deletion of *gdh* results in a deregulation of the nitrogen control network. It was demonstrated, that this effect is caused by the loss of GDH activity and not by the absence of the GDH protein itself. In the *gdh* deletion strain, internal 2-oxoglutarate is accumulated. A high 2-oxoglutarate pool seems to antagonize the nitrogen status and triggers a nitrogen starvation-like response even under nitrogen surplus. In addition, ammonium could be identified as a second metabolite that influences nitrogen control in *C. glutamicum.*

In the third part of this work, it was demonstrated that ammonium is not toxic for *C. glutamicum* and the formation of a putative futile cycle of ammonium was not observed.

Zusammenfassung

Globale Regulationsnetzwerke sind essentiell für die Adaptation an unterschiedliche Umweltbedingungen und ermöglichen Bakterien das Überstehen von Stress- und Mangelsituation. Die Stickstoffkontrolle ist ein solches Netzwerk. Sie reguliert die Aufnahme und Verstoffwechselung stickstoffhaltiger Substrate in Abhängigkeit von deren Verfügbarkeit. Bei der Stickstoffkontrolle des Gram-positiven Bodenbakteriums *Corynebacterium glutamicum*, welches eine große biotechnologische Bedeutung hat, scheint die Glutamatdehydrogenase (GDH) eine wichtige, bislang unbekannte Funktion einzunehmen. In dieser Arbeit wurde die Regulation der GDH und ihr Einfluss auf die Stickstoffkontrolle von *C. glutamicum* untersucht.

Die Transkription des *gdh*-Gens wird unter Stickstoffmangel induziert. Mit Hilfe magnetischer DNA-Affinitätsaufreinigung wurden vier Transkriptionsregulatoren isoliert, welche spezifisch an den Abschnitt der *gdh*-Promotorregion binden, der für die stickstoffabhängige Regulation verantwortlich ist. Dies sind die drei putativen Transkriptionsregulatoren FarR, WhiH, OxyR sowie der bereits charakterisierte Transkriptionsregulator AmtR, welcher ein zentraler Regulator der Stickstoffkontrolle von *C. glutamicum* ist. Die genauen Bindestellen von AmtR bzw. FarR innerhalb der *gdh*-Promotorregion wurden identifiziert und die prinzipielle Fähigkeit zur Repression *gdh*-Promotor-abhängiger Transkription für FarR gezeigt. Trotz allem führen weder Einfachdeletionen noch die Mehrfachdeletion aller Gene der vier Regulatoren zu einem Verlust der stickstoffabhängigen Transkriptionsregulation von *gdh*. Folglich regulieren AmtR, FarR, WhiH und OxyR die Transkription von *gdh* nicht in Abhängigkeit von der Stickstoffversorgung, könnten aber unter anderen Bedingungen aktiv sein. In dieser Arbeit wurden zahlreiche Stressbedingungen identifiziert, welche die Transkription von *gdh* beeinflussen. Außerdem wurde eine weitere Bindestelle von FarR vor dem *dtsR2*-Gen identifiziert, was auf eine mögliche Rolle von FarR bei der Regulation der Fettsäurebiosynthese und/oder Glutamatüberproduktion schließen lässt.

Im zweiten Teil dieser Arbeit wurde die Bedeutung der GDH für die Stickstoffkontrolle von *C. glutamicum* untersucht. Eine Deletion des *gdh*-Gens führt zu einer Deregulierung der Stickstoffkontrolle von *C. glutamicum*. Dieser Effekt beruht auf einem Verlust der GDH-Aktivität und nicht auf der Abwesenheit des GDH-Proteins an sich. Der Verlust der GDH-Aktivität führt zu einer Akkumulation von α-Ketoglutarat, was selbst unter guter Stickstoffversorgung eine Stickstoffmangelreaktion auszulösen scheint. Des Weiteren

wurde gezeigt, dass auch die Verfügbarkeit von Ammonium die Stickstoffkontolle von *C. glutamicum* direkt beeinflusst.

Im dritten Teil dieser Arbeit wurde gezeigt, dass Ammonium für *C. glutamicum* nicht toxisch ist. Die Anwesenheit eines putativen energieverschwendenden Transmembranzyklus von Ammonium konnte nicht beobachtet werden.

1. Introduction

Nitrogen is an essential element for all life-forms as it is part of many important biomolecules like proteins, nucleotides, and coenzymes. Many organisms have evolved regulatory networks to cope with changes in the nitrogen supply. Transport and metabolism of nitrogen-containing compounds are strictly regulated and adapted to the availability of nitrogen sources. These processes as well as the connecting regulatory networks are referred to as nitrogen control. Until now, nitrogen control has been investigated in a number of bacteria, e.g. *Escherichia coli* (Merrick and Edwards, 1995; Reitzer, 2003), *Bacillus subtilis* (Fisher, 1999), *Rhizobium* (Patriaca *et al*., 2002), cyanobacteria (Flores *et al*., 2005), and *Corynebacterium glutamicum* (Burkovski, 2003a; 2003b; 2005). In this thesis, new insights into the nitrogen control of *C. glutamicum* are described.

1.1. *Corynebacterium glutamicum*

C. glutamicum was first isolated form soil collected at Ueno Zoo in Tokyo/Japan during a screening program for glutamate-producing bacteria (Kinoshita *et al*., 1957). It is a Gram-positive, aerobic, and non-sporulating bacterium with a rod shape. Due to its complex mycolic acid-containing cell wall and its high G+C-content, *C. glutamicum* belongs to the mycolic acid-containing actinomycetes. This suborder also includes a considerable number of plant-, animal-, and human-pathogens, e.g. *Corynebacterium diphtheriae*, *Mycobacterium tuberculosis*, and *Mycobacterium leprae* (Pascual *et al*., 1995; Chun *et al*., 1996). In contrast to these, *C. glutamicum* is non-pathogenic and safe to handle. Therefore, it is suitable as a model organism for its pathogenic relatives.

Additionally, *C. glutamicum* is of great biotechnological relevance. First isolated due to its ability to excrete high amounts of glutamate (Konishita *et al*., 1957), it is now used for the industrial production of a diverse range of compounds. Amino acids like glutamate (1,500,000 tons per year), lysine (550,000 tons per year), and smaller amounts of tryptophan, glutamine, alanine, isoleucine, as well as nucleotides and vitamins are produced by the use of different *C. glutamicum* strains (Leuchtenberger, 1996; Hermann, 2003).

Because of its great industrial importance, *C. glutamicum* was intensively studied in the last decades. Nowadays, the genomic sequence of *C. glutamicum* is known

(Kalinowski *et al*., 2003) and several molecular biology tools for the genetic manipulation of *C. glutamicum* are well-established. The central carbon metabolism and amino acid biosynthesis pathways are well-investigated. Several enzymes have been characterized biochemically and flux analyses revealed a better knowledge about interacting metabolic pathways (Dominguez *et al*., 1998; Tesch *et al*., 1999; Wendisch *et al*., 2000; Kiefer *et al*., 2004; Krömer *et al*., 2004). The complex network of nitrogen control in *C. glutamicum* was investigated mainly in the last years (Burkovski, 2003a; 2003b; 2005).

1.2. Uptake of nitrogen sources

Bacteria can use a wide range of nitrogen-containing compounds as sole source of cellular nitrogen. Depending on the availability of nitrogen sources, bacteria express various uptake and utilization systems. In accordance with this, *C. glutamicum* is able to utilize urea, glutamate, glutamine, alanine, asparagine, serine, threonine, creatinine, and several dipeptides. Some of the corresponding uptake systems and metabolic utilization systems are characterized (Krämer *et al*., 1990; Erdmann *et al*., 1994; Zittrich *et al*., 1994; Kronemeyer *et al*., 1995; Siewe *et al*., 1995; Burkovski *et al*., 1996; Siewe *et al*., 1998; Trötschel *et al*., 2003; Bendt *et al*., 2004; Beckers *et al*., 2004). However, the preferred nitrogen source of *C. glutamicum* is ammonium. In general, two different uptake routes for ammonium are present (figure 1) and these are used in dependence on the availability of ammonium as described in the following. In aqueous solution, ammonium (NH_4^+) is in equilibrium with the uncharged and membrane permeable ammonia (NH_3). Ammonia can easily enter the cell by passive diffusion across the cytoplasmic membrane. Under ammonium surplus, diffusion of ammonia is sufficient to promote growth, whereas under nitrogen limitation, ammonium transporters are expressed to ensure a proper nitrogen supply of the cell. In *C. glutamicum*, two ammonium transporter, AmtA and AmtB, are present under nitrogen limitation (Siewe *et al*., 1996; Jakoby *et al*., 1999a; Meier-Wagner *et al*., 2001) to enhance ammonium uptake and to ensure nitrogen supply of the cell.

The mode of transport by these membrane proteins is not clear. Two models are discussed. On one hand, an energy-dependent transport of charged ammonium was observed, indicating that ammonium uptake depends on the membrane

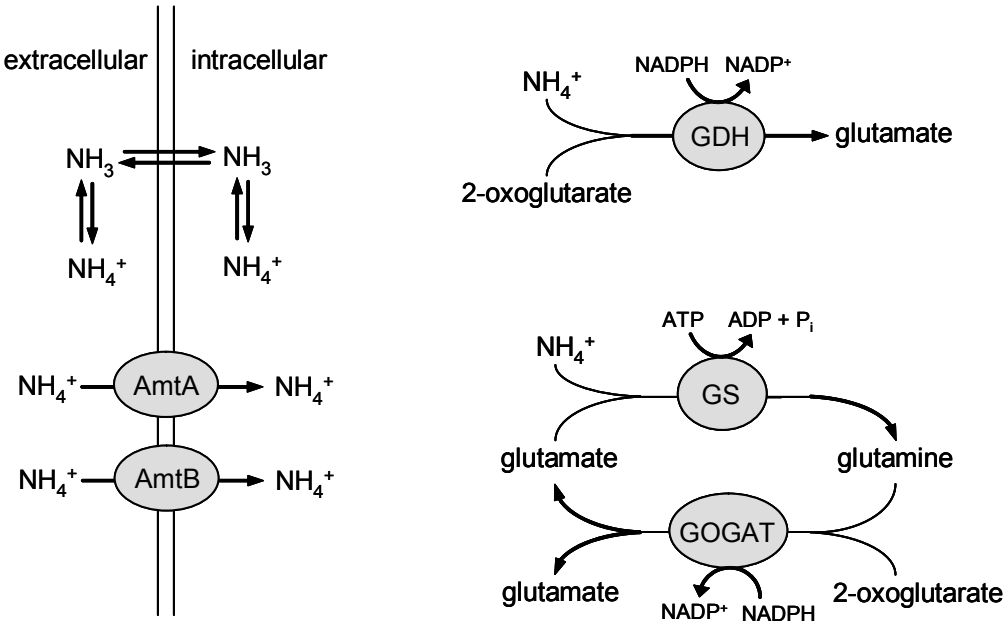

Figure 1: The uptake and assimilation of ammonium in *C. glutamicum.* The uptake of ammonium from the environment occurs either by diffusion of ammonia or *via* transport by AmtA and AmtB, respectively. It is not clear whether AmtA and AmtB actively transport ammonium depending on the membrane potential or if they facilitate passive diffusion of ammonia. Two assimilation pathways for ammonium are present in *C. glutamicum*. One is catalyzed by glutamate dehydrogenase (GDH), the other is a coupled reaction of glutamine synthetase (GS) and glutamate synthase (GOGAT). Both, transport and assimilation are regulated in dependence on the availability of ammonium. In all equations, free protons (H^+) are not given. (Burkovski, 2003a; 2003b; 2005)

potential (Kleiner, 1993, Siewe *et al*., 1996; Meier-Wagner *et al*., 2001). On the other hand, these transporters were described as gas channels that simply facilitate passive diffusion of uncharged ammonia across the cell membrane (Soupene *et al*., 1998, 2002; Khademi *et al*., 2004; Zheng *et al*., 2004; Javelle *et al*., 2005).

However, the strict regulation of ammonium transporters was ascribed to prevent the formation of a putative energy-costly futile cycle under ammonium surplus. Regarding to this theory, ammonium would first be transported into the cell by the use of energy and then it would diffuse passively back out of the cell resulting in a detrimental waste of energy (Castorph *et al*., 1984; Kleiner, 1985). Sensitivity to ammonium due to futile cycling is suspected to be a universal phenomenon of animals, plant, and bacteria (Wirén *et al*., 2004). In fact, a number of plant families (Britto *et al*., 2001; Kronzucker *et al*., 2001; Britto *et al*., 2002) as well as animal cells (Martinelle *et al*., 1993) are known to be sensitive to ammonium. Nevertheless,

ammonium toxicity has not been demonstrated in bacteria and the formation of a putative futile cycle in bacteria is still speculation.

1.3. Assimilation of ammonium

In many bacteria, the primary products of ammonium assimilation are glutamate and glutamine, which are the major intracellular nitrogen donors (Merrick and Edwards, 1995). Glutamate provides nitrogen for most of the transaminases, whereas glutamine donates nitrogen for the synthesis of purines, pyrimidines, arginine, asparagine, tryptophan, histidine, glucosamine, and *p*-aminobenzoate (Reitzer, 2003). In general, there are two pathways for the assimilation of ammonium forming glutamate or glutamine: the glutamate dehydrogenase (GDH) and the glutamine synthetase/glutamate synthase (GS/GOGAT) pathway (figure 1).

Glutamate dehydrogenases are broadly distributed enzymes which catalyze the reversible reductive amination of 2-oxoglutarate by ammonium to give L-glutamate in an NAD(P)H-dependent reaction (Barker, 1981; Merrick and Edwards, 1995). In contrast to most GDHs identified in higher eukaryotes, which have a dual coenzyme specificity (EC 1.4.1.3) using both, NADH and NADPH, GDHs of prokaryotes and lower eukaryotes act only with one particular coenzyme, NADH or NADPH (Minambres *et al*., 2000). In general, NADPH-dependent GDHs (EC 1.4.1.4) contribute to anabolism by assimilating ammonium to form glutamate (Consalvi *et al*., 1991), whereas NADH-dependent GDHs (EC 1.4.1.2) are usually catabolic enzymes for the reverse reaction, the oxidative deamination of glutamate (Duncan *et al*., 1992). All GDHs described so far are oligomeric enzymes, which consist either of six or four identical subunits. These subunits are either of 50 kDa, 115 kDa, or 180 kDa. According to the oligomeric structure, the subunit size, and the results of hierarchical homology grouping, four different well defined classes of GDHs exist: α_6-50_I and α_6-50_{II} (small GDHs) as well as α_6-180 and α_4-115 (large GDHs). The four classes share the same catalytic mechanism, very similar domain structures, and several well-conserved amino acid residues with distinct function. However, the function of the additional amino acids of large GDHs (α_6-180 and α_4-115 classes) is completely unknown. In bacteria, only hexameric GDHs have been reported yet (Minambres *et al*., 2000). GDH from *Clostridium symbiosum* is the most extensively studied GDH with regard to the three-dimensional structure, the catalytic

mechanism, and amino acid residues with distinct function. GDH from *C. symbiosum* is NADH-dependent and belongs to the α_6-50_I class (Minambres *et al*., 2000). Each subunit of this hexameric GDH consists of two domains separated by a cleft harbouring the active site. One domain binds NADH and the other glutamate and 2-oxoglutarate, respectively (Baker *et al*., 1992). During the catalytic cycle, a large movement between the two domains occurs, closing the cleft and bringing the substrate and NADH into the correct position for the reaction (Baker *et al*., 1997). The distinct functions of several amino acid residues are known (Pasquo *et al*., 1996; Millevoi *et al*., 1998; Baker *et al*., 1992; Baker *et al*., 1997). One of them is lysine-89 in the active site, which plays a key role for the interactions with the γ-carboxyl group of the substrate (Wang *et al*., 1994; Stillman *et al*., 1999). If this residue is altered by site-directed mutagenesis to a leucine residue, the resulting mutant has an almost identical conformation as the wild type GDH, but it is enzymatically inactive (Stillman *et al*., 1999).

GDH from *C. glutamicum* belongs to the α_6-50_I class of small GDHs (Minambres *et al*., 2000). It is NADPH-dependent, suggesting that it preferentially acts as an anabolic GDH for ammonium assimilation *in vivo*. The kinetic properties of GDH from *C. glutamicum* have been investigated by *in vitro* assays (Shiio *et al*., 1970). GDH from *C. glutamicum* catalyzes the formation as well as the degradation of glutamate *in vitro*, but the maximum velocity of the formation of glutamate (87.6 μmol/(min*mg)) is 4.6 times higher than that of the degradation (19.2 μmol/(min*mg)). High concentrations of glutamate (400 mM) inhibit the formation of glutamate (75 % inhibition) and the presence of ammonium (10 mM) inhibits the degradation of glutamate (95% inhibition) *in vitro*. As GDHs from many other organisms, GDH from *C. glutamicum* has only a low affinity to its substrates ammonium (K_m = 3.08 mM) and 2-oxoglutarate (K_m = 5.72 mM) and even lower affinity to its product glutamate (K_m = 100 mM) (Shiio *et al*., 1970). *In vivo*, GDH from *C. glutamicum* is the major consumer of cellular ammonium and NADPH under nitrogen surplus. Flux measurements revealed that about 72 % of ammonium assimilation is done by GDH (Tesch *et al*., 1999), which consumes about 50 % of cellular NADPH (Marx *et al*., 1999). The *gdh* gene encoding GDH from *C. glutamicum* has been identified. It is transcribed monocistronically and transcription starts 284 bp upstream of the start codon of *gdh* (Börmann *et al*., 1992).

The second pathway for ammonium assimilation is the glutamine synthetase/glutamate synthase (GS/GOGAT) system (figure 1). In this reaction, ammonium is first attached to glutamate to form glutamine by an ATP-dependent glutamine synthetase (GS), followed by the transfer of the amide nitrogen onto 2-oxoglutarate by an NADPH-dependent glutamate synthase (GOGAT) to form glutamate. In *C. glutamicum*, two genes encoding glutamine synthetases were identified: *glnA* coding for a GSI-β subtype enzyme (Jakoby *et al*., 1997) and *glnA2* coding for a GSI-α subtype enzyme (Nolden *et al*., 2001a). Analysis of a *glnA* deletion strain revealed that only *glnA* codes for an active enzyme for glutamine synthesis in *C. glutamicum*. The *glnA* mutant was observed to be glutamine-auxotrophic (Jakoby *et al*., 1996). Hence, the gene product of *glnA2* has obviously no glutamine synthetase activity in *C. glutamicum* and its physiological role is unclear. Glutamate synthase is encoded by the *gltBD* operon in *C. glutamicum* (Beckers *et al*., 2001; Schulz *et al*., 2001).

The overall reactions of both pathways, GDH and GS/GOGAT, are very similar (figure 1). Both catalyze the NADPH-dependent formation of glutamate from ammonium and 2-oxoglutarate. But in contrast to the GDH-pathway, the GS/GOGAT-system additionally utilizes energy in form of ATP. Consequently, the GS/GOGAT system is strictly regulated to prevent waste of energy. Ammonium is assimilated mainly by GDH if *C. glutamicum* is growing in ammonium-rich medium. Under these conditions, GDH activity is on a high level (1.7 U/mg protein), GOGAT activity is not detectable, and GS activity is maintained at a low level (0.1 U/mg protein) exclusively to satisfy the glutamine requirements of the cell (Tesch *et al*., 1998). As GDH from *C. glutamicum* has only a low affinity to ammonium (K_m = 3.08 mM), it is not able to sufficiently assimilate ammonium under nitrogen limitation. Glutamine synthetases are known to have a significantly higher affinity to ammonium than glutamate dehydrogenases. Consequently, the GS/GOGAT system is activated in *C. glutamicum* under nitrogen limitation (1.5 U/mg protein and 35 mU/mg protein, respectively) (Tesch *et al*., 1998). Thus, utilization of GS/GOGAT allows nitrogen assimilation even under ammonium limitation, but at the expense of energy.

1.4. Nitrogen-dependent regulation

As described above, bacteria regulate nitrogen uptake and assimilation in dependence on the availability of nitrogen sources. For this purpose, bacteria have evolved complex regulatory networks. The most extensive model of nitrogen-dependent regulation has been described for the Gram-negative enteric bacterium *E. coli* (Merrick and Edwards, 1995; Reitzer, 2003; Ninfa, 2005).

In *E. coli*, two proteins play a major role in the regulation of nitrogen uptake and metabolism (figure 2). These are uridylyltransferase (UTase) and the signal transduction protein PII. UTase is a sensor for the internal concentration of glutamine. The glutamine pool is low under nitrogen starvation and high under nitrogen surplus. UTase transfers this signal to PII by uridylylation and deuridylylation, respectively. Unmodified PII is present under nitrogen surplus, while PII-UMP is present under nitrogen starvation (Jiang *et al*., 1998a). In addition, PII itself is a sensor for the internal concentration of 2-oxoglutarate. Under nitrogen starvation, 2-oxoglutarate is accumulated. A high 2-oxoglutarate pool antagonizes the status of unmodified PII, which is present under high glutamine concentrations

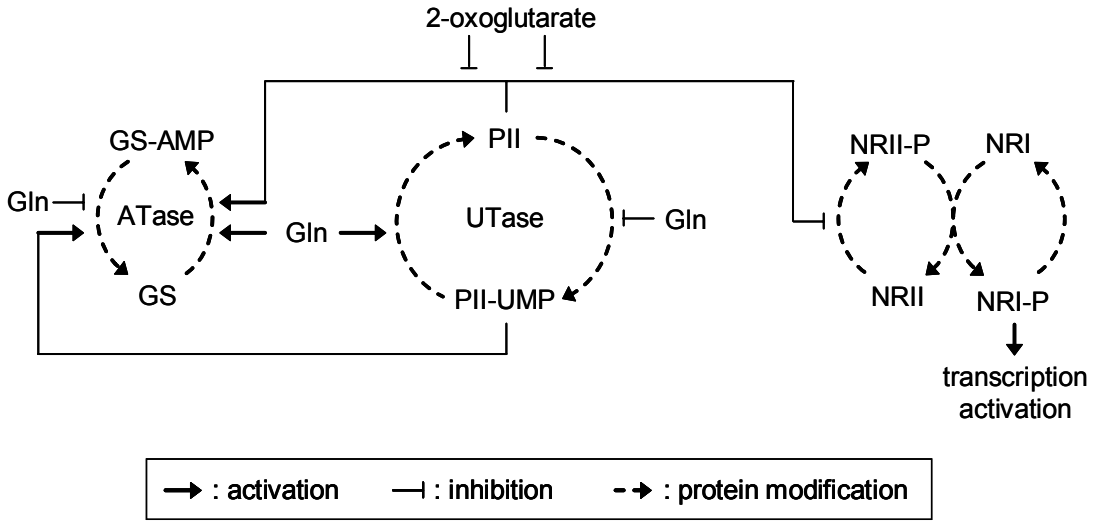

Figure 2: Nitrogen regulation network of *E. coli.* The nitrogen status is sensed by uridylyltransferase (UTase) in *E. coli*. UTase reversibly uridylylates PII in response to the internal glutamine pool. PII additionally senses 2-oxoglutarate. These signals are transferred by protein interactions of PII/PII-UMP to the NRII/NRI system for transcriptional control of nitrogen-regulated genes and adenylyltransferase (ATase), which regulates glutamine synthetase (GS) activity. ATase reversible adenylylates GS to regulate its activity, whereas NRII reversibly phosphorylates NRI to influence its ability to activate transcription (Ninfa *et al*., 2005).

(Kamberov *et al*., 1995; Jiang *et al*., 1998a; Jiang *et al*., 1998b). Thus, PII converts two input signals, the concentrations of glutamine and 2-oxoglutarate, in one output signal (Ninfa *et al*., 2005). This signal is transferred by PII to other regulatory proteins. On the one hand, PII and glutamine synergistically interact with adenylyltransferase (ATase), which regulates glutamine synthetase by adenylylation and deadenylylation. This results in unmodified and fully active GS under nitrogen starvation, whereas GS-AMP with reduced activity is present under nitrogen surplus (Stadtman, 1990; Jiang *et al*., 1998b). On the other hand, PII interacts with NRII, which is part of the NRII/NRI two component system. Under nitrogen surplus, PII binds the kinase NRII and thereby represses phosphorylation of the response factor NRI (Jiang *et al*., 1998b; 1998c). Under nitrogen limitation, NRII is released and phosphorylates NRI, which then activates transcription of σ^{54}-dependent genes. Among these are genes of nitrogen metabolism, transport, and regulation (Atkinson *et al*., 2002). For example, expression of *nac*, coding for the transcriptional regulator Nac, is activated by NRI under nitrogen limitation. Nac itself regulates the transcription of several genes of the glutamate and serine metabolism, e.g. *gdh* coding for glutamate dehydrogenase. Nac represses *gdh* transcription under nitrogen limitation and ammonium assimilation is taken over by the GS/GOGAT system (Camarena *et al*., 1998). Beside that, NRI activates the expression of the *glnK* gene, coding for GlnK, under nitrogen limitation. GlnK is another PII-type protein. It is also modified by UTase in response to the nitrogen status in the same manner as PII. GlnK is responsible for fine tuning of the nitrogen regulation cascade under nitrogen limitation by the formation of heterotrimers of PII-UMP and GlnK-UMP (Atkinson *et al*., 1998; 1999; 2002; Forchhammer *et al*., 1999; van Heeswijk *et al*., 2000). Additionally, GlnK binds to the ammonium transporter AmtB, if nitrogen-starved cells are exposed to an ammonium rich environment. This deactivates AmtB presumably to prevent the formation of a futile cycle under ammonium surplus. Additionally, AmtB is discussed to be a sensor for external ammonium and thereby influences the uridylylation state of GlnK (Javelle *et al*., 2004).

Nitrogen control of *C. glutamicum* differs substantially from that of the model organism *E. coli* (Burkovski, 2003a; 2003b). In *C. glutamicum*, a signal cascade of at least three proteins plays a major role in nitrogen control (figure 3). This cascade

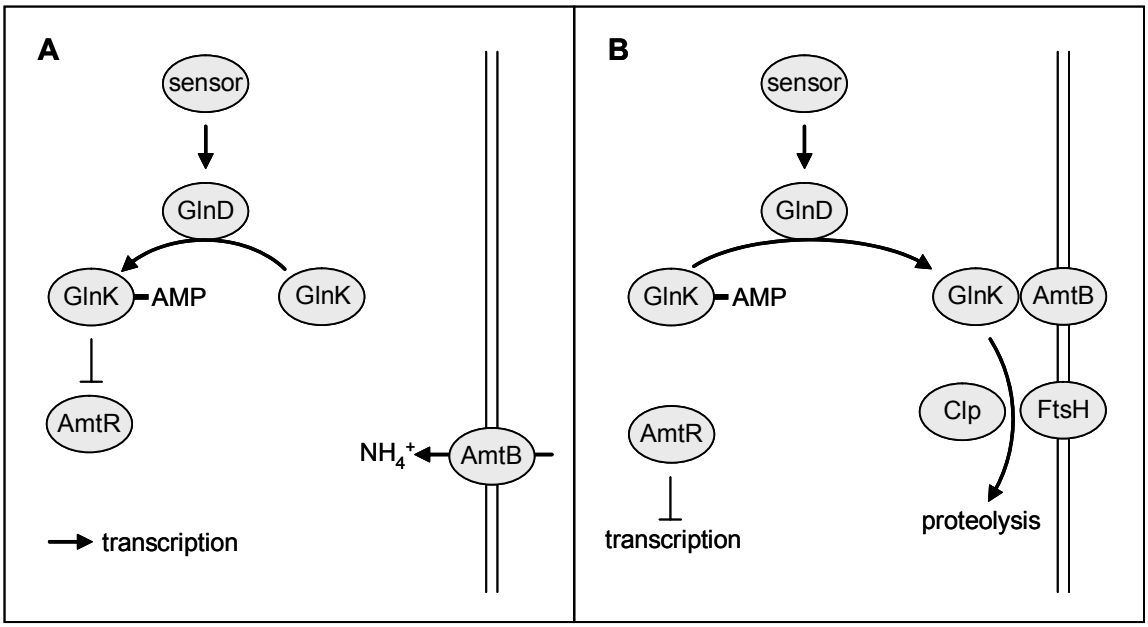

Figure 3: The nitrogen regulation network of *C. glutamicum*. A: Under nitrogen limitation, a so far unknown sensor protein induces the adenylylation of GlnK by GlnD. GlnK-AMP binds the transcriptional repressor AmtR to inactivate it. Consequently, AmtR-controlled genes are transcribed. B: After a shift of nitrogen starved cells to an ammonium rich environment, GlnD deadenylylates GlnK-AMP. Unmodified GlnK does not deactivate AmtR anymore. Consequently, AmtR represses the transcription of its target genes. Unmodified GlnK is sequestered to the membrane. It binds AmtB and thereby most probably deactivates AmtB. Beside that, binding to AmtB induces degradation of GlnK by proteolysis, which is depending on the proteases FtsH, ClpCP, and ClpXP. (Stösser *et al*., 2004)

consists of the GlnD protein, which is similar to the UTase from *E. coli*, the GlnK protein, which is the only PII-type protein in *C. glutamicum*, and AmtR, which is a TetR-type transcriptional repressor (Jakoby *et al*., 1999; 2000; Nolden *et al*., 2001b). Under nitrogen surplus, AmtR represses transcription of several genes involved in nitrogen metabolism, transport, and regulation (figure 4) (Jakoby *et al*., 2000; Nolden *et al*., 2001b; Beckers, 2004). Under this condition, GlnD and GlnK are present only on a low basal level. In response to nitrogen starvation, GlnD adenylylates GlnK (Strösser *et al*., 2004), which then binds to AmtR (figure 3A). AmtR bound by GlnK-AMP does not bind DNA anymore (Beckers *et al*., 2005). Consequently, repression of transcription by AmtR is released by GlnK-AMP and the expression of corresponding genes is induced under nitrogen limitation. If nitrogen-starved cells are shifted to an ammonium rich enviroment, GlnD deadenylylates GlnK (Stösser *et al*., 2004). AmtR cannot be bound by unmodified GlnK, which allows repression of target gene transcription again (figure 3B) (Beckers *et al*., 2005). Moreover, unmodified GlnK binds to the ammonium

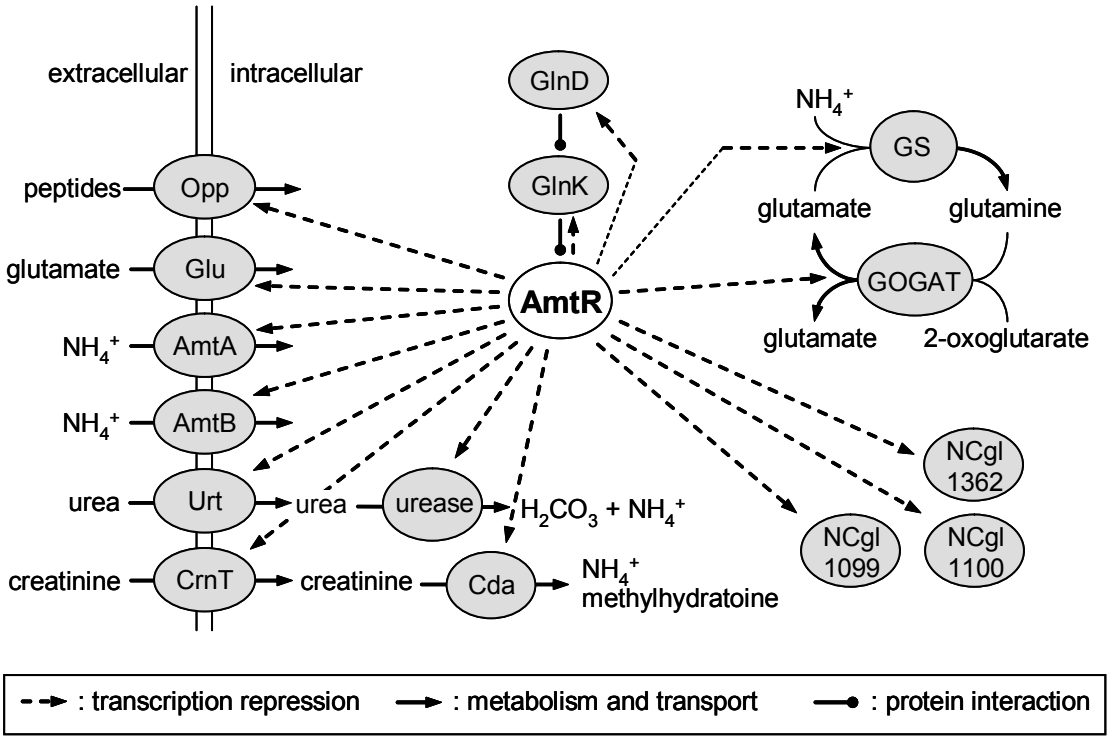

Figure 4: The AmtR-regulon of *C. glutamicum*. The transcriptional repressor AmtR from *C. glutamicum* regulates the expression of genes coding for transporters, enzymes, and signal transduction proteins as indicated. Repression occurs under nitrogen surplus and is released under nitrogen limitation. (Beckers, 2004)

transporter AmtB in response to an ammonium upshift. On the one hand, this is suspected to inactivate AmtB, as described for *E. coli*, to prevent an energy-costly futile cycle in the presence of ammonium. On the other hand, binding of GlnK to AmtB leads to a rapid degradation of GlnK by a process, that involves the proteases FtsH, ClpCP, and ClpXP. Nevertheless, around 5 % of GlnK are protected against proteolysis. The role and the mechanism of protection of GlnK is still unknown (Strösser *et al*., 2004).

In addition to the transcriptional regulation by the GlnD/GlnK/AmtR cascade, glutamine synthetase is regulated on the level of activity by adenylylation/deadenylylation. In accordance to *E. coli*, GS-AMP is present under nitrogen surplus and is less active than unmodified GS, which is present under nitrogen starvation (Nolden *et al*., 2001a). The modification/demodification of GS is catalyzed by ATase. But in contrast to *E. coli*, ATase works independently of GlnK (Burkovski, 2003b).

While the signal transduction *via* the GlnD/GlnK/AmtR cascade is well-investigated, the sensor of the nitrogen status in *C. glutamicum* is still unknown. An overexpression of the corresponding *glnD* gene leads to a loss of nitrogen control (Nolden *et al*., 2001b). This observation is inconsistent with a putative role of GlnD as a primary sensor, as described for in *E. coli*. Consequently, the presence of at least one additional protein was postulated, which functions as a sensor for the nitrogen status of the cell and controls GlnD activity in response to nitrogen supply (figure 3). Beside that, the signal indicating the nitrogen status is unknown as well. The question if the internal concentrations of glutamate, glutamine, and ammonium, respectively, indicate the nitrogen status in *C. glutamicum* was investigated (Nolden *et al*., 2001b). The cellular concentration of glutamate is high under nitrogen surplus as well as under nitrogen starvation. Thus, glutamate can be excluded. For glutamine, Nolden *et al*. (2001b) observed only a slight drop of the internal concentration from approximately 18 mM to 8 mM 10 minutes after the removal of nitrogen sources. This indicates, that glutamine does not play a major role in sensing the nitrogen status in *C. glutamicum*. To measure internal ammonium, Nolden *et al*. (2001) initially used the indophenol method (Jahns *et al*., 1988). But this method is significantly influenced by high amino acid pools as present in *C. glutamicum* and is not reliable under these conditions (L. Nolden, personal communication). Because of that, the values of internal ammonium concentrations presented by Nolden *et al.* (2001b) might be incorrect.

Glutamate dehydrogenase plays an important but so far less investigated role in nitrogen control of *C. glutamicum*. The presence of the *gdh* gene, coding for glutamate dehydrogenase, is essential for a functional nitrogen-dependent regulation in *C. glutamicum*. GS and GOGAT activity are normally downregulated in the *C. glutamicum* wild type under nitrogen surplus. Deletion of *gdh* causes a significantly increase of GS activity and deregulation of GOGAT activity (Tesch *et al*., 1998). In accordance to this, a loss of transcription control by the GlnD/GlnK/AmtR signal cascade was observed upon deletion of *gdh*. In the *C. glutamicum* wild type, transcription of *amtA* and *amtB* is repressed by AmtR under nitrogen surplus. Deletion of *gdh* leads to the loss of repression of *amtA* and *amtB* transcription. Consequently, a deletion of *gdh* abolishes transcription control by the

GlnD/GlnK/AmtR signal cascade (L. Nolden, personal communication). The underlying mechanism for the interaction between *gdh* and the signal cascade is unknown so far.

In addition to that, GDH seems to have a so far unknown function under nitrogen limitation. In other bacteria, expression of NADPH-dependent GDH is either downregulated under nitrogen starvation or it remains constant (Brenchley *et al*., 1975; Schwacha *et* al., 1993; Merick and Edwards, 1995; Camarena *et al*., 1998). In agreement with this, GDH from *C. glutamicum* was first reported to be unaffected by nitrogen supply. Tesch and co-workers (1999) could not observe a significant change in GDH activity of *C. glutamicum* under nitrogen limitation. This observation was supported by transcriptome analyses of *C. glutamicum* cultivated under nitrogen excess and nitrogen limitation, where *gdh* transcription was observed to be unaffected (Beckers, 2004; Silberbach, 2004). In contrast to this, L. Nolden observed a significant increase in *gdh* transcription as well as GDH activity under nitrogen limitation (personal communication). This is remarkable, as an upregulation of NADPH-dependent GDH in bacteria under nitrogen limitation was unknown at that time. Recently published data show, that NADPH-dependent GDH from *Ruminococcus flavefaciens* is also upregulated on the level of transcription under ammonium limitation (Antonopoulos *et al*., 2003). The physiological reason for this regulation in *R. flavefaciens* is still unknown. Interestingly, GDH from *R. flavefaciens* and GDH from *C. glutamicum* are closely related. Both are members of the α_6-50_I class of small GDHs, and with an amino acid identity of 63 %, GDH from *R. flavefaciens* is the most similar homolog of *C. glutamicum* GDH known so far (Antonopoulos *et al*., 2003). Because of these observations, one can speculate about a putative new and so far unknown physiological role of certain NADPH-dependent GDHs in bacteria under nitrogen limitation. However, the induction of *gdh* transcription under nitrogen limitation in *C. glutamicum* seems not to depend on the global nitrogen regulator AmtR. A deletion of the *amtR* gene did not affect *gdh* transcription (L. Nolden, personal communication). Consequently, an additional and so far unknown regulatory system for nitrogen-dependent transcription control seems to be present in *C. glutamicum*, which regulates *gdh* transcription in response to the nitrogen supply.

1.5. Objectives

Expression of the *gdh* gene is induced under nitrogen limitation. This regulation does not depend on the global nitrogen regulator AmtR. Consequently, a putative new regulatory system for nitrogen-dependent transcription control is present in *C. glutamicum*. The main aim of this work is the identification and characterization of the putative new regulator of *gdh* transcription.

Glutamate dehydrogenase plays a crucial role for a functional nitrogen control by the GlnD/GlnK/AmtR signal cascade. Deletion of the *gdh* gene leads to a complete loss of transcription control by AmtR. The underlying mechanism is still unknown. The characterization of this effect is the second aim of this work.

Ammonium is suspected of being toxic for bacteria due to the formation of a putative energy-wasting transmembrane cycle. An additional aim of this work is to investigate putative ammonium toxicity in *C. glutamicum* and the presence of a putative futile cycle.

2. Materials and methods

2.1. Bacterial strains, plasmids, and primers

Bacterial strains used in this study are listed in table 1, plasmids are listed in table 2.

Table 1: *E. coli* and *C. glutamicum* strains that were used in this work. For strains that were constructed as part of this work, a detailed description is given in the appendix. Nx^R: resistant to nalidixic acid.

Strain	Genotype, phenotype	Reference
E. coli		
DH5α*mcr*	*endA1 supE44 thi-1* λ^- *recA1 GyrA96 relA1 deoR* Δ*(lacZYA-argF) U169* ϕ80Δ*lacZ* Δ*M15mcrA* Δ*(mmr hsdRMS mcrBC)*	Grant *et al*., 1990
JM109	F' *traD36 lacI*^{q} Δ*(lacZ)M15 proA*$^+$*B*$^+$ *I e14*$^-$ *(McrA*$^-$*)* Δ*(lac-proAB) thi gyrA96 (Nx*^{R}*) endA1 hsdR17 (*$r^-_k m^-_k$*) relA1 supE44 recA1*	Yanisch-Perron *et al*., 1985
M15 pREP4	RecA$^+$, Uvr$^+$, Lon$^+$ *lac, ara, gal, mtl,* pREP4	Qiagen, Hilden
C. glutamicum		
ATCC 13032	wild type	Abe *et al*., 1967
RES167	ATCC 13032 Δ*(cglIM-cglIRR-cglIIR)*	Tauch *et al*., 2002
MJ6-18	ATCC 13032 Δ*amtR*	Jakoby *et al*., 2000
TMΔfarR	RES167 Δ*farR*	this work
TMΔwhiH	RES167 Δ*whiH*	this work
TMΔoxyR	RES167 Δ*oxyR*	this work
TMΔfarRΔamtR	RES167 Δ*farR* Δ*amtR*	this work
TMΔfarRΔamtR ΔwhiH	RES167 Δ*farR* Δ*amtR* Δ*whiH*	this work
TMΔfarRΔamtR ΔwhiHΔoxyR	RES167 Δ*farR* Δ*amtR* Δ*whiH* Δ*oxyR*	this work

LNΔGDH	ATCC 13032 Δ*gdh*	Nolden, unpublished
LNΔGS	ATCC 13032 Δ*glnA*	Nolden, unpublished
TMΔgdhΔglnA	LNΔGDH Δ*glnA*	this work
JS-1	ATCC 13032 Δ*amtA* Δ*amtB*	Strösser, unpublished

Table 2: Plasmids that were used in this work. For plasmids that were constructed as part of this work, a detailed description is given in the appendix. Ap^R: resistant to ampicilin. Km^R: resistant to kanamycin.

Plasmid	Description	Reference
pK18mobsacB	Km^R, *ori* pUC, *mob*, *sacB*	Schäfer *et al.*, 1994
pK18ΔamtR	Deletion vector for *amtR* of *C. glutamicum*, derived from pK18mobsacB, Km^R, *ori* pUC, *mob*, *sacB*	Nolden, 2001
pK18ΔfarR	Deletion vector for *farR* of *C. glutamicum*, derived from pK18mobsacB, Km^R, *ori* pUC, *mob*, *sacB*	this work
pK18ΔwhiH	Deletion vector for *whiH* of *C. glutamicum*, derived from pK18mobsacB, Km^R, *ori* pUC, *mob*, *sacB*	this work
pK18ΔoxyR	Deletion vector for *oxyR* of *C. glutamicum*, derived from pK18mobsacB, Km^R, *ori* pUC, *mob*, *sacB*	this work
pK18ΔglnA	Deletion vector for *glnA* of *C. glutamicum*, derived from pK18mobsacB, Km^R, *ori* pUC, *mob*, *sacB*	Nolden, unpublished
pZ8-1	Km^R, *ptac*, *ori C. glutamicum*	Degussa AG, Halle
pUC18	Ap^R, *lacZ*α	Viera & Messing, 1982
pUC11-1.8	Expression vector of *amtR* of *C. glutamicum* derived from pUC19, Ap^R, *lacZ*α	Jakoby *et al.*, 2000
pUCfarR	Expression vector of *farR* of *C. glutamicum* derived from pUC18, Ap^R, *lacZ*α	this work

pUCwhiH	Expression vector of *whiH* of *C. glutamicum* derived from pUC18, Ap^R, *lacZ*α	this work
pUCoxyR	Expression vector of *oxyR* of *C. glutamicum* derived from pUC18, Ap^R, *lacZ*α	this work
pZgdh	Expression vector of *gdh* from *C. glutamicum*, derived from pZ8-1, Km^R, *ptac*, *ori C. glutamicum*	this work
pZgdhEC	Expression vector of *gdh* from *E. coli*, derived from pZ8-1, Km^R, *ptac*, *ori C. glutamicum*	this work
pZgdh-K92L	Expression vector for an enyzmatical inactive mutant of GDH from *C. glutamicum*, derived from pZ8-1, Km^R, *ptac*, *ori C. glutamicum*	this work
pQE30Xa	Ap^R, *ori* ColE1, PT5	Qiagen, Hilden
pQE30Xagdh	Expression vector for his-tagged GDH from *C. glutamicum,* Ap^R, *ori* ColE1, PT5	this work
pJC1	Km^R, *ori C. glutamicum*	Cremer *et al*., 1990
pJCgdhlacZ	Km^R, *ori C. glutamicum,* harbouring a fusion of the *gdh* promoter of *C. glutamicum* and *lacZ*	this work
pK18gdh-lacZ	Km^R, *ori* pUC, *mob*, *sacB,* harbouring a fusion of the *gdh* promoter of *C. glutamicum* and *lacZ*	Nolden, unpublished
PGEM3z-amt	Ap^R, *lacZ*α, harbouring a 0.5 kb fragment of the *amtA* gene	Nolden, 2001
PGEM3z-amtB	Ap^R, *lacZ*α, harbouring a 0.5 kb fragment of the *amtB* gene	Nolden, 2001
PGEM3z-gltB	Ap^R, *lacZ*α, harbouring a 0.5 kb fragment of the *gltB* gene	Nolden, 2001
PGEM3Z-glnA	Ap^R, *lacZ*α, harbouring a 0.5 kb fragment of the *glnA* gene	Nolden, 2001
PGEM4z-gdh	Ap^R, *lacZ*α, harbouring a 0.5 kb fragment of the *gdh* gene	Nolden, 2001
PGEM3z-glnD	Ap^R, *lacZ*α, harbouring a 0.5 kb fragment of the *glnD* gene	Nolden, 2001
pDrive	Ap^R, *lacZ*α, A-T insertion vector	Qiagen, Hilden

2.2. Cultivation of bacteria

Culture media used in this study are listed in table 3. If appropriate, antibiotics were added to the media in the following final concentrations: 50 μg/mL carbenicillin, 25 μg/mL kanamycin, or 10 μg/mL kanamycin (latter only for *C. glutamicum* strains after electroporation). *E. coli* strains were routinely grown at 37 °C in LB medium or on LB plates. *C. glutamicum* strains were routinely cultivated at 30 °C in CgC medium, in Brain Heart Infusion (BHI) medium, or on BHI plates. To study various stress conditions under highly reproducible conditions, a standard inoculation schema was applied. *C. glutamicum* strains were first cultivated in 3 mL BHI medium for 8 hours. This culture was used to inoculate 25 mL CgC medium for overnight growth. This culture, with an overnight OD_{600} of approximately 25-33, was used to inoculate 100 mL of fresh CgC medium to an OD_{600} of approximately 1 and cells were grown until the exponential phase was reached (OD_{600} approximately 4-5). In case of LNΔGS and TMΔgdhΔglnA, all media were additionally supplemented with 100 mM glutamine. To analyze the effect of various cultivation conditions or medium compositions, the cells were treated in the following as listed in table 4.

Table 3: Culture media used in this study.

Medium	Ingredients (per L)
LB	10 g Tryptone, 5 g yeast extract, 10 g NaCl
LB plates	15 g Bacto-Agar in LB medium
BHI	37 g/L Brain Heart Infusion
BHI plates	15 g Bacto-Agar in BHI medium
CgC	42 g MOPS, 20 g $(NH_4)_2SO_4$, 5 g urea, 0.5 g KH_2PO_4, 0.5 g K_2HPO_4, pH (NaOH) = 7.0, after autoclavation: 10 mL 100 mM $CaCl_2$, 10 mL 1 M $MgSO_4$, 200 mg biotin, 1 mL trace element solution, 50 mL 50 % glucose
CgCoN	42 g MOPS, 0.5 g KH_2PO_4, 0.5 g K_2HPO_4, pH (NaOH) = 7.0, after autoclavation: 10 mL 100 mM $CaCl_2$, 10 mL 1 M $MgSO_4$, 200 mg biotin, 1 mL trace element solution, 50 mL 50 % glucose
CgCoC	42 g MOPS, 20 g $(NH_4)_2SO_4$, 5 g urea, 0.5 g KH_2PO_4, 0.5 g K_2HPO_4, pH (NaOH) = 7.0, after autoclavation: 10 mL 100 mM $CaCl_2$, 10 mL 1 M $MgSO_4$, 200 mg biotin, 1 mL trace element solution
Trace element solution	28.5 g $FeSO_4$ x 7 H_2O, 16.5 g $MnSO_4$ x H_2O, 6.4 g $ZnSO_4$ x 7 H_2O, 764 mg $CuSO_4$ x 5 H_2O, 129 mg $CoCl_2$ x 6 H_2O, 44 mg $NiCl_2$ x 6 H_2O, 64 mg Na_2MoO_4 x 2 H_2O, 48 mg H_3BO_3, 50 mg $SrCl_2$, 50 mg $BaCl_2$ x 2 H_2O, 28 mg $KAl(SO_4)_2$ x 12 H_2O, pH (H_2SO_4) = 1, sterilization by filtration.

Table 4: Cultivation protocols for the analysis of various conditions. To study the effect of various conditions, *C. glutamicum* strains was treated as described in this table.

Condition	Practical procedure
Nitrogen starvation	Cells were harvested by centrifugation and resuspended in 100 mL pre-warmed CgCoN medium. Cells were cultivated again at 30 °C. After a certain period of time, 200 mM $(NH_4)_2SO_4$ was added to the culture medium to restore nitrogen surplus conditions. LNΔGS was pulsed with either 200 mM $(NH_4)_2SO_4$, or 100 mM glutamine, or both, 200 mM $(NH_4)_2SO_4$ and 100 mM glutamine.
Variation of the nitrogen source	Cells were harvested by centrifugation and resuspended in 100 mL pre-warmed CgCoN medium supplemented with 1 % of the appropriate nitrogen source. Cells were cultivated again at 30 °C.
Carbon starvation	Cells were harvested by centrifugation and resuspended in 100 mL pre-warmed CgCoC medium. Cells were cultivated again at 30 °C. After a certain period of time, 1 % glucose was added to the culture medium to restore carbon surplus conditions.
Variation of the carbon source	Cells were harvested by centrifugation and resuspended in 100 mL pre-warmed CgCoC medium supplemented with 1 % of the appropriate carbon source. Cells were cultivated again at 30 °C.
Osmotic stress	1 M NaCl was added to the culture medium, and cells were cultivated at 30 °C.
Oxidative stress	Either 100 μM paraquat (superoxide stress) or 58 μM H_2O_2 (peroxide stress) was added to the culture medium, and cells were cultivated at 30 °C.
Oxygen limitation	50 mL of a culture was transferred to a 50 mL falcon tube. The falcon tube was sealed. In this airtight container, cells were cultivated at 30 °C.
Chill stress	Cells were harvested by centrifugation and resuspended in 100 mL CgC medium with a temperature of 15 °C. Cells were cultivated at 15 °C.
Heat stress	Cells were harvested by centrifugation and resuspended in 100 mL CgC medium with a temperature of 37 °C. Cells were cultivated at 37 °C.
Growth phase	Cells were cultivated at 30 °C until the stationary phase was reached.
Addition of intermediates of arginine biosynthesis	1 % of arginine, citrulline, and ornithine, respectively, was added to the culture medium, and cells were cultivated at 30 °C.
High ammonium concentrations	Cells were harvested by centrifugation and resuspended in 100 mL pre-warmed CgCoN medium supplemented with either 0.25 M $(NH_4)_2SO_4$, 0.5 M $(NH_4)_2SO_4$, or 1 M $(NH_4)_2SO_4$. As control, cells were resuspended in prewaremd CgCoN medium supplemented with either 0.25 M $(NH_4)_2SO_4$ + 0.25 M Na_2SO_4 or 0.25 M $(NH_4)_2SO_4$ + 0.75 M Na_2SO_4. After resupending, cells were cultivated at 30 °C. Cultures of TMΔgdhΔglnA were additionally supplemented with 100 mM glutamine.

2.3. Genetic manipulation of bacteria

2.3.1. Preparation of competent *E. coli* cells and transformation

To prepare competent *E. coli* cells, 20 mL LB medium was inoculated with *E. coli* cells and cultivated for 8 h at 37 °C. 1 mL of this culture was used to inoculate 250 mL SOB medium for overnight growth at 20 °C in a 2 L flask. On the next day, the culture was chilled on ice for 10 min. Cells were harvested by centrifugation (4000 x g, 4 °C, 8 min). The cell pellet was resuspended in 80 mL ice-cold TB buffer and centrifuged again (4000 x g, 4 °C, 10 min). After resuspending in 40 mL TB buffer supplemented with 1.4 mL DMSO, the cells were incubated for 10 min on ice. Aliquots of 100 µL were transferred to pre-cooled reaction tubes. These were immediately frozen in liquid nitrogen and stored at -80 °C.

For transformation, a 100 µL aliquot of competent *E. coli* cells was thawed on ice and plasmid DNA was added. The cells were incubated for 30 min on ice. After a heat shock at 42 °C for 30 s, cells were again incubated for 2 min on ice and 900 µL SOC medium was added. The cell suspension was cultivated for 1 h at 37 °C. After that, 200 µL of the cell suspension was plated on LB plates containing the appropriate antibioticum.

TB buffer: 10 mM Pipes, 15 mM $CaCl_2$, 250 mM KCl, pH (KOH) = 6.7. After adjustment of pH, 55 mM $MnCl_2$ were added, sterilization by filtration.

SOB medium: 20 g/L Tryptone, 5 g/L yeast extract, 0.5 g/L NaCl, 2.5 mM KCl. After autoclavation, 5 mL 2 M $MgCl_2$ were added.

SOC medium: 10 g/L Tryptone, 5 g/L yeast extract, 5 g NaCl, 3.6 g/L glucose. After autoclavation, 5 mL 2 M $MgCl_2$ were added.

2.3.2. Preparation of competent *C. glutamicum* cells and transformation

To prepare competent *C. glutamicum* cells, 20 mL BHI medium was inoculated with *C. glutamicum* cells and cultivated for 8 h at 30 °C. Subsequently, this culture was used to inoculate 200 mL LB medium with growth inhibitors to an OD_{600} of 0.35. This was cultivated at 20 °C in a 2 L flask overnight. On the next day, cells were

harvested by centrifugation (4000 x g, 4 °C, 8 min). The cell pellet was washed five times with ice-cold 10 % glycerol. Finally, the cell pellet was resuspended in 1 mL ice-cold 10 % glycerol. Aliquots of 50 µL were transferred to pre-cooled reaction tubes. These were immediately frozen in liquid nitrogen and stored at -80 °C.
For transformation, a 50 µL aliquot of competent *C. glutamicum* cells was thawed on ice and transferred to a pre-cooled electroporation cuvette (Biorad, München). Plasmid DNA was added and electroporation was performed with a Gene-Pulser (Biorad, München) at 2.5 kV, 600 Ω, and 25 µF. After that, the cell suspension was transferred to a cultivation tube and 1 mL BHIS medium was added. The cells were cultivated for 90 min at 30 °C. After that, 200 µL of the cell suspension was plated on a BHI plate containing the appropriate antibioticum.

LB medium with growth inhibitors: 10 g/L Tryptone, 5 g/L yeast extract, 5 g/L NaCl, 4 g/L isonicotine acid hydrazide, 25 g/L glycine, 0.1 % (v/v) Tween 80, sterilization by filtration.

BHIS medium: 37 g/L Brain Heart Infusion, 91 g/L sorbitol, sterilization by filtration.

2.3.3. Generation of deletion strains of *C. glutamicum*

To introduce a chromosomal deletion in the *C. glutamicum* genome, a method similar to the protocols described by Schäfer *et al*. (1994) and Niebisch *et al*. (2001) was used. The flanking genomic sequences of the target gene were cloned into the plasmid pK18mobsacB. *C. glutamicum* was transformed with the resulting plasmid. Cells carrying the plasmid were selected by their resistance to kanamycin and their sensitivity to sucrose. A single colony carrying the plasmid was used to inoculate 3 mL BHI medium containing 25 µg/mL kanamycin. After overnight growth at 30 °C, the cells were harvested by centrifugation (14,000 x g, 30 s, RT) and wash four times with 2 mL CgXIIoNoPoPC medium. Finally, the cells were resuspended in 3 mL CgXIIoNoPoPC medium and cultivated for 6 h at 30 °C in the absence of kanamycin. After that, the culture was diluted 1:1000 and 1:10000, respectively, in 100 µl BHI medium. These cell suspensions were plated on BHI plates containing 10 % sucrose. Colonies that were resistent to sucrose and sensitive to kanamycin were analyzed by PCR to identify clones carrying the desired deletion.

CgXIIoNoPoPC: 42 g/L MOPS, pH (NaOH) = 7.0, after autoclavation: 1 mM $MgSO_4$. 0.1 mM $CaCl_2$, 0.2 mg/L biotin, 1 mL/L trance element solution, 0.5% glucose.

2.4. Working with DNA

2.4.1. Isolation of plasmid DNA from *E. coli*

To isolate plasmid DNA from *E. coli*, the NucleoSpin® Extract kit (Macherey-Nagel, Düren) was used as recommended by the supplier.

2.4.2. Isolation of genomic DNA from *C. glutamicum*

The isolation of genomic DNA from *C. glutamicum* was performed as described by Eikmanns *et al.* (1994). *C. glutamicum* cells were cultivated overnight in 5 mL LB medium. After that, cells were harvested by centrifugation (14.000 x g, 30 s, RT) and the cell pellet was resuspended in 1 mL TE buffer supplemented with 15 mg lysozyme (Sigma, Deisenhofen). After shaking for 3 h at 37 °C, 200 µL 10 % SDS was added. After an incubation of 2 min at 37 °C, 3 mL lysis buffer and 125 µL proteinase K (Roche Diagnostics) were added. The suspension was incubated overnight at 37 °C. On the next day, 2 mL of a saturated solution of NaCl was added and the suspension was gently mixed. After centrifugation (4000 x g, 30 min, RT), the supernatant was transferred to a 50 mL tube and ice-cold ethanol was added to a final volume of 50 mL. The precipitated genomic DNA was washed three times with 70 % ethanol, dried, and resuspended in water.

2.4.3. Gel electrohoresis and extraction of DNA from agarose gels

Gel electrophoresis of DNA was performed in 0.8 – 2 % agarose gels in 1 x TAE buffer as described by Sambrook *et al*. (1989). Samples were mixed with 5 x Loading Dye (MBI Fermentas, St. Leon-Roth). After electrophoresis, DNA was stained with ethidium bromide. For detection of stained DNA, the Image Master VDS system (Amersham Biosciences, Freiburg) was used. DNA was isolated from agarose gels using the NucleoSpion® Extract kit (Macherey-Nagel, Düren) as recommended by the supplier.

1x TAE buffer: 40 mM Tris, 0.5 mM EDTA, pH (acetic acid) = 7.5.

2.4.4. PCR and SOE-PCR

The selective amplification of specific DNA fragments was performed by PCR using the Taq PCR Master Mix (Qiagen, Hilden) as recommended by the supplier. For a total reaction volume of 25 µL, 10 pmol of each primer and 1 µL of the template DNA solution were added. Primers were supplied by Sigma-ARK (Darmstadt), Carl Roth GmbH (Karlsruhe), and Operon (Köln). The PCR was performed with a Mastercycler® personal or Mastercycler® gradient (Eppendorff, Hamburg) using the following program: 5 min, 95°C; 30x (30 s, 95 °C; 30 s, 60 °C; 1 min/kb, 72°C); 5 min, 72°C; 4°C. If appropriate, the PCR product was purified either with the NucleoSpin® Extract Kit (Macherey-Nagel, Düren) as recommended by the supplier or by gel electrophoresis as described in section 2.4.3..

Using SOE-PCR (splicing by overlapping extension-PCR) (Horton *et al*., 1989), two DNA fragments were amplified and fused together by PCR without the use of restriction digestion. For this purpose, the 3' primer of one fragment was designed to overlap the 5' primer of the other fragment and *vice versa*. In a first step, each DNA fragment was amplified separately by PCR using the standard protocol described above. After that, 1 µL of each reaction mix was applied as template for another PCR to synthesize the fusion DNA. The outer primers were added in excess (100 pmol) and the PCR was performed using the standard protocol described above. The fusion DNA was purified by gel electrophoresis followed by extraction of the DNA as described in section 2.4.3..

2.4.5. Restriction, ligation, and sequencing of DNA

For restriction of DNA, restriction enzymes were used as recommended by the suppliers (NEB, Frankfurt/Main; MBI Fermentas, St. Leon-Roth). If appropriate, 1 µL shrimp alkaline phosphate (SAP) or 1 µL calf intestinal alkaline phosphate (CIP) was added to dephosphorylate 5' ends (NEB, Frankfurt/Main). For fill-in of 5' overhangs to form blunt ends, the large Klenow fragment of DNA polymerase I (NEB, Frankfurt/Main) was used as recommended by the supplier. After restriction, dephosphorylation, or blunting, DNA was purified either with the NucleoSpin® Extract kit (Macherey-Nagel, Düren) following the supplier's protocol or by gel electrophoresis as described in section 2.4.3..

For the ligation of DNA fragments to restricted vectors, the Rapid DNA Ligation kit (MBI Fermentas, St. Leon-Roth) was used as recommended by the supplier. For direct ligation of PCR products to the pDrive vector by T/A-cloning, the QIAGEN PCR Cloning kit (Qiagen, Hilden) was used following the supplier's protocol. After ligation, 5 μL of the reaction mix was used to transform competent *E. coli* cells as described in section 2.3.1..
DNA sequence analyses were carried out by the bioanalytics service unit at the *Center for Molecular Medicine Cologne* (ZMMK).

2.4.6. Site-directed mutagenesis

For the site-directed mutagenesis of DNA plasmids, the QuikChange™ Site-Directed Mutagenesis Kit (Stratagene, La Jolla, USA) was used as recommended by the supplier. To produce the methylated template DNA plasmid, the *E. coli* strain JM109 was transformed with the respective unmethylated DNA plasmid as described in section 2.3.1.. From the resulting strain, the methylated DNA plasmid was isolated as described in section 2.4.1.. Primers were supplied by Operon (Köln).

2.5. Working with RNA

2.5.1. Isolation of total RNA from *C. glutamicum*

0.5 mL of a *C. glutamicum* culture with an OD_{600} of 4-5 were centrifuged (14000 x g, 30 s, 30 °C) and the cell pellet was immediately frozen in liquid nitrogen and stored at -80 °C. The cell pellet was thawed at room temperature while resuspensing the cells in RA1 buffer (NucleoSpin RNA II Kit, Macherey-Nagel, Düren). Immediately after resuspention of the cell pellet, the suspension was transferred to a tube containing glass beads and cells were disrupted by vigorous shaking at 6.5 m/s for 1 min using a FastPrep FP120 instrument (Q-BIOgene, Heidelberg). Cell debris and glass beads were removed by centrifugation (14000 x g, 2 min, RT) and the supernatant was mixed with 350 μL 70 % ethanol. In the following, total RNA was isolated using the NucleoSpin® RNA II kit (Macherey-Nagel, Düren) as recommended by the supplier. The purity of total RNA isolated by this approach was

sufficient for dot blot hybridization experiments. However, for DNA microarray experiments and quantitative real-time RT-PCR experiments, total RNA was additionally treated with TURBO-DNase (Ambion, Austin, USA) and subsequently purified using again the NucleoSpin® RNA II kit (Macherey-Nagel, Düren) as recommended by the suppliers.

The integrity of isolated total RNA was analyzed by gel electrophoresis. Three μL of purified total RNA was mixed with 10 μL RNA loading buffer and incubated for 10 min at 70 °C. After that, the sample was placed on ice for 5 min. In the following, gel electrophoresis and detection of RNA was performed in accordance to the analysis of DNA described in section 2.4.3..

The concentrations of RNA samples used for dot blot hybridization experiments or DNA microarray analyses were measured spectroscopically at a wavelength of 260 nm (ε = 25 cm^2/mg) and their purity was analyzed by determine the quotient of A_{260} / A_{280}, which is 2.0 for pure RNA. The concentrations of RNA samples used for quantitative real-time RT-PCR experiments were measured using the RiboGreen RNA Quantitation kit (Moleculare Probes, Leiden, NL) as recommended by the supplier.

RNA loading buffer: 250 μL formamide, 83 μL 37 % formaldehyde, 50 μL 10 x MOPS buffer, 50 μL glycerol, 0.01 % bromphenol blue, 0.01 % xylene cyanole, 1 μL 10 g/L ethidium bromide, 120 μL RNase-free water.

MOPS buffer: 200 mM MOPS, 50 mM sodium acetate, 10 mM EDTA, pH = 7.0.

2.5.2. Synthesis of digoxigenin-labelled RNA probes

Digoxigenin-labelled RNA probes were produced by *in vitro* transcription. For this purpose, a DNA plasmid that harbours an insert with the appropriate DNA sequence was used as template. Depending on the orientation of the insert, the plasmid was restricted either upstream or downstream of the insert and *in vitro* transcription was started from a SP6 or T7 promoter that was located at the opposite end of the insert. The probe was labelled by the use of digoxigenin-11-dUTP instead of dUTP for the *in vitro* transcription. The reaction mixture for the *in vitro* transcription was composed of:

1 μg template DNA (restricted plasmid)
2 μL DIG RNA Labeling Mix (Roche, Mannheim)
2 μL 10 x Transcription Buffer (Roche, Mannheim)
2 μL SP6 or T7 RNA polymerase (Roche, Mannheim)
13 μL RNase-free water

The reaction mixture was incubated for 2 h at 37 °C. After that, 1 μL DNase (Roche, Mannheim) was added and the solution was incubated for another 20 min at 37 °C. The resulting digoxigenin-labelled RNA probe was stored at -80 °C.

2.5.3. Dot blot analysis and slot blot analysis

For the preparation of RNA blots, 2.5 μg of total RNA was mixed with 100 μL 10 x SSC and spotted onto a nylone membrane (BioBond^{TM} Nylon Membrane, Sigma, Taufkirchen), which was pre-equilibrated in 10 x SSC, using either the Minifold I Dot Blotter (Schleicher & Schuell, Dassel) or the Slot Blotter (Fisher Science, Schwerte). Subsequently, the nylon membrane was dried and RNA was crosslinked by UV radiation (125 mJ/cm^2) using a Bio-Link instrument (LFT-Labortechnik, Wasserburg). The membrane was incubated for 1 h in 20 mL hybridization mix. Subsequently, 1 μL digoxigenin-labelled RNA probe (its preparation is described in section 2.5.2.) was added and hybridization was performed at 68 °C overnight. On the next day, the membrane was washed twice with 20 mL washing buffer 1 for 15 min at room temperature. Then, the membrane was washed twice with 20 mL washing buffer 2 for 15 min at 68 °C and subsequently, with 20 mL washing buffer 3 for 1 min at room temperature. After that, the membrane was incubated for 30 min in 20 mL 1 x blocking buffer. Then, 2 μL alkaline phosphatase conjugated anti-digoxigenin Fab fragments (Roche, Mannheim) were added and the membrane was incubated for another 30 min at room temperature. After three washing steps with washing buffer 3 for 30 minutes at room temperature, the membrane was equilibrated in detection buffer for 3 minutes. 15 μL CSPD reagent (Roche, Mannheim) was dissolved in 1.5 mL detection buffer. This solution was used to moisten the membrane, which was subsequently covered with and heat-sealed in transparent plastic foil. After an incubation of 15 min at 37 °C, light emission was detected using a Fuji Luminescent Image Analyser LAS1000 (Raytest,

Straubenhardt). The intensities of hybridization signals were determined using the software AIDA 2.0 (Raytest, Straubenhardt).

20 x SSC: 3 M NaCl, 0.3 M sodium citrate, pH (HCl) = 7.0.

Hybridization mix: 50 mL formamide, 20 mL 10 x blocking buffer, 25 mL 20 x SSC, 1 mL 10 % sodium lauryl sarconisate, 0.2 mL 10 % SDS, 3.8 mL water.

Washing buffer 1: 2 x SSC, 0.1 % SDS.

Washing buffer 2: 0.2 x SSC, 0.1 % SDS.

10 x blocking buffer: 10 % blocking reagent (Roche, Mannheim) in maleic acid buffer. 10 x blocking buffer was dissolved 1:10 in maleic acid buffer to obtain 1 x blocking buffer.

Maleic acid buffer: 0.1 M maleic acid, 0.15 M NaCl, pH (NaOH) = 7.5.

Washing buffer 3: 0.3 % (v/v) Tween 20 in maleic acid buffer.

Detection buffer: 0.1 M Tris, 0.1 M NaCl, pH (NaOH) = 9.0.

2.5.4. Quantitative real-time RT-PCR

Quantitative real-time RT-PCR was used to quantify the amount of a specific mRNA present in *C. glutamicum* cells. For this purpose, total mRNA was isolated from *C. glutamicum* cells as described in section 2.5.1.. One μg of total RNA was applied for a reverse transcription reaction using the QuantiTect® Reverse Transcription kit (Qiagen, Hilden) as recommended by the supplier. 5 μL of the resulting cDNA solution was used as template for quantitative real-time PCR using the QPCR Mastermix Plus For SYBR® Green I kit (Eurogentec, Seraing, Belgium) as recommended by the supplier, primers supplied by Operon (Köln), and the real-time thermocycler ABI Prism® 7000 (Applied Biosystems, Weiterstadt). The following program was used: 5 min, 95°C; 40x (15 s, 95 °C; 30 s, 60 °C; 30 s, 72°C); 4°C.

After each temperature cycle, the amount of PCR product was determined based on the fact that the applied SYBR® green I dye specifically interacts with double-stranded DNA to become highly fluorescent upon excitation. At the end of the run, the specificity and the purity of the PCR product were analyzed by performing of melt curve. As negative control, total RNA was directly applied for quantitative real-time PCR instead of the corresponding cDNA.

2.5.5. DNA-Microarray analysis

The DNA microarrays that were used in this work were developed and produced by the group of Dr. J. Kalinowski at the University of Bielefeld/Germany as described by Hüser *et al*. (2003). The preparation of the labelled probes, the hybridization of the microarrays, and subsequent detection of the hybridization signals were performed as described Hüser *et al*. (2003).

In order to compare the transriptomes of two different *C. glutamicum* strains, total RNA of both strains was isolated as described in section 2.5.1.. Fluorescently labelled cDNA copies of the total RNA samples were prepared by an indirect labelling technique. Aminoallylmodified nucleotides (aa-dUTP) were incorporated during a first strand reverse transcription, which was started by random priming using 5'-amino-modified hexamer nucleotides (Operon, Köln). For each *C. glutamicum* strain, 8 μg total RNA and 2.5 μg 5'-amino-modified hexamers were mixed, incubated at 70 °C for 10 min, and chilled on ice for 5 min to anneal the primers. Subsequently, the following components were added to each reaction mixture:

0.5 mM	of each dNTP
0.8 mM	aa-dUTP (Sigma–Aldrich, Deisenhofen)
300 units	Super-Script II RNase H Reverse Transcriptase (Invitrogen, Karlsruhe)
6 μL	5 x first-strand buffer (Invitrogen, Karlsruhe)
3 μL	100 mM DTT
0.5 μL	RNase inhibitor (Roche Diagnostics, Mannheim, Germany)
ad. 30 μL	water

The reverse transcription reactions were performed for 4.5 h at 42 °C. Subsequently, 10 μL 0.5 mM EDTA and 10 μL 1 M NaOH were added and the reaction mixtures were incubated for 10 min at 70 °C. After that, 10 μL 1M HCl was added. The resulting cDNA was purified using the MinElute PCR Purification kit (Qiagen, Hilden) as recommended by the supplier. Then, 1 M sodium bicarbonate buffer (pH 9.0) was added to a final concentration of 0.1 M. One cDNA solutions was transferred to an aliquot of Cy3 monofunctional NHS-esters (Amersham Biosciences, Freiburg), the other to an aliquot of Cy5 monofunctional NHS-esters (Amersham Biosciences, Freiburg). Both solutions were incubated for 60 min in the dark. Non-reactive NHS-esters were quenched by the addition of 4.5 mL 4 M hydroxylamine and incubation for 15 min in the dark. Subsequently, the labelld cDNA probes were purified using the MinElute PCR Purification kit (Qiagen, Hilden) as recommended by the supplier.

For microarray hybridization, both cDNA probes were combined, vacuum-dried and dissolved in 70 μL DIG Easy-Hyb hybridization solution (Roche, Mannheim). The DNA microarray was pre-hybridized in DIG EasyHyb hybridization solution for 45 min at 45 °C. The microarray was washed in water for 1 min and in ethanol for 10 s and finally centrifuged (185 x g, 3 min, RT). The hybridization probe was incubated for 5 min at 65 °C for denaturation. Hybridization was performed in a final volume of 65 μL inside an *in situ* hybridization chamber (TeleChem International, Sunnyvale, USA) which was sealed with a cover slip. After 16 h at 45 °C, the microarray was washed for 5 min in washing buffer 1 at 42 °C, for 2 min in washing buffer 2 at room temperature, for 1 min in 0.2 x SSC at room temperature, and for 10 s in 0.1 x SSC at room temperature. Subsequently, the microarray was dried by centrifugation (185 x g, 3 min, RT). Signal acquisition was performed with a ScanArray 4000 microarray scanner (Perkin-Elmer, Boston, USA) and data analysis by the Ima-Gene 5.0 software (BioDiscovery, Los Angeles, USA) and the EMMA Microarray Data Analysis software (Dondrup *et al*., 2003).

Washing buffer 1: 2 x SSC, 0.2 % SDS.

Washing buffer 2: 0.2 x SSC, 0.2 % SDS.

2.5.6. Analysis of mRNA degradation rates

To analyze the degradation rate of a specific mRNA *in vivo*, 100 µL 10 g/L rifampicin was added to 100 mL of a *C. glutamicum* culture (OD_{600} = 4-5) in order to stop transcription. Samples of 0.5 mL were taken before and 2, 4, 6, and 8 min after the addition of rifampicin. These samples were used to prepare total RNA as described in section 2.5.1.. The total RNA samples were used for RNA slot blot hybridization analysis as described in section 2.5.3. using an antisense probe for the investigated mRNA, which was prepared as described in section 2.5.2.. The intensities of hybridization signals were determined using the software AIDA 2.0 (Raytest, Straubenhardt). From these values, the degradation rate of the investigated mRNA was determined.

2.6. Working with proteins

2.6.1. Analysis of protein concentrations

The concentration of protein was measured as described by Bradford (1976). For this purpose, the Roti®-Nanoquant reagent (Carl Roth GmbH, Karlsruhe) was used as recommended by the supplier. Solutions of bovine serum albumine (NEB, Frankfurt/Main) with distinct concentrations were used for standardization. The concentration was determined by measuring the absorbance at 450 nm and 590 nm. The concentration of protein correlates with the quotient A_{590}/A_{450}.

2.6.2. SDS-PAGE and Coomassie staining

The electrophoretic separation of proteins was performed in 12 % SDS polyacrylamide gels (Schägger *et al*., 1987). A separation gel was composed of:

12 mL	acrylamide : bisacrylamide (30 : 0.8)
10 mL	gel buffer
10.8 g	urea
ad. 30 mL	water
10 µL	TEMED
100 µL	10 % ammonium persulphate

The stocking gel was composed of:

1 mL	acrylamide : bisacrylamide (30 : 0.8)
3.1 mL	gel buffer
8 mL	water
10 μL	TEMED
100 μL	10 % ammonium persulphate

Protein samples were mixed with loading buffer, incubated for 5 min at 65 °C, and loaded onto the gel. Gel electrophoresis was performed in BlueVertical 101 apparatus (Serva Electrophoresis GmbH, Heidelberg) at 30 V for 30 min and subsequently at 100 V for 2 h.
For Coomassie staining, the polyacrylamide gel was first incubated in staining solution at room temperature overnight. On the next day, the gel was incubated in neutralization solution for 2 min and for 45 s in 25 % methanol. Subsequently, the gel was incubated in fixation solution for 8 h. If appropriate, the staining procedure was repeated several times to increase the staining efficiency and to be able to detect even small amounts of protein.

Gel buffer: 3 M Tris, 1M HCl, 0.3 % SDS.

5 x Loading buffer: 20 % SDS, 60 % glycerol (w/v), 250 mM Tris, 10 % mercaptoethanol (v/v), 0.01 % serva blue G, pH (HCl) = 6.8.

Cathode buffer: 0.1 M Tris, 0.1 M tricine, 0.1 % SDS.

Anode buffer: 0.2 M Tris, pH (HCl) = 8.9.

Staining solution: 98 % solution A, 2 % solution B, stirred overnight.

Solution A: 10 % ammonium sulphate, 2 % phosphoric acid.

Solution B: 5 % Coomassie Brilliant Blue G-250.

Neutralization solution: 0.1 M Tris, pH (H_3PO_4) = 6.5.

Fixation solution: 20 % ammonium sulphate.

2.6.3 Peptide mass fingerprinting

The identification of proteins was carried out by the bioanalytics service unit at the *Center for Molecular Medicine Cologne* (ZMMK). To identify a protein, the regarding band was excised from a Coomassie-stained polyacrylamide gel. The protein was digested by trypsin and subsequently analyzed by MALDI-TOF mass spectrometry. The resulting data were used to identify the investigated protein using the GPMAW 6.0 software (Lighthouse Data, Odense, DK) and a data base of all predicted proteins of *C. glutamicum* (Kalinowski *et al*., 2003).

2.6.4. Analysis of β-galactosidase activity

The analysis of β-galactosidase activity was performed as described by Miller (1972). In this assay, *o*-nitrophenyl β-D-galactoside (OPNG) is converted by β-galactosidase into β-D-galactoside and *o*-nitrophenyl. The concentration of *o*-nitrophenyl can be measured spectroscopically.

Either 10 mL of a *C. glutamicum* culture with an OD_{600} of 4-5 or 10 mL of an overnight culture of *E. coli* were centrifuged (4000 x g, 8 min, RT). The cell pellet was washed with 10 mL 0.1 M K_2HPO_4 (pH = 7.5) and subsequently frozen in liquid nitrogen and stored at -80 °C. The cell pellet was thawed on ice and resuspended in 1 mL reaction buffer. The optical density at 600 nm of this cell suspension was measured. Subsequently, 0.5 mL of the cell suspension was mixed with 1.3 mL reaction buffer and 0.2 mL 1 % CTAB. From the resulting suspension, 100 µL were transferred into a new reaction tube. 800 µL reaction buffer was added and the sample was incubated for 1 min in a water bath at 30 °C. To start the reaction, 200 µL ONPG solution was added and the suspension was incubated for 10 min in a water bath at 30 °C. The reaction was stopped by the addition of 500 µL 1 M sodium carbonate. Cell debris was removed by centrifugation (14000 x g, 1 min, RT) and the absorbance at 420 nm was measured spectroscopically. The specific activity of β-galactosidase was determined using the following equation:

$$activity = \frac{\Delta A \cdot V}{\varepsilon \cdot t \cdot m \cdot d}$$

activity: β-galactosidase activity
ΔA: absorbance at 420 nm
V: total volume
ε: extinction coefficient (4.5 cm^2 μmol^{-1})
t: reaction time
m: cell dry weight
d: layer thickness

Reaction buffer: 5 mM Tris, 5 % glycerol, 10 mM KCl, pH = 7.5.

ONPG solution: 4 mg/mL *o*-nitrophenyl β-D-galactoside, 0.1 M K_2HPO_4, pH = 7.5.

2.6.5. Analysis of GDH activity

To measure GDH activity as described by Meers *et al*. (1970), 15 mL of a *C. glutamicum* culture (OD_{600} = 4-5) was centrifuged (4000 x g, 8 min, RT). The cell pellet was washed with 15 mL ice-cold potassium phosphate buffer (200 mM, pH 7.0). Subsequently, the cell pellet was resuspended in 1.5 mL ice-cold potassium phosphate buffer (200 mM, pH 7.0). The cell suspension was transferred to a tube containing glass beads and cells were disrupted by vigorous shaking at 6.5 m/s for 1 min using a FastPrep FP120 instrument (Q-BIOgene, Heidelberg). Cell debris and glass beads were removed by centrifugation (14000 x g, 30 min, 4 °C). To measure the GDH activity of this cell extract, the following reaction mixture was added to an UV-cuvette:

100 µL 1 M Tris, pH 8.0
100 µL 2.5 mM NADPH
100 µL 200 mM ammonium chloride
10 µL cell extract
590 µL water

The reaction was started by the addition of 100 μL 100 mM 2-oxoglutarate and the initial rate of absorbance decrease at 340 nm was measured using the DU-640 Spectrophotometer (Beckman, München). In addition to that, the concentration of total protein in the cell extract was determined as described in section 2.6.1.. From the resulting data, the specific GDH-activity was calculated using the following equation:

$$activity = \frac{\Delta A \cdot V}{\varepsilon \cdot t \cdot m \cdot d}$$

activity: specific GDH activity
ΔA: decrease of absorbance at 340 nm
V: total volume
ε: extinction coefficient (6.3 cm^2 μmol^{-1})
t: reaction time
m: mass of total protein in the reaction mixture
d: layer thickness

2.6.6. DNA affinity purification with magnetic beads

The approach of DNA affinity purification with magnetic beads was used to isolate transcriptional regulators by their ability to bind specifically to certain DNA sequences. For this purpose, a biotinylated target DNA was coupled to magnetic beads. Subsequently, these beads were suspended in a cell extract of *C. glutamicum* in order to allow the protein of interest to bind.

Preparation of biotinylated target DNA:

The target DNA was amplified by PCR using the standard protocol described in section 2.4.4.. For a reaction mixture with a total volume of 50 μL, 12.5 pmol of the 5'-primer, which was biotin-labelled, and 17.5 pmol of the unlabelled 3'-primer were applied. The PCR was carried out 10 times. Subsequently, the reaction products of the 10 PCRs (each 50 μL) were combined and concentrated using Microcon-30 columns (Millipore, Billerica, USA). For this purpose, the PCR products were loaded onto a column and centrifuged (12000 x g, 12 min, RT). The DNA was washed three

times by the addition of 500 µL 1 x DNA binding buffer followed by centrifugation (12000 x g, 12 min, RT). After that, the DNA was eluted by inversion of the column and centrifugation (1000 x g, 4 min, RT). The resulting biotinylated target DNA was stored at -20 °C.

Preparation of DNA-coated magnetic beads:

4 mg of Dynabeads®M-280 Streptavidin (Dynal, Oslo, Norway) were washed twice in 500 µL PBS pH 7.4 + 0.1 % BSA and twice in 500 µL 2 x DNA binding buffer. Finally, the magnetic beads were resuspended in 200 µL 1 x DNA binding buffer. The purified biotinylated target DNA obtained by PCR as described above was added and the suspension was incubated for 30 min at room temperature under shacking in order to allow the biotinylated DNA to bind to the streptavidine-coated magnetic beads. The binding efficiency was checked by analyzing the amount of DNA present in the supernatant before and after the incubation period using gel electrophoresis (section 2.4.3.). Then, the magnetic beads were washed three times with 500 µL 1 x DNA binding buffer. The DNA-coupled magnetic beads were stored at 4 °C in TE buffer containing 0.02 % NaN_3.

Preparation of the total protein extracts:

The *C. glutamicum* wild type strain ATCC 13032 was used to inoculate 25 mL BHI medium. After cultivation at 30 °C for 8 h, the culture was used to inoculate 100 mL CgC medium for overnight growth. This culture, with an overnight OD_{600} of approximately 30-33, was used to inoculate 1000 mL of fresh CgC medium to an OD_{600} of approximately 1 and cells were grown until the exponential phase was reached (OD_{600} approximately 4-5). This culture was used to prepare a total protein extract of cells cultivated under nitrogen surplus, To prepare a total protein extract of cells cultivated under nitrogen starvation, the cells were first harvested by centrifugation (4000 x g, 10 min, 30 °C), transferred to 1000 mL CgCoN medium, and cultivated for 30 min at 30 °C. To isolate total protein, the cells were harvested by centrifugation (4000 rpm, 10 min, 4 °C). The cell pellet was resuspended in 4 mL ice-cold lysis buffer. This cell suspension was transferred to tubes containing glass beads and cells were disrupted by vigorous shaking at 6.5 m/s for 1 min using a FastPrep FP120 instrument (Q-BIOgene, Heidelberg). Cell debris and glass beads

were removed by centrifugation (14000 x g, 4 min, 4 °C). The protein extract was further purified by ultracentrifugation (267000 x g, 30 min, 4 °C). 1 mL-aliquots of the supernatant were transferred to reaction tubes and stored at -80°C.

Isolation of transcriptional regulators:

The DNA coated magnetic beads were washed three times in 500 µL 1 x DNA binding buffer and equilibrated in 1 mL ice-cold protein binding buffer. Subsequently, the beads were resuspended in 1 mL of ice-cold total protein extract and incubated for 45 min at 4 °C under shacking. The beads were separated from the protein extract at 4 °C and washed with 500 µL ice-cold protein binding buffer. Then, the beads were suspended again another 1 mL-aliquot of ice-cold total protein extract and incubated and washed again. This procedure was repeated three times in total. Finally, the magnetic beads were washed three times in 500 µL ice-cold protein binding buffer. Subsequently, the proteins that were bound to the DNA were eluted in several steps. For this purpose, the beads were resuspended in 20 µL-portions of elution buffer while rising sodium chloride concentrations from 200 mM to 1000 mM in 100 mM-steps. The elutions fractions were analyzed by SDS-PAGE and Coomassie staining as described in section 2.6.2. and proteins were identified by peptide mass fingerprinting (section 2.6.3.).

2 x DNA binding buffer: 2 M NaCl, 1mM EDTA, 10 mM Tris, pH (HCl) = 7.5.

PBS: 8 g NaCl, 0.2 g KCl, 2.68 g Na_2HPO_4 x 7 H_2O, 0.24 g KH_2PO_4, pH (HCl) = 7.4.

TE buffer: 10 mM Tris, 1 mM EDTA, pH = 8.0.

Lysis buffer: 50 mM Tris, 70 mM KCl, 1 mM EDTA, 1 mM DTT, 10 % (v/v) glycerol, 400 µL Complete, pH = 8.0.

Protein binding buffer: 20 mM Tris, 100 mM NaCl, 1 mM EDTA, 1 mM DTT, 10 % (v/v) glycerol, 0.05 % (w/v) triton X-100, 400 µL Complete, pH = 8.0.

Elution buffer: 20 mM Tris, 1 mM EDTA, 1 mM DTT, 10 % (v/v) glycerol, 0.05 % (w/v) triton X-100, 400 µL Complete, pH = 8.0, NaCl in rising concentrations from 200 mM to 1M.

2.6.7. Gel shift assays and competition assays

By gel shift assays, binding of a transcriptional regulator to a distinct DNA fragment can be analyzed. For this purpose, a protein extract of an *E .coli* strain heterologously expressing the investigated transcriptional regulator was prepared. The corresponding strain was cultivated in 2 L LB medium at 37 °C overnight. On the next day, cells were harvested by centrifugation (4000 x g, 10 min, 4 °C). The cell pellet was resuspended in 10 mM Tris (pH = 7.5) (2 mL per g cell pellet weight). The cell suspension was transferred to tubes containing glass beads and cells were disrupted by vigorous shaking at 6.5 m/s for 1 min using a FastPrep FP120 instrument (Q-BIOgene, Heidelberg). Cell debris and glass beads were removed by centrifugation (14000 x g, 20 min, 4 °C). The protein extract was stored at -80°C.
The 200 bp target DNA for the gel shift assay was synthesized by PCR (section 2.4.4.) and purified by gel electrophoresis (section 2.4.3.). For labelling of the DNA and the setup of the reaction mixture for the gel shift assay, the DIG Gel Shift Kit (Roche, Mannheim) was used following the supplier's protocol.. Separation by gel electrophoresis was performed in native 6 % polyacrylamide gels (Anamed Electrophorese GmbH, Darmstadt) using 0.5 x TBE buffer as running buffer. Subsequently, the labelled DNA was blotted on a nylone membrane (BioBond™ Nylon Membrane, Sigma, Taufkirchen) by elctro-blotting as described in the protocol of the the DIG Gel Shift Kit (Roche, Mannheim). Detection of the labelled DNA was performed as described in section 2.5.3..
Competition assays were performed in accordance to the protocol of gel shift assays but additionally either unlabelled oligonucleotides (in 1500-fold excess over the labelled DNA) or certain substances were added in order to analyze their ability to inhibit a shift of the labelled target DNA.

10 x TBE buffer: 890 mM Tris, 890 mM boric acid, 20 mM EDTA, pH = 8.0.

2.6.8. Purification of GDH protein by Ni-NTA chromatography, dialysis, and electro-elution, and the production of antibodies for GDH

The *E. coli* strain M15 pREP4 was transformed with the expression vector pQE30Xagdh. The resulting strain produces his-tagged GDH of *C. glutamicum*. This strain was used to isolate his-tagged GDH of *C. glutamicum* by Ni-NTA chromatography using the Ni-NTA Spin kit (Qiagen, Hilden). Cultivation of the *E. coli* strain and purification of the protein was performed as recommended by the supplier. However, instead of the standard buffer B containing 8 M urea, the alternative buffer A containing 6 M guanidine hydrochloride was used for cell lysis in order to disrupt inclusion bodies of his-tagged GDH. After the isolation of his-tagged GDH, guanidine hydrochloride was removed by dialysis against water at 4°C for 2 days (cut off: 16 kDa). The isolated protein was then further purified by SDS-PAGE and Coomassie staining as described in section 2.6.2.. Protein bands of his-tagged GDH were excised and the protein was isolated by electro-elution using the Electro Eluter 422 (Biorad, München). To verify that the isolated protein was GDH of *C. glutamicum*, peptide mass fingerprinting analysis was carried out as described in section 2.6.3.. Purified his-tagged GDH was used for antibody production, which was carried out by Eurogentec (Seraing, Belgium) in rabbit.

2.6.9. Western blotting

For the preparation of a *C. glutamicum* cell extract for Western blotting, a 1 mL-aliquot of a *C. glutamicum* culture (OD_{600} = 4-5) was transferred to a tube containing glass beads and immediately frozen in liquid nitrogen. The sample was thawed on ice and cells were disrupted by vigorous shacking using a FastPrep FP120 instrument (Q-BIOgene, Heidelberg) at 4 °C. Subsequently, glass beads and cell debris were removed by centrifugation. SDS-PAGE was carried out as described in section 2.6.2.. After electrophoresis, the gel-separated proteins were transferred onto a polyvinylidene difluoride membrane by electroblotting (PVDF, Carl Roth GmbH, Karlsruhe) and incubated with GDH-specific anti-sera generated in rabbits as described in section 2.6.8.. Antibody binding was visualized by using appropriate antiantibodies coupled to alkaline phosphatase or peroxidase (Sigma-Aldrich, Deisenhofen) and the BCIP/NBT alkaline phosphatase substrate (Sigma-Aldrich, Deisenhofen).

2.7. Chromatography

2.7.1. Determination of internal 2-oxoglutarate and glutamate by gas chromatography

10 mL of a *C. glutamicum* culture (OD_{600} approximately 4-5) was harvested by centrifugation. The cell pellet was washed with pre-warmed fresh culture medium and then resuspended in 1 mL methanol. For internal standardisation, 100 µL of an aqueous solution of 1 mM 2-oxoadipic acid was added. After an incubation of 20 minutes at 70 °C, cell debris was removed by centrifugation. The supernatant was dried under continuous nitrogen flow at 60 °C. The residue was dissolved in 50 µL of a solution of 20 g/L methoxylamine in pyridine and incubated for 90 minutes at 30 °C. 80 µL MSTFA were added followed by an incubation of 60 minutes at 65 °C. The resulting solution was analyzed by gas chromatography using the TraceGC system (Thermo Finnigan, Woburn, USA) and the FS-Supreme 5 column (CS-Chromatographie, Langerwehe). For this purpose, 0.3 µL were injected (split ration 1:25) and separation was performed under nitrogen gas flow (flowrate: 1 mL/min) using the following time program: 2 min at 60 °C, temperature gradient of 30 °C/min up to 140 °C, temperature gradient of 2 °C/min up to 175 °C, temperature gradient of 30 °C/min up to 320 °C, 5 min at 320 °C. At the end of the run, initial conditions were restored. Column effluents were monitored by flame ionization detection (FID) at 300 °C. Standard solution of 2-oxoglutarate were treated in the same way starting with the addition of 1 mL methanol.

2.7.2. Determination of internal ammonium by HPLC

2 mL of a *C. glutamicum* culture (OD_{600} approximately 4-5) was harvested by centrifugation. The supernatant (culture medium) was saved for further analysis. The cell pellet was weighted and then resuspended in 100 µL of an aqueous solution of 0.1 % CTAB. After incubation of 10 minutes at room temperature, cell debris was removed by centrifugation. The ammonium concentrations of this supernatant (cell pellet extract) as well as of the supernatant obtained in the first centrifugation step (culture medium) were determined by reversed-phase HPLC using a protocol based on the method described by Lindroth & Mopper (1979). Ammonium was labelled by pre-column derivatisation using *ortho*-phthaldialdehyde

(OPA). For separation, the Agilent 1100 system (Agilent, Waldbronn) with a LiChrosher RP 18 (150 x 3 mm, 5 mm) column (Merck, Darmstadt) and 60 % methanol as mobile phase with a low rate of 0.8 mL/min at 40 °C were used. Column effluents were monitored with a G1321A Fluorimenter (Agilent, Waldbronn) at an excitation wavelength of 330 nm and a detection wavelength of 455 nm.

From the ammonium concentrations of the cell pellet extract and the culture medium, the intracellular concentration of ammonium was calculated based on the observation that 62.0 % (± 1.0 %) of a cell pellet consists of surrounding culture medium. This percentage was determined by a scintillation assay using ^{3}H-labelled water and ^{14}C-labelled taurine as described by Rönsch (2000).

2.7.3. Determination of internal glutamine, glutamate, and arginine by HPLC

1 mL of a *C. glutamicum* culture (OD_{600} approximately 4-5) was filtrated in order to separate the cells form the culture medium. If standard culture medium was used, the cells were washed with 1 mL pre-warmed fresh culture medium. If the culture medium was supplemented with glutamine, cells were washed three times with 1 mL pre-warmed fresh culture medium without glutamine. The cells were resuspended in 1 mL of an aqueous solution of 0.1 % CTAB. After incubation of 10 minutes at room temperature, cell debris was removed by centrifugation. The supernatant was analyzed by reversed-phase HPLC after pre-column derivatisation using ortho-phthaldialdehyde (OPA). For separation, the Agilent 1100 system (Agilent, Waldbronn) with a 125/4 Nucleodur 100-5 C18 ec column (Macherey-Nagel, Düren) was used. The following buffer system was applied: A: 40 mM sodium acetate buffer (pH 6.5) : methanol : acetonitrile (95 : 2.5 : 2.5); B: methanol : acteobitrile (50:50). Column effluents were monitored with a G1321A Fluorimenter (Agilent, Waldbronn) at an excitation wavelength of 330 nm and a detection wavelength of 455 nm.

2.8. Bioinformatic approaches

2.8.1. Identification of open reading frames

To investigate if *gdh* transcription is controlled by translation-dependent attenuation, the sequence between the start of transcription and the initiation codon of the *gdh* gene was screened for open reading frames coding for polypeptides of at least five amino acids. This search was performed using the Clone Manager 5.2 software.

2.8.2. Identification of putative binding sites

Putative binding sites of FarR were identified within the genome of *C. glutamicum* by their homology to a known binding motif of FarR from *C. glutamicum*. For this purpose, the FUZZNUC program (http://bioweb.pasteur.fr/seqanal/interfaces/fuzznuc.html) was used. FUZZNUC allows nucleic acid pattern searches with various ambiguities. The sequence GGTTATATAACC, which is the predicted FarR binding motif upstream of *gdh*, was applied as pattern, whereby, up to three mismatches were allowed. From the resulting putative binding sites, those were selected that were located in non-coding regions of the genome, upstream of genes, and within putative promoter regions, i.e. not more than 600 bp upstream of the start codons of genes. This selection was performed using Microsoft Excel 2000 and a database of all predicted open reading frames of the genome of *C. glutamicum* (accession number: NC003450).

2.8.3. Sequence alignments and presentation of consensus sequences

The sequences of the FarR-binding sites upstream of *gdh* and *dtsR2*, respectively, were used for a sequence alignment to deduce a consensus binding motif of FarR. For this purpose, the CLUSTALW algorithm was used (http://www.expasy.org). The resulting consensus binding motif of FarR was depicted using the program Sequence Logos (http://weblogo.berkeley.edu).

3. Results

3.1. Regulation of glutamate dehydrogenase

3.1.1. Characterization of the nitrogen-dependent regulation of glutamate dehydrogenase

The regulation of glutamate dehydrogenase in response to nitrogen supply has been described controversially in the past. On the one hand, GDH activity and *gdh* transcription were found to by unaffected by changes in nitrogen supply (Tesch *et al*., 1999; Beckers, 2004; Silberbach, 2004). On the other hand, a significant increase of GDH activity and *gdh* transcription under nitrogen limitation was observed (L. Nolden, personal communication). To reinvestigate nitrogen-dependent regulation of glutamate dehydrogenase, the *C. glutamicum* wild type strain ATCC13032 was cultivated under nitrogen surplus. Then, the cells were exposed to nitrogen starvation. After that, an excess of ammonium was added to the culture of nitrogen-starved cells. Regulation of glutamate dehydrogenase was analyzed by RNA dot blotting, Western blotting, and enzymatic activity measurements. The level of *gdh* mRNA, GDH protein, and GDH activity are

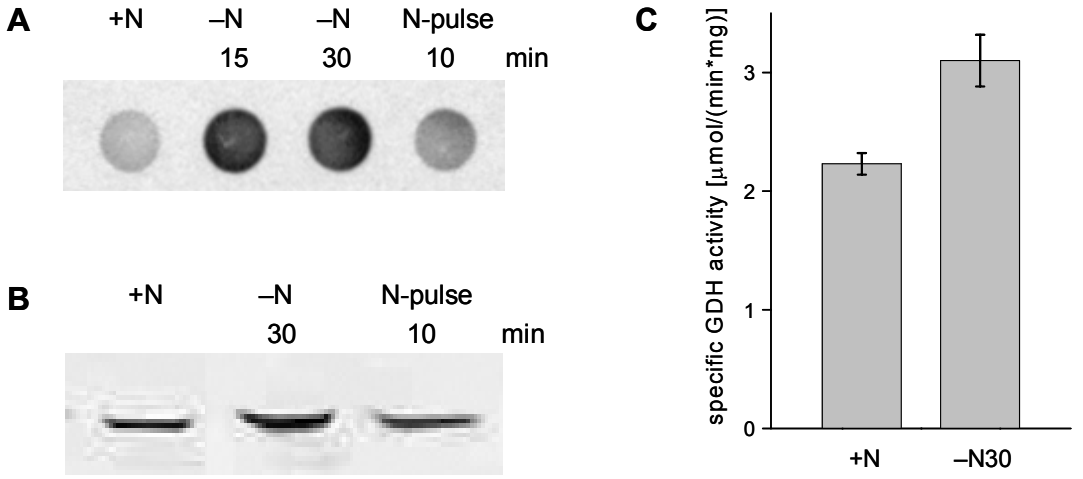

Figure 5: The nitrogen-dependent regulation of glutamate dehydrogenase. The expression of *gdh* is induced if *C. glutamicum*, which has been cultivated under nitrogen surplus (+N), is exposed to nitrogen starvation (-N) for 15 and 30 minutes, respectively. The initial level is reached again 10 minutes after an excess of ammonium is added to the nitrogen starved cells (N-pulse). The induction of *gdh* expression is detectable by RNA dot blotting using *gdh* as probe (A), by Western blotting using antibodies for GDH (B), and at the level of enzymatic activity of GDH (C).

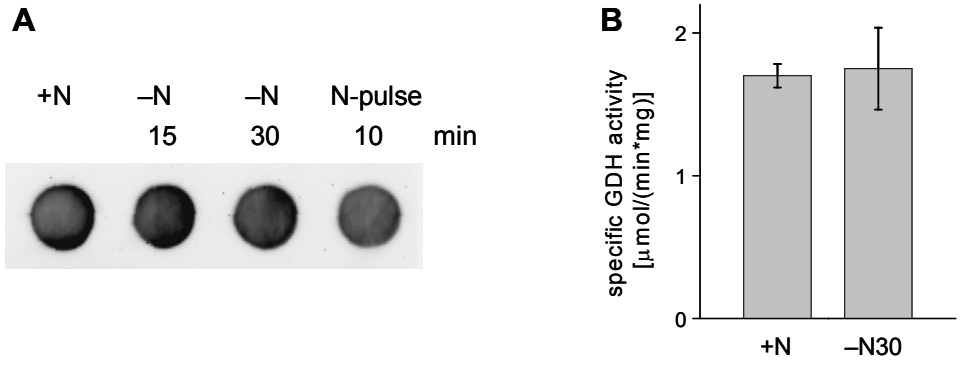

Figure 6: The nitrogen-dependent regulation of GDH activity depends on transcriptional regulation of *gdh*. In the *C. glutamicum* strain LNΔGDH pZgdh, expression of *gdh* is under the control of the *tac* promoter. This strain was cultivated under nitrogen surplus (+N) and then exposed to nitrogen starvation (-N) for 15 and 30 minutes, respectively. After that, an excess of ammonium was added to the nitrogen starved cells (N-pulse). Transcription of *gdh* was analyzed by RNA dot blotting using *gdh* as probe (A). In addition, GDH activity was measured (B). Both, transcription of *gdh* and GDH activity, are not regulated in response to nitrogen supply in the *C. glutamicum* strain LNΔGDH pZgdh.

significantly increased under nitrogen limitation (figure 5). Thus, glutamate dehydrogenase is nitrogen-regulated under the tested conditions.

At this point, it was not clear if the nitrogen-dependent regulation of glutamate dehydrogenase occurs only on the level of expression or if GDH is additionally regulated by posttranslational processes. This was investigated based on the fact, that a putative posttranslational regulation should still be observable even if *gdh* is transcribed constantly. For this purpose, the *gdh* gene was cloned into the vector pZ8-1. In the resulting plasmid pZgdh, expression of *gdh* is under the control of the *tac* promoter and is consequently not nitrogen-regulated. The strain LNΔGDH, which lacks endogenous *gdh*, was transformed with pZgdh. In the resulting strain, *gdh* is transcribed constantly irrespective the nitrogen conditions as expected (figure 6). As the enzymatic activity of glutamate dehydrogenase is also unaffected by the nitrogen supply (figure 6), an additional regulation of GDH activity by posttranslational processes in response to nitrogen limitation can be excluded. Hence, the induction of glutamate dehydrogenase under nitrogen limitation occurs most likely exclusively on the level of expression.

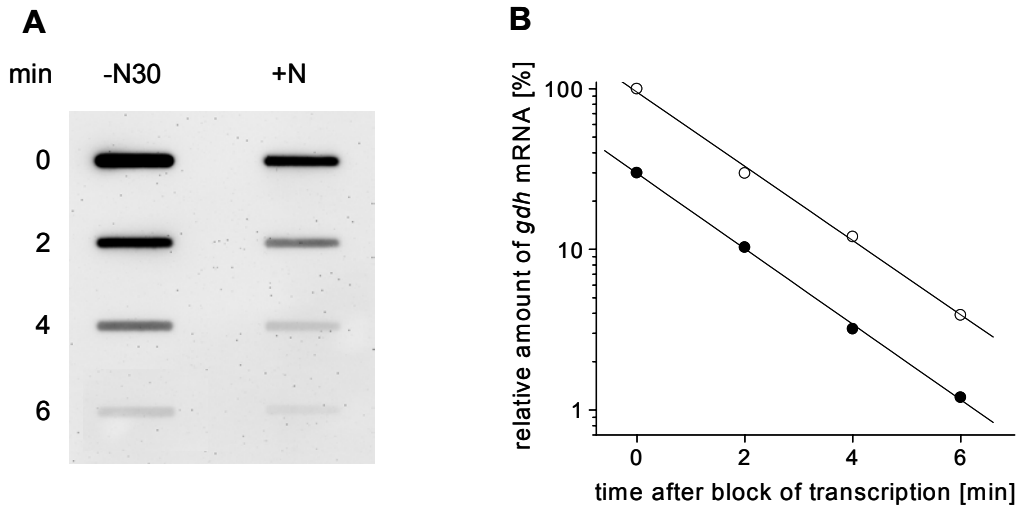

Figure 7: Degradation of *gdh* mRNA under nitrogen surplus and nitrogen limitation. A: *C. glutamicum* RES167 was cultivated under nitrogen surplus (+N) and for 30 minutes under nitrogen starvation (-N30). Transcription was blocked by the addition of rifampicin to the culture medium. Samples were taken before the addition of rifampicin (0 minutes) and 2, 4, and 6 minutes after the addition. The samples were used for an RNA slot blot hybridization experiment using *gdh* as probe. B: The intensities of the bands of the RNA slot blot were determined and converted into relative amounts of *gdh* transcript, whereby the highest value was set to 100 %. Higher amounts of *gdh* transcript are present after 30 minutes of nitrogen starvation (open circles) than under nitrogen surplus (black circles). The degradation rate of *gdh* is not affected by nitrogen supply.

Expression is generally regulated by varying the amounts of the respective mRNA present in the cell. In principle, this can be achieved in two different ways: firstly, by regulation of the transcription rate or, secondly, by a regulation of mRNA degradation whereas transcription itself remains constant. To investigate, which mechanism is responsible for the regulation of *gdh* expression, degradation rates of *gdh* mRNA were analyzed. *C. glutamicum* RES167 was cultivated under nitrogen surplus and under nitrogen limitation, respectively. Transcription was stopped by the addition of rifampicin to the culture medium. After that, the degradation of *gdh* mRNA was analyzed during a period of 6 minutes using RNA slot blot hybridization (figure 7). Higher amounts of *gdh* mRNA are present under nitrogen limitation as described before, but the degradation of *gdh* mRNA is not affected by the nitrogen conditions. The half-life of *gdh* mRNA is 1.29 minutes under nitrogen surplus and 1.30 minutes under nitrogen starvation. Thus, *gdh* expression is regulated only on the level of transcription under the investigated conditions, but not by a regulated degradation of *gdh* mRNA.

orf-1: MAQVHTLKSCAHAAEMGTRK
orf-2: MYMVPSMGTTNITKWPRYTL
orf-3: MQPRWERGN
orf-4: MTSRLM
orf-5: MPAVS
orf-6: MNAVFKSFRIRFFTGILLQQTPRMYMVPSMGTTNITKWPRYTL
orf-7: MRACSRDGNEEI

Figure 8: Predicted open reading frames of the leader mRNA of *gdh*. The sequence between the start of transcription and the start of translation of the *gdh* gene was screened for open reading frames coding for peptides of at least five amino acids. The corresponding peptide sequences are given. None of them contains an accumulation of a certain amino acid. Thus, translation-dependent attenuation seems not to be involved in transcription control of *gdh*.

Different mechanisms of transcription control are known. One is translation-dependent attenuation. Attenuation describes the control of transcription by regulated termination of mRNA synthesis. The decision between termination and readthrough is triggered by the translation of a small leader peptide from the growing mRNA chain. This leader peptide is located upstream of the structural gene and contains a cluster of certain amino acids. If this amino acid and therefore the respective charged tRNA are present in sufficient concentrations in the cell, translation of the leader peptide is fast, which triggers termination of transcription. In contrast, a lack of the respective tRNA decelerates translation of the leader peptide and transcription continues into the structural gene (Wagner, 2000). To investigate if *gdh* transcription is controlled by translation-dependent attenuation, the sequence between the start of transcription and the initiation codon of the *gdh* gene was screened for open reading frames coding for polypeptides of at least five amino acids. Seven open reading frames could be identified, but none of them contains a significant accumulation of a certain amino acid (figure 8). As such an accumulation is essential for translation-dependent attenuation, *gdh* transcription is most likely not regulated by this mechanism.

3.1.2. Identification of transcriptional regulators of glutamate dehydrogenase

Transcription of *gdh* is regulated in response to nitrogen supply, but the underlying regulatory mechanism is still unknown. To identify putative transcriptional regulators of *gdh*, the following approaches were used. First, it was analyzed, which part of the *gdh* promoter is responsible for nitrogen-dependent control, i.e. harbours a binding site for a putative transcription factor. For this purpose, the 550 bp DNA sequence upstream of *gdh* was investigated in a reporter gene assay. As shown in figure 10A, this sequence harbours the transcription start and all basic elements of the core promoter of *gdh* (Börmann *et al*., 1992). A fusion of this DNA fragment and the *lacZ* gene coding for β-galactosidase was cloned into the plasmid pJC1 and then transformed into the *C. glutamicum* strain RES167. In the resulting strain, expression of *lacZ* is under the control of the 550 bp fragment of the *gdh* promoter from *C. glutamicum* and can be monitored by β-galactosidase activity measurements. The activity of β-galactosidase was determined under nitrogen surplus and nitrogen limitation (figure 9). Expression of *lacZ* was induced under nitrogen limitation. Thus, the investigated 550 bp DNA fragment of the *gdh* promoter is sufficient for a nitrogen-dependent expression and harbours the corresponding regulatory element, e.g. a binding site for a putative transcriptional regulator.

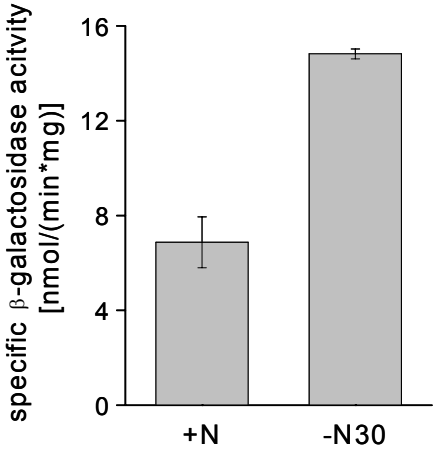

Figure 9: Reporter gene assay of a distinct part of the *gdh* promoter region. The *C. glutamicum* strain RES167 was transformed with the plasmid pJCgdhlacZ, which harbours a fusion of a 550 bp fragment of the *gdh* promoter and the *lacZ* gene coding for β-galactosidase. The resulting strain was cultivated under nitrogen surplus (+N) and for 30 minutes under nitrogen limitation (-N30). The activity of β-galactosidase was determined.

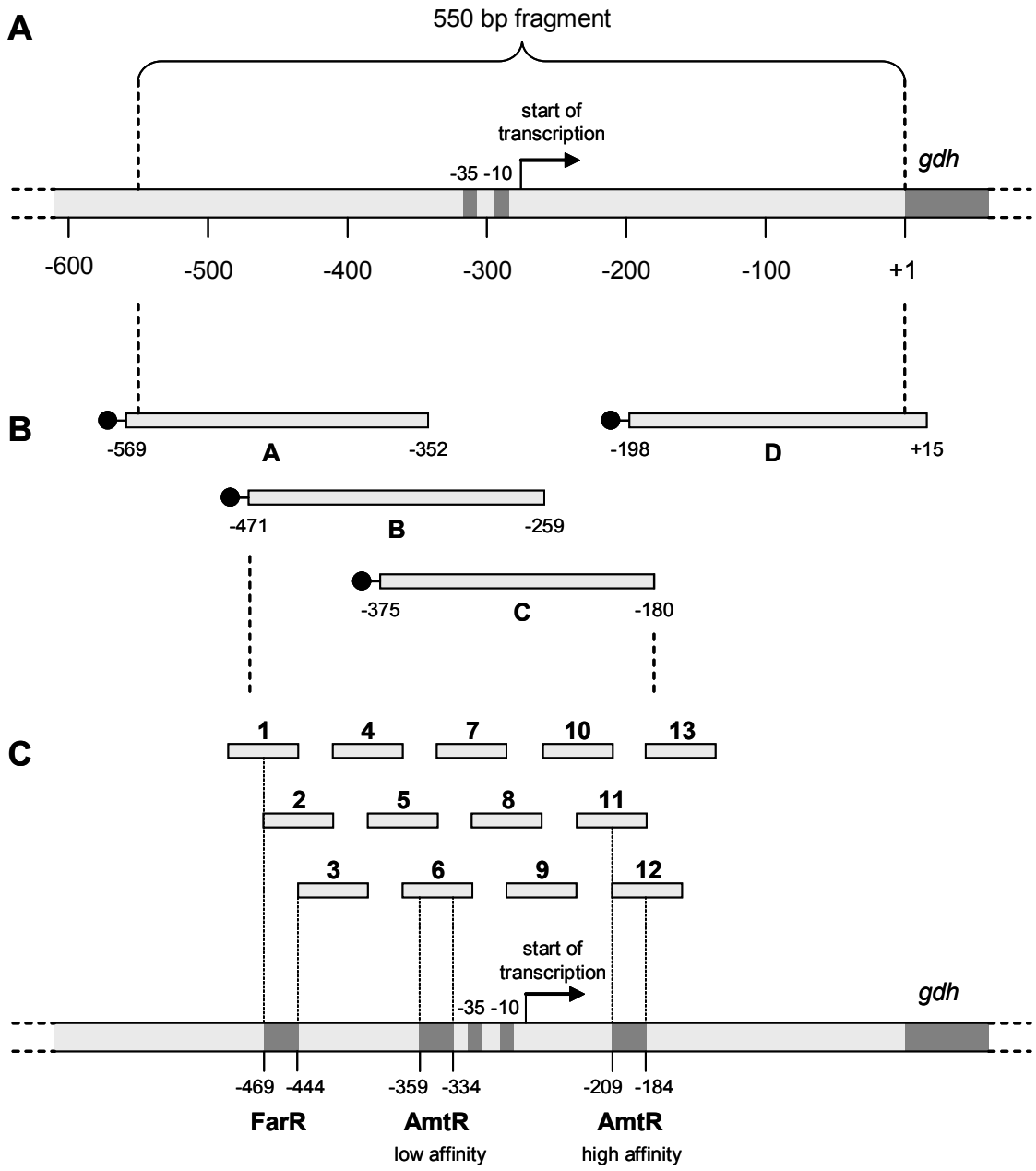

Figure 10: Schematic presentation of the *gdh* promoter region of *C. glutamicum* and the DNA fragments used for DNA affinity purification with magnetic beads and gel shift assays. A: Scheme of the promoter region upstream of the *gdh* gene containing the -10 region and the -35 region as well as the start of transcription (arrow). Numbers indicate the position upstream of the translation start of *gdh*. The given 550 bp DNA fragment was analyzed by reporter gene assays, showing that this region harbours the regulatory element for nitrogen-dependent transcription control of *gdh*. B: The overlapping DNA fragments A, B, C, and D were used for DNA affinity purification with magnetic beads of putative transcriptional regulators of *gdh*. They span the 550 bp DNA fragment as indicated. The DNA fragments were bound to magnetic beads at their 5'-ends (black balls). C: The given 50 bp DNA fragments (1 - 13) were used for competition assays. One FarR binding site and two AmtR binding sites could be identified upstream of *gdh* as indicated.

This knowledge was used to isolate putative transcriptional regulators of *gdh* by DNA affinity purification with magnetic beads. By this approach, transcription factors can be isolated from total protein extracts by their capacity to bind specifically to an immobilized DNA fragment. To isolate putative transcription factors of *gdh*, four different 200 bp DNA fragments were applied as target DNA (figure 10B). These overlapping DNA fragments span the 550 bp fragment of the *gdh* promoter that harbours the putative transcription factor binding site. The DNA fragments were coupled to magnetic beads and thereby immobilized. The beads were then suspended in protein extracts of *C. glutamicum* to allow the proteins of interest to bind specifically to the immobilized DNA. Protein extracts of *C. glutamicum* cultivated under nitrogen surplus and under nitrogen starvation, respectively, were applied. The purification was carried out separately for each combination of the four DNA sequences (A, B, C, D) and the two total protein extracts. After three washing steps, the DNA-bound proteins were eluted by increasing the concentration of

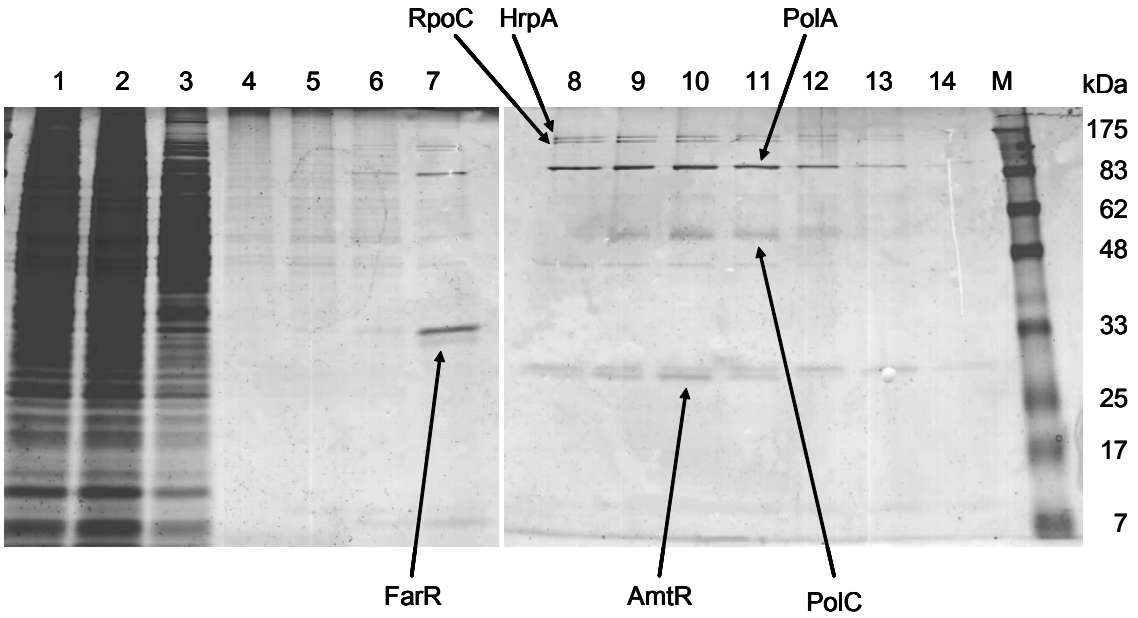

Figure 11: Coomassie-stained gel of the washing and elution fractions of DNA affinity purification with magnetic beads. This figure shows a Coomassie-stained SDS-polyacrylamide gel of the washing and elution fractions of DNA affinity purification with magnetic beads using the DNA fragment C of the *gdh* promoter as target DNA. The DNA-coated beads were suspended in a total protein extract of *C. glutamicum* cultivated under nitrogen surplus (lane 1). After magnetic separation the unbound proteins were removed by several washing steps (lane 2-4). After that, the DNA-bound proteins were eluted by raising the sodium chloride concentration from 100 mM up to 1M (lane 5-14). Proteins were excised and identified by peptide mass fingerprinting as indicated. M: molecular weight marker.

Table 5: Proteins isolated by DNA affinity purification with magnetic beads coupled to DNA fragments of the *gdh* promoter region. The given proteins were isolated by DNA affinity purification with magnetic beads. Only AmtR has been characterized in *C. glutamicum* yet. For the other proteins, the most similar homolog from other organism and the predicted function is given. +: protein could be isolated, -: protein could not be isolated, +N: isolation from a total protein extract of *C. glutamicum* cultivated under nitrogen surplus, -N: isolation from a total protein extract of *C. glutamicum* cultivated under nitrogen starvation, A, B, C, D: isolated using DNA fragment A, B, C, and D from the *gdh* promoter.

ORF-number	name of protein / most similar protein of other organims	proposed or known function in *C. glutamicum*	+N				-N			
			A	B	C	D	A	B	C	D
984	RpoC (*B. subtilis*)	RNA polymerase β chain	+	+	+	+	+	+	+	+
2011	HrpA (*E. coli*)	ATP-dependent helicase	+	+	+	+	+	+	+	+
2682	PolA (*Bacillus stearothermophilus*)	DNA polymerase I	+	+	+	+	+	+	+	+
2242	PolC (*B. subtilis*)	DNA polymerase III α chain	+	+	+	+	+	+	+	+
1416	AmtR (*C. glutamicum*)	transcriptional regulator	-	-	+	-	-	-	+	-
289	FarR (*E. coli*)	transcriptional regulator	+	+	+	-	-	-	-	-
3471	WhiH (*S. coelicolor*)	transcriptional regulator	+	-	-	-	+	-	-	-
2008	OxyR (*M. leprae*)	transcriptional regulator	-	-	-	-	-	-	+	-

sodium chloride in the elution buffer. The elution fractions were analyzed by SDS-PAGE and Coomassie staining as shown in figure 11. Purified proteins were excised from the gels and identified by peptide mass fingerprinting. The results are given in table 5.

All isolated proteins were DNA-binding proteins. Among these were DNA- and RNA-polymerase subunits and a helicase. These proteins bound unspecifically to all four DNA fragments. Additionally, four transcriptional regulators were isolated. These bound only to distinct fragments of the *gdh* promoter as given in table 5. Thus, binding of these proteins was sequence-specific as one would expect for transcriptional regulators. One of them was AmtR, the global transcriptional regulator of nitrogen control (for details, see section 1.4.). The binding of AmtR to the *gdh* promoter is astonishing, as a deletion of *amtR* does not affect *gdh* transcription monitored by RNA hybridization experiments (L. Nolden, personal communication). The other putative transcription factors have not been

characterized in *C. glutamicum* yet, but by sequence alignments, they were found to by similar to the transcriptional regulators FarR from *E. coli*, WhiH from *Streptomyces coelicolor*, and OxyR from *M. leprae*. None of them has been described as a regulator of *gdh* transcription yet. The function of FarR from *E. coli*, which is HutC/FarR-type regulator of the GntR family, has been described controversially as a fatty acyl responsive regulator of TCA cycle genes (Quail *et al*., 1994) and as a regulator of genes coding for a 2-*O*-α-mannosyl-D-glycerate transport and metabolism system (Sampaio *et al*., 2004). During the magnetic DNA affinity purification described here, FarR from *C. glutamicum* exhibited an interesting binding behaviour. It was isolated only from a total protein extract of *C. glutamicum* cultivated under nitrogen excess, but not from a total protein extract of *C. glutamicum* cultivated under nitrogen limitation (table 5). A putative nitrogen-dependency could also be observed for OxyR, which was isolated only from a total protein extract of *C. glutamicum* cultivated under nitrogen limitation. In other organisms, OxyR regulates transcription in response to oxidative stress (Christman *et al*., 1989; Storz *et al*., 1990). WhiH from *S. coelicolor* is also a member of the GntR-family and regulates genes in the late sporulation phase (Ryding *et al*., 1998). During the DNA affinity purification with magnetic beads, WhiH from *C. glutamicum* bound to the *gdh* promoter irrespective of the nitrogen conditions.

3.1.3. Characterization of the binding behaviour of AmtR, FarR, OxyR, and WHiH to the *gdh* promoter region

To verify the binding behaviour of AmtR, FarR, OxyR, and WhiH from *C. glutamicum* to the *gdh* promoter, gel shift assays were performed. For this purpose, total protein extracts of *E. coli* DH5αmcr transformed with expression vectors for AmtR, FarR, WhiH, and OxyR from *C. glutamicum* and the empty vector, respectively, were used. As target DNA, the digoxigenin-labelled 200 bp fragments A, B, C, and D of the *gdh* promoter region (figure 10B) were applied. The results are given in figure 12. AmtR retarded the DNA fragments B and C, whereas FarR retarded the DNA fragments A and B. WhiH and OxyR, respectively, did not retard any of the DNA fragments under the tested conditions. The results of the gel shift assays are summarized and compared to the results of the DNA affinity purification with magnetic beads in table

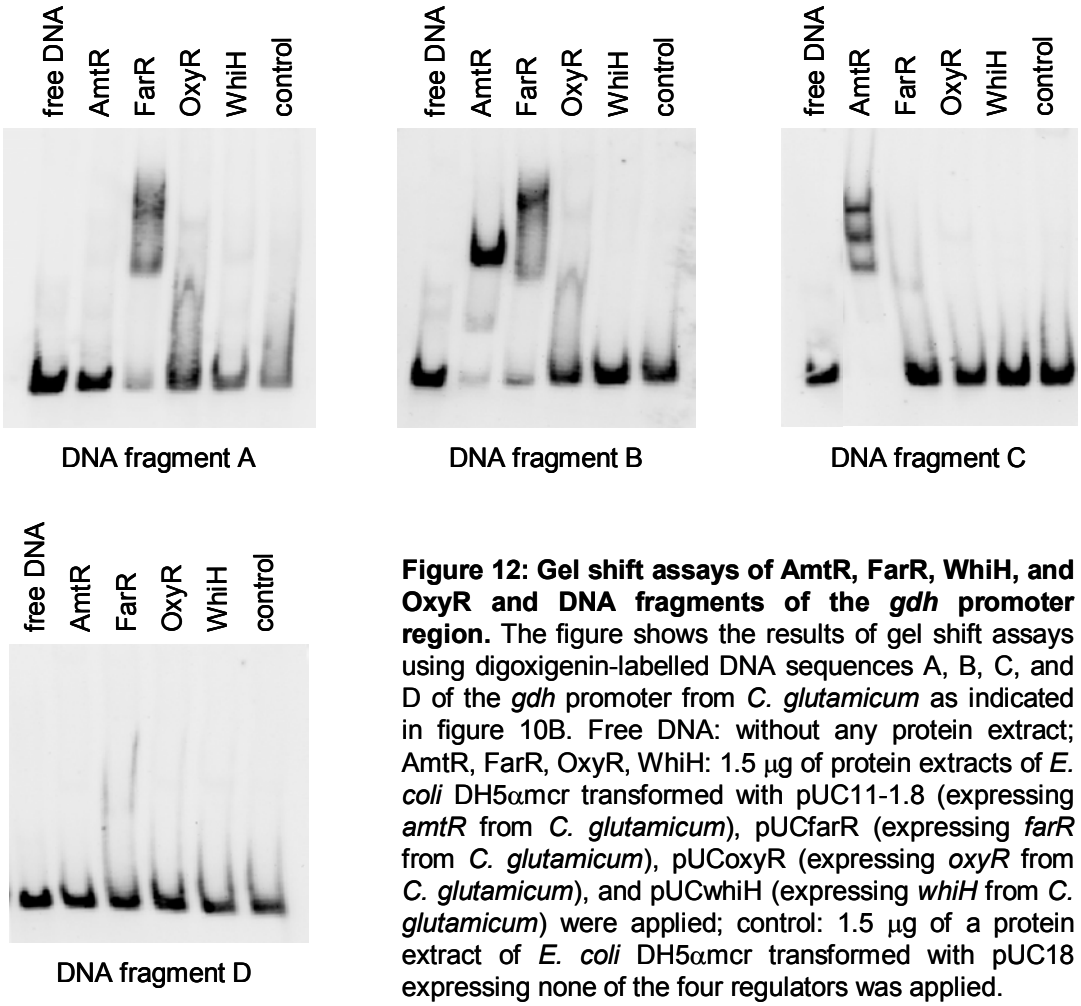

Figure 12: Gel shift assays of AmtR, FarR, WhiH, and OxyR and DNA fragments of the *gdh* promoter region. The figure shows the results of gel shift assays using digoxigenin-labelled DNA sequences A, B, C, and D of the *gdh* promoter from *C. glutamicum* as indicated in figure 10B. Free DNA: without any protein extract; AmtR, FarR, OxyR, WhiH: 1.5 µg of protein extracts of *E. coli* DH5αmcr transformed with pUC11-1.8 (expressing *amtR* from *C. glutamicum*), pUCfarR (expressing *farR* from *C. glutamicum*), pUCoxyR (expressing *oxyR* from *C. glutamicum*), and pUCwhiH (expressing *whiH* from *C. glutamicum*) were applied; control: 1.5 µg of a protein extract of *E. coli* DH5αmcr transformed with pUC18 expressing none of the four regulators was applied.

Table 6: Comparison of the results of the DNA affinity purification with magnetic beads and the gel shift assays. The binding of AmtR, FarR, WhiH, and OxyR from *C. glutamicum* to the DNA fragments A, B, C, and D (figure 10B) observed by gel shift assays and during the magnetic DNA affinity purification, respectively, is indicated. +: binding could be observed; -: binding could not be observed.

	gel shift assays				magnetic DNA affinity purification			
	A	B	C	D	A	B	C	D
AmtR	-	+	+	-	-	-	+	-
FarR	+	+	-	-	+	+	+	-
WhiH	-	-	-	-	+	-	-	-
OxyR	-	-	-	-	-	-	+	-

6. In principle, the capacity of AmtR and FarR to bind specifically to the *gdh* promoter region as demonstrated by magnetic DNA affinity purification could be verified by gel shift assays. However, an additional affinity of AmtR to the DNA fragment B was revealed by gel shift assays, whereas binding of FarR to DNA fragment C could not be stated.

As observable in figure 12, addition of AmtR and FarR, respectively, resulted in multiple shifts of the tested DNA fragments, indicating that the DNA fragments bound more than one AmtR or FarR molecule. This observation was further investigated by gel shift assays applying increasing amounts of the protein extracts. A protein extract containing AmtR retarded the DNA fragment C up to four times depending on the amount of protein extract added (figure 13A), whereas DNA fragment B was shifted only twice (figure 13B). Thus, at least four AmtR units (i.e. four AmtR monomers or four AmtR oligomers) bound to the DNA fragment C, from which two AmtR units bound in the overlapping region of DNA fragment B and C. FarR retarded the DNA fragments A as well as B twice (figure 13CD). Thus, at least two FarR units (i.e. two FarR monomers or two FarR oligomers) bound to the overlapping region of sequence A and B.

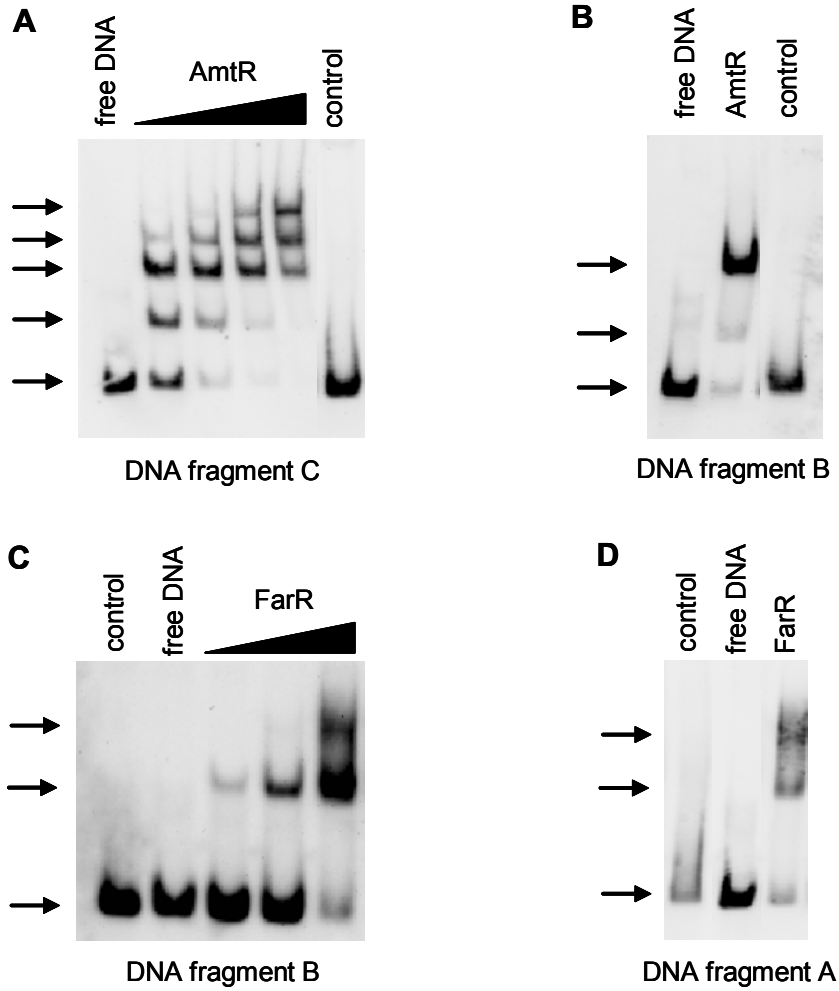

Figure 13: Mutiple shifts of DNA fragments of the *gdh* promoter region by AmtR or FarR. A: Gel shift assay of DNA fragment C and rising amounts (0.15 µg, 0.3 µg, 0,7 µg, 1.5 µg) of a protein extract of *E. coli* DH5αmcr transformed with pUC11-1.8, which expresses *amtR* from *C. glutamicum*. B: Gel shift assay of DNA fragment B and 1.5 µg of a protein extract of *E. coli* DH5αmcr transformed with pUC11-1.8, which expresses *amtR* from *C. glutamicum*. C: Gel shift assay of DNA fragment B and rising amounts (0.06 µg, 0.3 µg, 1.5 µg) of a protein extract of *E. coli* DH5αmcr transformed with pUCfarR, which expresses *farR* from *C. glutamicum*. D: Gel shift assay of DNA fragment A and 1.5 µg of a protein extract of *E. coli* DH5αmcr transformed with pUCfarR, which expresses *farR* from *C. glutamicum*. Free DNA: without any protein extract; control: 1.5 µg of a protein extract of *E. coli* DH5αmcr transformed with pUC18 expressing none of the four regulators was applied. Arrows indicate the presence of a band.

A

protein [μg]	0	0.15	0.3	0.75	1.5
DNA-AmtR$_4$ [fmol]	N/D	N/D	0.04	0.25	0.61
DNA-AmtR$_3$ [fmol]	N/D	0.08	0.28	0.49	0.53
DNA-AmtR$_2$ [fmol]	N/D	0.57	0.78	0.67	0.40
DNA-AmtR [fmol]	N/D	0.41	0.31	0.10	N/D
DNA [fmol]	1.55	0.49	0.13	0.04	N/D

B

$$K_4 = \frac{\text{DNA AmtR}_4}{\text{DNA AmtR}_3 \text{ x protein}}$$

$$K_3 = \frac{\text{DNA AmtR}_3}{\text{DNA AmtR}_2 \text{ x protein}}$$

$$K_2 = \frac{\text{DNA AmtR}_2}{\text{DNA AmtR x protein}}$$

$$K_1 = \frac{\text{DNA AmtR}}{\text{DNA x protein}}$$

C

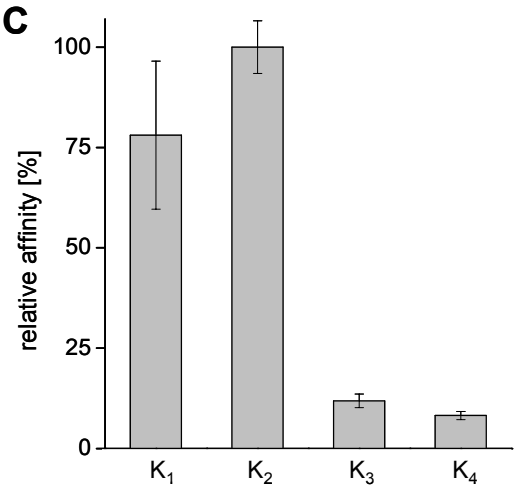

Figure 14: Relative affinities of AmtR to the *gdh* promoter region. A: The intensities of the bands of the gelshift assay of the digoxigenin-labelled DNA fragment C and rising amounts of a protein extract containing AmtR (figure 9A) were used to determine the amounts of DNA fragment C bound by one (DNA-AmtR), two (DNA-AmtR$_2$), three (DNA-AmtR$_3$), or four (DNA-AmtR$_4$) AmtR unit and the amount of free DNA (DNA) in dependence on the applied amount of protein extract (protein). N/D: not detectable. B: Equations used to estimate the binding affinities of the first (K_1), the second (K_2), the third (K_3), and the fourth (K_4) AmtR unit bound to the DNA fragment C. C: Relative affinities of the first (K_1), the second (K_2), the third (K_3), and the fourth (K_4) AmtR unit bound to the DNA fragment C, whereby the highest affinity was set to 100 %.

From the multiple shifts of DNA fragment C by AmtR (figure 13A), further predictions about the binding affinities of the four AmtR units units (i.e. four AmtR monomers or four AmtR oligomers) could be derived. The intensities of the bands directly correlate with the amount of digoxigenin-labelled DNA present in the bands. Thus, the amount of DNA fragment C bound by one, two, three, or four AmtR units in dependence on the applied amount of protein extract could be determined (figure 14A). From these values, the affinities for the first, the second, the third, and the

fourth AmtR unit could be estimated using the equations given in figure 14B. As shown in figure 14C, the affinities for the first and the second AmtR unit were approximately on the same level and were about eight times higher than the affinities for the third and fourth AmtR unit, which were approximately at the same relatively low level. Thus, the DNA sequence C binds two AmtR units with a relatively high affinity and another two AmtR units with a lower affinity.

To further localize the binding sites of AmtR and FarR within the *gdh* promoter, competition assays with unlabelled 50 bp DNA fragments (figure 10C) were performed. Addition of the 50 bp DNA fragments 11 an 12 in an 1500-fold molar excess partially inhibited retardation of the digoxigenin-labelled DNA fragment C by AmtR (figure 15A). In contrast, the partially overlapping DNA fragments 10 and 13 were not able to inhibit a shift. From that it can be concluded that a binding site of AmtR is located in the 25 bp overlapping region of DNA fragment 11 and 12. Moreover, addition of DNA fragment 6 caused a slight complementation of the shift, indicating a relatively low affinity of AmtR to DNA fragment 6 (figure 15A). To verify this, the digoxigenin-labelled DNA fragment B was used, which harbours only the putative low affinity binding site. A shift of DNA fragment B could be complemented by DNA fragment 6 (figure 15B). Thus, a low affinity binding site for is located within fragment 6. Conclusively, two 25 bp binding sites for AmtR could be identified within the *gdh* promoter region, one binding site with a higher affinity, which is located downstream of the start of transcription, and another one with a lower affinity, which is located upstream of the start of transcription (figure 10C). Both binding sites are able to bind two AmtR units. This observation is in accordance with the estimated affinities of AmtR to sequence C described above. The two binding sites are homologous to the consensus binding motif of AmtR described by G. Beckers (2004) (figure 16A).

A shift of DNA fragment B by FarR was inhibited by an 1500-fold molar excess of DNA fragment 1 and DNA fragment 2 (figure 15C). In contrast, DNA fragment 3 did not complement the shift. Thus, one FarR binding site is present in the overlapping region of DNA fragment 1 and 2, which binds two FarR molecules (figure 10C). This

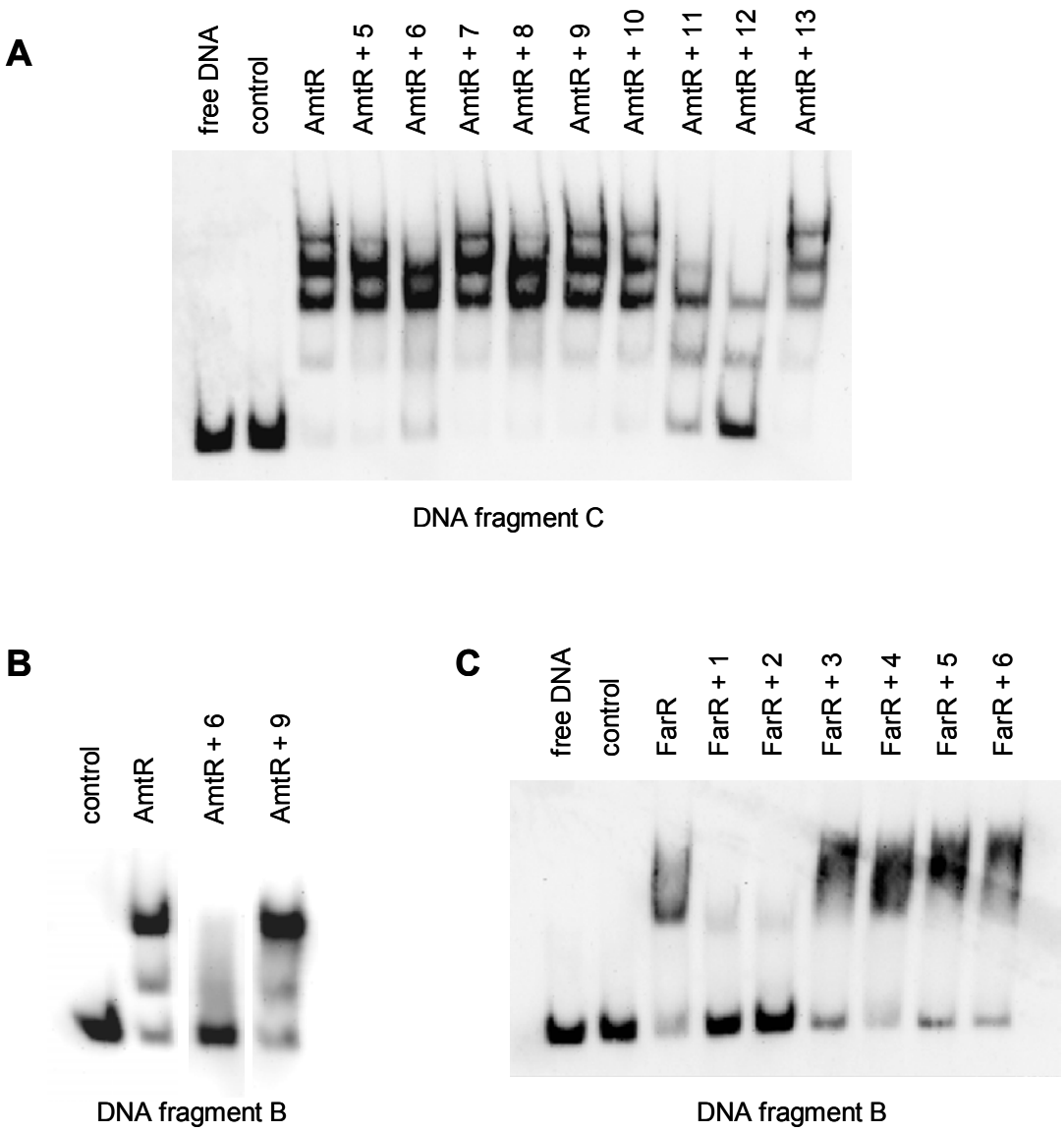

Figure 15: Competition assays to identify the exact binding site of AmtR and FarR within the *gdh* promoter region. Competition assays using the digoxigenin-labelled DNA fragments B and C, respectively, and an 1500-fold molar excess of the unlabelled 50 bp DNA fragments 1, 2, 3, 4, 5, 6, 7, 8, 9, 10, 11, 12, and 13, respectively. For details about the DNA fragments, see figure 10C. AmtR: a protein extract of *E. coli* DH5αmcr transformed with pUC11-1.8, which expresses *amtR* from *C. glutamicum*, was applied; FarR: a protein extract of *E. coli* DH5αmcr transformed with pUCfarR, which expresses *farR* from *C. glutamicum*, was applied; control: a protein extract of *E. coli* DH5αmcr transformed with pUC18, which expresses none of the regulators, was applied. Free DNA: without any protein extract.

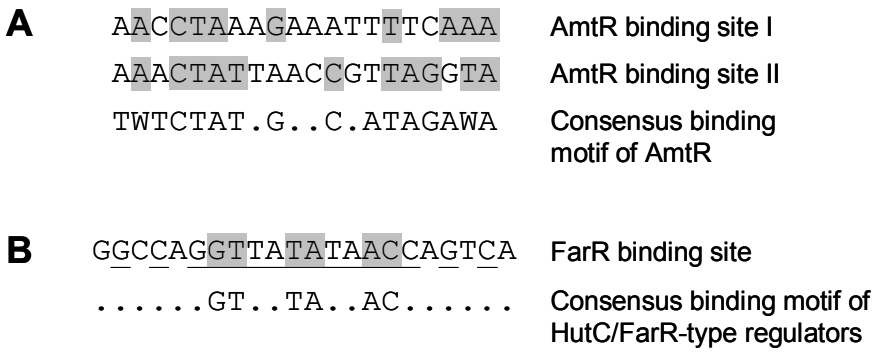

Figure 16: Sequence alignments of the identified binding sites and known binding motifs. A: Sequence alignment of the two AmtR binding sites, which are located upstream of *gdh*, and the consensus binding motif of AmtR described by G. Beckers (2004). AmtR binding site I is located upstream of the start of transcription and AmtR binding site II downstream of the start of transcription. Nucleotides, which are homologous to the consensus binding motif are highlighted in grey. W: A or T; Dot: any nucleotide. B: Sequence alignment of the FarR binding site located upstream of *gdh* and the consensus binding motif of HutC/FarR-like regulators of the GntR family (Rigali *et al*., 2002). Underlined nucleotides indicate the palindrome of the FarR binding site. Nucleotides, which are identical to the consensus binding motif are highlighted in grey. Dot: any nucleotide.

25 bp binding site harbours a highly palindromic sequence, which is homolog to the consensus binding motif of HutC/FarR-type regulators of the GntR family already described for other organisms (figure 16B) (Rigali *et al*., 2002).

To investigate if AmtR, FarR, OxyR, and WhiH may also bind *in vivo* to the *gdh* promoter and thereby affect transcription, β-galactosidase assays were used. For this purpose, the *E. coli* strain DH5αmcr was transformed with two different plasmids. The first plasmid harboured the *gdh* promoter of *C. glutamicum* fused to the reporter gene *lacZ* coding for the β-galactosidase, i.e. expression of *lacZ* was under the control of the *gdh* promoter in this plasmid. The second plasmid was one of the expression vectors for AmtR, FarR, WhiH, and OxyR, respectively, from *C. glutamicum*. In the resulting strains, the regulators were heterologously expressed and their effect on the *gdh* promoter was monitored by β-galactosidase activity measurements. As a control, the plasmid without insert was used instead of the expression vectors. The results are given in figure 17. Expression of AmtR, OxyR,

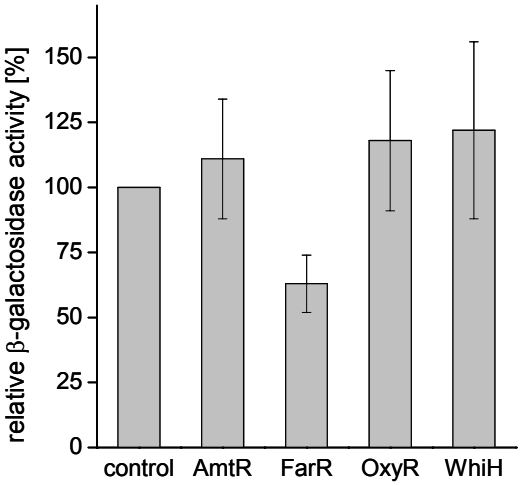

Figure 17: Reporter gene assay of the *gdh* promoter in *E coli* heterologously expressing AmtR, FarR, WhiH, and OxyR. An *E. coli* strain harbouring a plasmid-coded fusion of the *gdh* promoter from *C. glutamicum* and *lacZ* coding for β-galactosidase was transformed with the following expression vectors: pUC18 (control), pUC11-1.8 (AmtR), pUCfarR (FarR), pUCoxyR (OxyR), and pUCwhiH (WhiH). In the resulting strains, the putative transcriptional regulators from *C. glutamicum* AmtR, FarR, OxyR, and WhiH, respectively, were expressed heterologously. In the control strain, none of the regulators was expressed. The relative β-galactosidase activities were determined. The control strain was set to 100 %.

and WhiH, respectively, did not affect β-galactosidase activity. In contrast, expression of FarR caused a significant decrease of the β-galactosidase activity down to 62 % compared to the control strain. Thus, FarR was able to bind *in vivo* to the *gdh* promoter in order to repress transcription of the gene downstream of the *gdh* promoter.

3.1.4. Analysis of the role of AmtR, FarR, WhiH, and OxyR in the nitrogen-dependent regulation of *gdh* transcription

Single deletion strains of the four transcriptional regulators, AmtR, FarR, WhiH, and OxyR, were used to analyze their role in regulation of *gdh* transcription in *C. glutamicum*. The *amtR* deletion strain MJ6-18, which was derived form the *C. glutamicum* wild type strain ATCC 13032, was available (Jakoby *et al*., 2000). For *farR*, *whiH*, and *oxyR*, the single deletion strains TMΔfarR, TMΔwhiH, and TMΔoxyR were constructed by allelic replacement. These were derived from the *C. glutamicum* strain RES167, a defined restriction-deficient mutant of ATCC 13032 that is easier to manipulate. The deletion strains as well as ATCC 13032 and

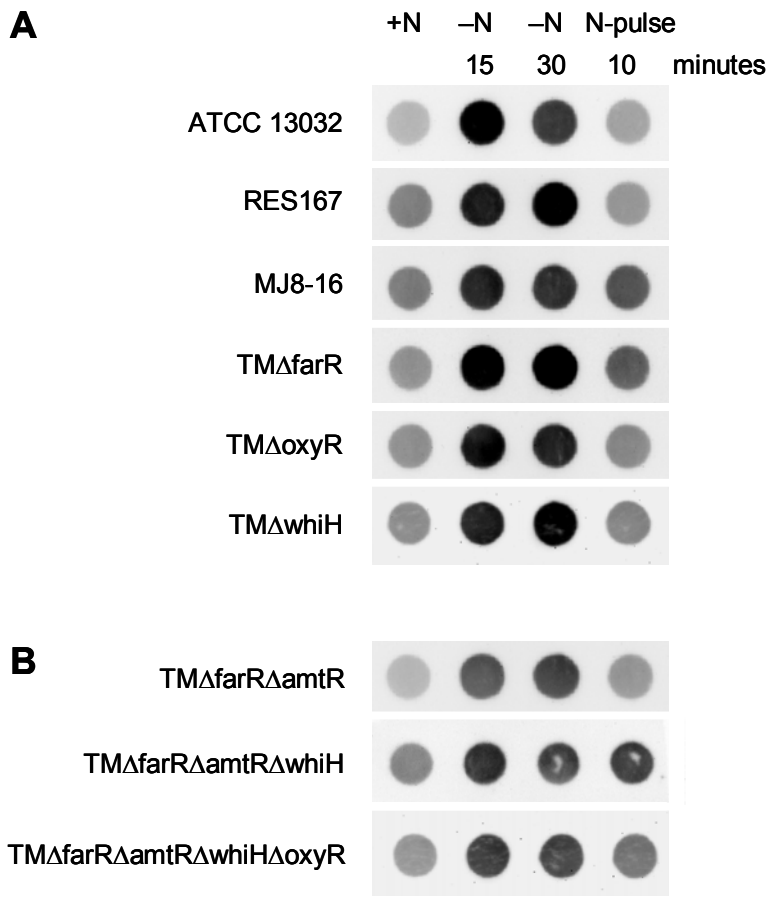

Figure 18: Transcription of *gdh* in single and multiple deletion strains of *amtR*, *farR*, *whiH*, and *oxyR*. *C. glutamicum* strains were cultivated under nitrogen surplus (+N), under nitrogen starvation (-N). Then a nitrogen-pulse was given to the nitrogen-starved cells (N-pulse). Transcription of *gdh* was analyzed by RNA dot blot hybridization after the given periods of time.

RES167 were cultivated under nitrogen surplus. The cells were then exposed to nitrogen limitation for 15 and 30 minutes, respectively. After that, an excess of ammonium was added. Transcription of *gdh* was analyzed by RNA dot blot hybridization. In the wild type strain ATCC 13032 and in RES167, transcription of *gdh* is regulated in dependence on the availability of nitrogen sources as described before (figure 18A). Surprisingly, single deletions of *amtR*, *farR*, *whiH*, and *oxyR*, respectively, did not affect *gdh* transcription at all. Nitrogen-dependent regulation of *gdh* transcription was still observable in the mutant strains. Thus, AmtR, FarR, WhiH, and OxyR, respectively, are not essential for transcription control of *gdh* under the tested conditions.

To verify these results, *gdh* transcription was investigated by quantitative real time RT-PCR. The single deletion strains as well as ATCC 13032 and RES167 were

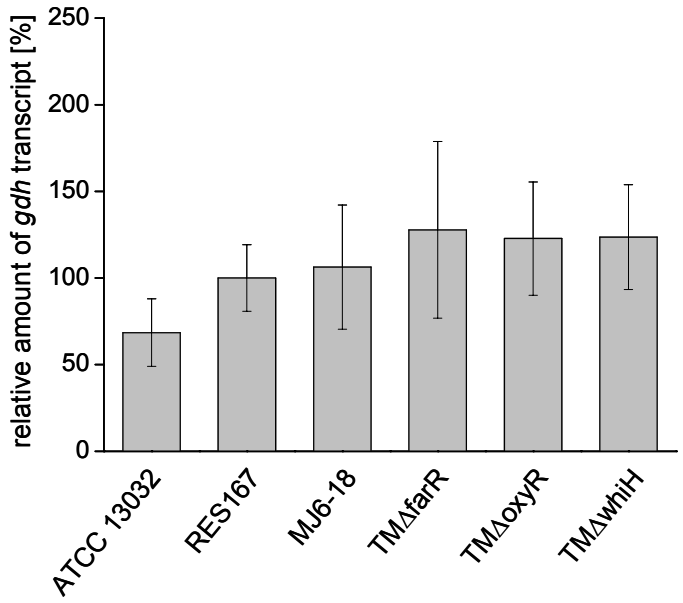

Figure 19: Quantitative real-time RT-PCR of *gdh* mRNA in the wild type and single deletion strains of *amtR*, *farR*, *whiH*, and *oxyR*. The relative amounts of *gdh* transcript were analyzed by quantitative real-time RT-PCR in the *C. glutamicum* wild type strain (ATCC 13032), in RES167, in the *amtR* deletion strain (MJ6-18), in the *farR* deletion strain (TMΔfarR), in the *oxyR* deletion strain (TMΔoxyR), and in the *whiH* deletion strain (TMΔwhiH). The strains were cultivated in CgC medium. The amount of *gdh* transcript of RES167 was set to 100 %.

cultivated under nitrogen surplus. Total RNA was isolated and the relative amounts of *gdh* transcript were determined by quantitative real time PCR. Again, single deletions of *amtR*, *farR*, *whiH*, and *oxyR*, respectively, did not affect *gdh* transcription significantly (figure 19).

However, it is possible that the transcription of *gdh* is regulated by more than one regulator and that only the combined deletion of two or more regulators leads to the loss of the nitrogen-dependent regulation. To investigate a putative functional redundancy of AmtR, FarR, WhiH, and OxyR, multiple deletion strains were derived from RES167 by allelic replacement. Nitrogen control of *gdh* transcription was investigated by RNA dot blot hybridization in the resulting strains TMΔfarRΔamtR, TMΔfarRΔamtRΔwhiH, and TMΔfarRΔamtRΔwhiHΔoxyR. None of the multiple deletions affected nitrogen-dependent *gdh* transcription (figure 18B). Thus, AmtR, FarR, WhiH, and OxyR, respectively, are not essential for transcription control of *gdh* under the tested conditions and functional redundancy among the regulators was not observed.

3.1.5. Identification of conditions that trigger regulation of *gdh* transcription by AmtR, FarR, OxyR, and WhiH

The absence of a distinct effect on *gdh* transcription in the deletion strains is astonishing, as it could be demonstrated *in vitro* that AmtR, FarR, WhiH, and OxyR bind specifically to the *gdh* promoter. For FarR, this could also be observed *in vivo* by β-galactosidase assays in *E. coli*. One possible explanation for this discrepancy is that AmtR, FarR, WhiH, and OxyR regulate *gdh* transcription only under conditions which have not been tested so far, i.e. they respond to other stress conditions than nitrogen starvation. To identify conditions that trigger regulation of gdh transcription by AmtR, FarR, WhiH, and OxyR, these regulators were further characterized as described in the following.

3.1.5.1. Growth rates of the single deletion strains

The single deletions of *amtR*, *farR*, *whiH*, and *oxyR* were further characterized with regard to growth rates. The single deletion strains as well as ATCC13032 and RES167 were cultivated in CgC medium and the optical density at 600 nm was monitored. Single deletions of *farR*, *oxyR*, and *whiH* had no effect on the growth rate, whereas a single deletion of *amtR* slightly induced growth (figure 20).

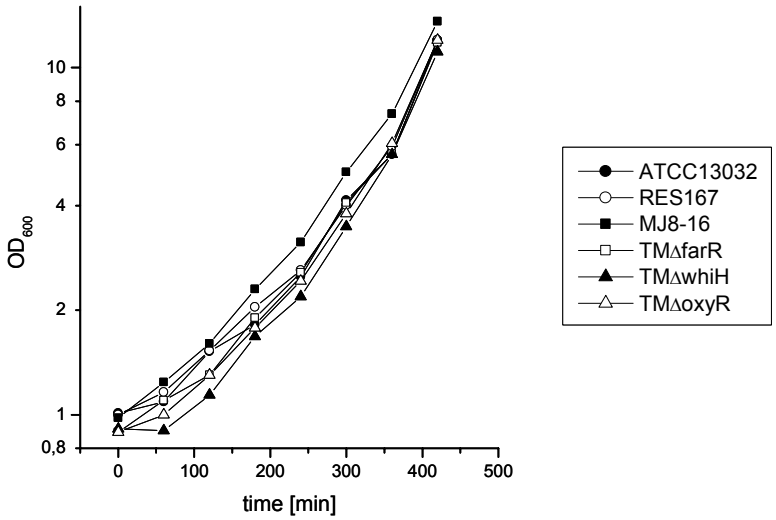

Figure 20: Growth curves of the wild type and the single deletion strains of *amtR*, *farR*, *whiH*, and *oxyR*. The *C. glutamicum* wild type strain (ATCC 13032), the strain RES167, the *amtR* deletion strain (MJ6-18), the *farR* deletion strain (TMΔfarR), the *oxyR* deletion strain (TMΔoxyR), and the *whiH* deletion strain (TMΔwhiH) were cultivated in CgC medium and growth was analyzed by monitoring of the optical density at 600 nm. Only the *amtR* deletion strain MJ8-16 exhibited a slight alteration in growth.

3.1.5.2. Identification of putative target genes of FarR and WhiH by DNA microarray hybridization

To characterize the *in vivo* function of FarR and WhiH, DNA microarrays were used to identify putative target genes of FarR and WhiH. The applied DNA microarrays, consisted of 93.4 % of the predicted *C. glutamicum* genes. Each gene was spotted in quadruplicate onto a glass slide. Analysis of the technical variance revealed that *C. glutamicum* genes detected with different intensities resulting in ratios greater than 1.52 or smaller than -1.52 can be regarded as differentially expressed with a confidence level of greater than 95 % (Hüser *et al*., 2002).

Total mRNA of the *C. glutamicum* strains RES167, TMΔfarR, TMΔwhiH, and TMΔfarRΔamtR was isolated. These mRNA samples were used for the synthesis of fluorescently labelled cDNA samples, which were then hybridized with DNA microarrays. The following combinations were analyzed: RES167 *vs*. TMΔfarR, RES167 *vs*. TMΔwhiH, and RES167 *vs*. TMΔfarRΔamtR. For each combination, the hybridization signals were detected and analyzed. Each experiment was carried out in duplicate. Only those genes, which are significantly regulated in both experiments, were taken into account. A complete list of all differentially expressed genes is given in table 8 in the appendix.

The level of *gdh* transcript was unaltered in all experiments. This result is consistent with previous results obtained from dot blot hybridization experiments and quantitative real time RT-PCR. Interestingly, 93 genes were differentially expressed in all three tested combinations, i.e. these genes were differentially expressed in TMΔfarR, TMΔwhiH, and TMΔfarRΔamtR compared to RES167. Because of that, these genes were considered to be affected by general metabolic perturbations and not to be specific targets of the regulators. In the following, only those genes which were differentially expressed in only one or two of the deletion strains were taken into account.

From the microarray analyses of RES167 *vs*. TMΔwhiH and RES167 *vs*. TMΔfarΔamtR, putative target genes of FarR and WhiH could not be deduced. Genes that were differentially expressed in RES167 *vs*. TMΔwhiH did not show any clear pattern or any physiological link to *gdh*. Comparing the transcriptomes of RES167 and TMΔfarRΔamtR, many genes were found to be differentially

expressed. Among these were 18 transcriptional regulators. Thus, differentially expressed genes might have been affected by one of these regulators instead of AmtR and FarR. Consequently, identification of specific targets of FarR and AmtR was not possible. However, several known target genes of AmtR were found to be differentially expressed, e.g. *amtA*, *amtB*, *glnA*, *gltBD*, *glnD*, *glnK*, and *ureACDEFG*, validating this experimental approach.

Analysis of RES167 *vs*. TMΔfarR revealed 132 differentially expressed genes in total. Among these were *glnA* coding for glutamine synthetase, *carB* coding for carbamoylphosphate synthase and several genes of the arginine biosynthesis pathway (*argBCDFJ*). Together, these genes code for enzymes that catalyze the formation of the arginine precursor citrulline using glutamate as the major substrate. The expression of these genes was upregulated in the *farR* deletion strain compared to RES167 by factors between 1.53 and 4.19. Because of that, a putative role of FarR as a transcriptional repressor of arginine biosynthesis genes was assumed. However, *argR*, coding for a transcriptional regulator of arginine biosnthesis, was also upregulated in the *farR* mutant. Because of that, it is possible, that the regulation of genes of the arginine biosynthese is just a secondary effect mediated by ArgR.

To further investigate, if FarR is a repressor of arginine biosynthesis, the internal concentrations of arginine in RES167 and TMΔfarR, respectively, were measured by HPLC. If FarR was a repressor of arginine biosynthesis, a deletion of *farR* might cause an increase of internal arginine. However, analysis by HPLC revealed only a slight increase of internal arginine in the *farR* deletion strain (figure 21A).

Beside that, a putative role of FarR in transcription control of *gdh* in response to the addition of arginine was investigated. For this purpose, RES167 and TMΔfarR were cultivated in standard minimal medium. Then, arginine was added to a final concentration of 1 % to the culture medium. Samples were taken before (0 min) as well as 30 and 60 minutes after the addition of arginine and analyzed by RNA dot blot hybridization using *gdh* as probe. In response to the addition of arginine, transcription of *gdh* was slightly induced in RES167 (figure 21B). This arginine-dependent regulation was not affected by the deletion of *farR*. Thus, FarR is not essential for the regulation of *gdh* transcription in response to arginine. This experiment was also carried out with the arginine precursors citrulline and ornithine.

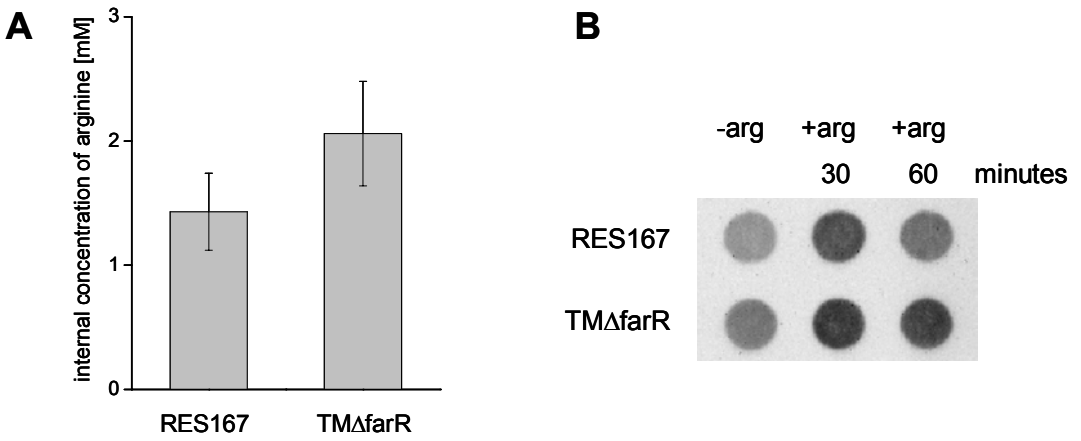

Figure 21: Internal concentrations of arginine and *gdh* transcription in response to the addition of arginine. A: The internal concentrations of arginine in the *C. glutamicum* strains RES167 and TMΔfarR cultivated in CgC medium. B: RNA dot blot hybridization using *gdh* as probe and RNA samples of the *C. glutamicum* strains RES167 and TMΔfarR before (-arg) and 30 or 60 minutes after the addition of arginine (+arg) to a final concentration of 1 %.

Additon of citrulline and ornithine, respectively, did not affect *gdh* transcription, neither in RES167 nor in TMΔfarR (data not shown).

Conclusively, the putative role of FarR as repressor of arginine biosynthesis genes revealed by DNA microarray experiments could not be verified by measurements of internal arginine concentrations or by analysis of arginine-dependent transcription control of *gdh*. Thus, the role of FarR remains unclear.

3.1.5.3. Identification of putative target genes of FarR using a bioinformatic approach

A binding motif of FarR upstream of *gdh* from *C. glutamicum* could be identified as described before. This motif was applied in a bioinformatical approach to identify other putative binding sites of FarR within the genome of *C. glutamicum*. For this purpose, the FUZZNUC program was used, which allows nucleic acid pattern searches with various ambiguities (http://bioweb.pasteur.fr/seqanal/interfaces/fuzznuc.html). The sequence GGTTATATAACC, which is the predicted FarR binding motif upstream of *gdh*, was applied as pattern, whereby, up to three mismatches were allowed. The search revealed 576 putative binding sites for FarR in total. However, transcription factors normally bind close to promoters in order to interact with RNA polymerase. Consequently, only those putative binding sites of

Table 3: A selection of genes that were predicted to harbour FarR binding sites within their promoter regions. Several putative binding sites of FarR could be identified by a bioinformatic approach. Out of these, 13 were further analyzed because of their location upstream of genes involved in nitrogen metabolism and transport, fatty acid metabolism, or upstream of genes which were found to be differentially expressed in the DNA microarray analysis of RES167 *vs.* TMΔfarR. The respective genes as well as the location of the binding sites upstream of the genes are given in this table.

NCgl-No.	gene name	annotation	location upstream of the start codon [bp]	differential expression (RES167 vs. TMΔfarR)
NCgl0328	*noxC*	nitroreductase	70	no
NCgl0406	-	permease of major facilitator superfamily	44	yes
NCgl0677	*dtsR2*	detergent sensitive rescuer	174	no
NCgl1143	*narK*	nitrate/nitrite transporter	184	no
NCgl1151	*fadD4*	acyl-CoA synthetase	462	no
NCgl1235	*serA*	phosphoglycerate dehydrogenase	100	yes
NCgl1266	*gpsA*	glycerol-3-phosphate dehydrogenase	3	no
NCgl1521	*amtA*	ammonium transporter	108	no
NCgl1521	*amtA*	ammonium transporter	196	no
NCgl1875	*gluA*	glutamate transporter	148	no
NCgl2016	*hisH*	glutamine amidotransferase	73	no
NCgl2108	-	cell wall-associated hydrolase	257	yes
NCgl2972	*plsC*	1-acyl-sn-glycerol-3-phosphate acyltransferase	25	no

FarR were taken into account, which were located in non-coding regions of the genome, upstream of genes, and within putative promoter regions, i.e. not more than 600 bp upstream of the start codons of genes. From the resulting 143 putative binding sites, a selection of 13 putative binding sites was further investigated (table 7). These 13 putative binding sites were located upstream of genes of nitrogen metabolism, fatty acid metabolism, or genes which were observed to be differential expressed in the *farR* deletion strain vs. RES167 by DNA microarray experiments.

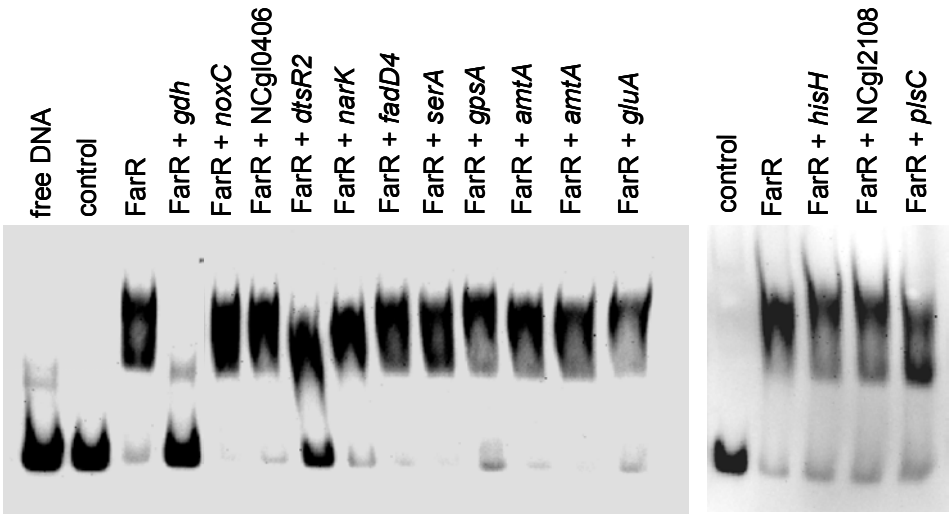

Figure 22: Competition assay to identify FarR binding sites. Competition assays of the digoxigenin-labelled DNA fragment B of the *gdh* promoter region harbouring a FarR binding site from *C. glutamicum* and a cell extract of *E. coli* heterologously expressing FarR from *C. glutamicum* were performed. Unlabelled 30 bp DNA fragments harbouring putative FarR binding sites located upstream of the given genes were added in a 1500-fold molar excess. Only the DNA fragments of the *gdh* promoter and the *dtsR2* promoter, respectively, inhibited a complete shift of the labelled DNA. Free DNA: without protein extract. Control: cell extract of *E. coli* containing the empty vector.

To verify binding of FarR to these putative binding sites, competition gel shift assays were performed using the digoxigenin-labelled DNA fragment B of the *gdh* promoter and a 1500-fold excess of unlabelled 40 bp DNA fragments containing the putative FarR binding sites for complementation. A protein extract of *E. coli* heterologously expressing FarR from *C. glutamicum* was applied and, as a control, an extract of *E. coli* containing the control vector without *farR*. Addition of the 40 bp DNA fragment harbouring the putative FarR binding site upstream of *dtsR2* partially inhibited the shift (figure 22). Thus, an additional FarR binding site could be identified, which is located 174 bp upstream of *dtsR2*. However, inhibition of the shift by the FarR binding site of *dtsR2* was not as strong as by the FarR binding site of *gdh*, showing that FarR had a higher affinity to the *gdh* promoter than to the *dtsR2* promoter. The *dtsR2* gene codes for the detergent sensitive rescuer protein DtsR2, which is presumed to be a counterpart of biotin-binding acyl-CoA carboxylase (AccBC). This protein complex is involved in fatty acid biosynthesis in *C. glutamicum* (Kimura, 2002).

Figure 23: Consensus binding motif of FarR from *C. glutamicum*. This consensus binding motif of FarR from *C. glutamicum* was derived from the sequences of the binding site of FarR upstream of *gdh* and *dtsR*2, respectively.

The sequences of the FarR-binding sites upstream of *gdh* and *dtsR*2, respectively, were used for a sequence alignment to deduce a consensus binding motif of FarR. For this purpose, the CLUSTALW algorithm was used (http://www.expasy.org). The resulting consensus binding motif of FarR was depicted using the program Sequence Logos (http://weblogo.berkeley.edu) and is given in figure 23.

3.1.5.4. Identification of putative effector molecules of FarR

HutC/FarR-like transcription factors of the GntR family typically consist of a DNA-binding domain fused to a signalling domain. These signalling domains exhibit small-molecule-binding pockets and trigger conformational changes upon recognizing specific ligands. Thereby, binding of ligands influences the DNA-binding properties of the transcription factors which results in activation or repression of transcription (Aravind *et al*., 2003). Due to sequence homologies, FarR from *C. glutamicum* is predicted to be a HutC/FarR-like transcription of the GntR family, thus, might be regulated upon binding of a ligand. This was investigated by the use of gel shift assays.

As target DNA, the digoxigenin-labelled DNA fragment B was used, which contains a FarR binding site as described above. A protein extract of *E. coli* heterologously expressing *farR* from *C. glutamicum* was applied. To identify putative effector molecules of FarR, a diverse range of metabolites were added and their ability to inhibit binding of FarR to the labelled DNA was analyzed. Most of the tested substances had no effect on the shift caused by FarR (figure 24). In contrast, the addition of sodium myristate and sodium palmitate, respectively, inhibited a shift of the DNA by FarR. Thus, sodium myristate and sodium palmitate prevented binding of FarR to the DNA under the tested conditions. However, it was not clear, if this

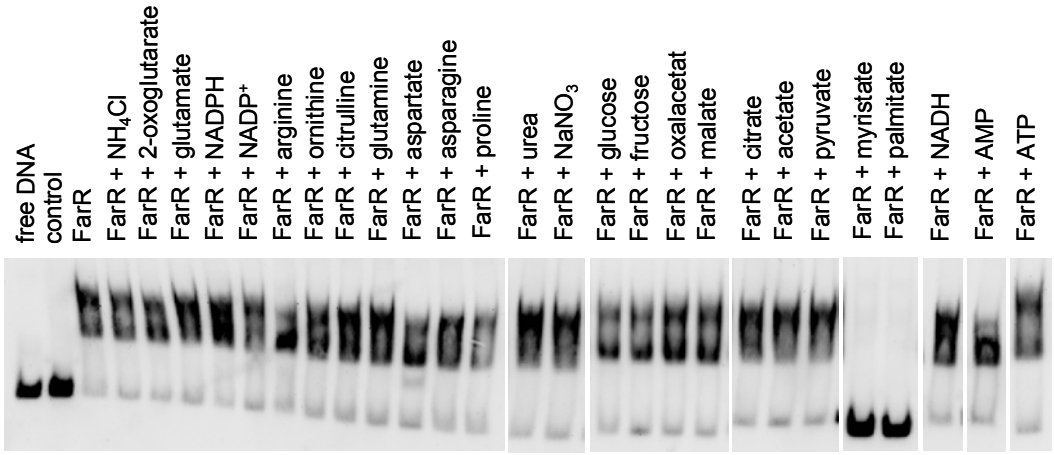

Figure 24: Gel shift assays for the identification of effector molecules of FarR. Gel shift assay were performed with the digoxigenin-labelled DNA fragment B of the *gdh* promoter from *C. glutamicum* and a cell extract of *E. coli* heterologously expressing FarR from *C. glutamicum*. The indicated substances were added to a final concentrations of 10 mM, except myristate and palmitate, which were added to a final concentration of 1 mM together with triton X-100 in a final concentration of 0.2 % (w/v). Only myristate and palmitate inhibited a shift of the DNA. Control: cell extract of *E. coli* containing the empty plasmid. Free DNA: without any protein extract.

was the result of a specific interaction of myristate and palmitate with a putative signalling domain of FarR, or if myristate and palmitate just denatured FarR in a detergent-like manner. To investigate this, the effect of detergents similar to myristate and palmitate was analyzed. Sodium dodecylsulfate (SDS), cetyl trimethyl ammonium bromide (CTAB), and sodium oleate also inhibited a shift of the DNA by FarR (figure 25A). Especially the ability of CTAB to partially inhibit DNA-binding by FarR is remarkable, as this molecule is positively charged in contrast to myristate and palmitate, which are negatively charged. Thus, inhibition by sodium myristate and sodium palmitate was most probably unspecific and not caused by a specific binding of myristate and palmitate to a putative signalling domain of FarR. In addition, sodium myristate and sodium palmitate were added in a relatively high concentration of 1 mM. This concentration is not in the physiological range. Because of that, another gel shift assays was carried out applying sodium palmitate in a range of concentrations of 1 μM up to 100 μM. In these concentrations, sodium palmitate did not inhibit a shift of the DNA by FarR (figure 25B). Thus, sodium palmitate has no effect on FarR in the physiological range of concentrations.

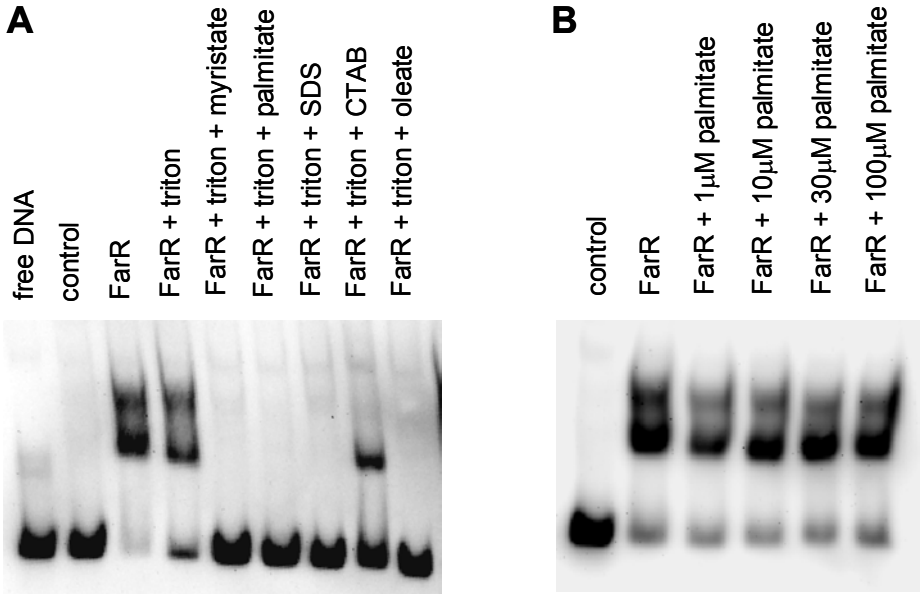

Figure 25: Analysis of the ability of fatty acids to inhibit DNA binding by FarR. Gel shift assays were performed with the dioxigenin-labelled DNA fragment B of the *gdh* promoter from *C. glutamicum* and a cell extract of *E. coli* heterologously expressing FarR from *C. glutamicum*. Control: cell extract of *E. coli* containing the empty plasmid. Free DNA: without any protein extract. A: The indicated substances were added to a final concentrations of 1 mM, except triton X-100, which was added to a final concentration of 0.2 %. B: sodium myristate was added to a final concentration as given without the addition of triton X-100.

3.1.5.5. Regulation of *gdh* transcription in response to various stress conditions

AmtR, FarR, WhiH, and OxyR do not regulate *gdh* transcription in response to nitrogen starvation but might regulate *gdh* transcription in response to other stress conditions. However, other stress conditions that affect *gdh* transcription have not been described yet. Therefore, the *C. glutamicum* wild type ATCC 13032 was exposed to various conditions and *gdh* transcription was analyzed by RNA dot blot hybridization experiments. Variation of the carbon sources as well as carbon starvation affected *gdh* transcription (figure 26A). The use of alternative nitrogen sources affected *gdh* transcription as well (figure 26B). Additionally, *gdh* was regulated in response to the growth phase (figure 26C) and to oxygen limitation (figure 26D). Chill stress at 15 °C induced *gdh* transcription, whereas heat stress at 37 °C had no effect compared to the standard conditions at 30 °C (figure 26F). Beside that, oxidative stress caused by superoxide and peroxide, respectively

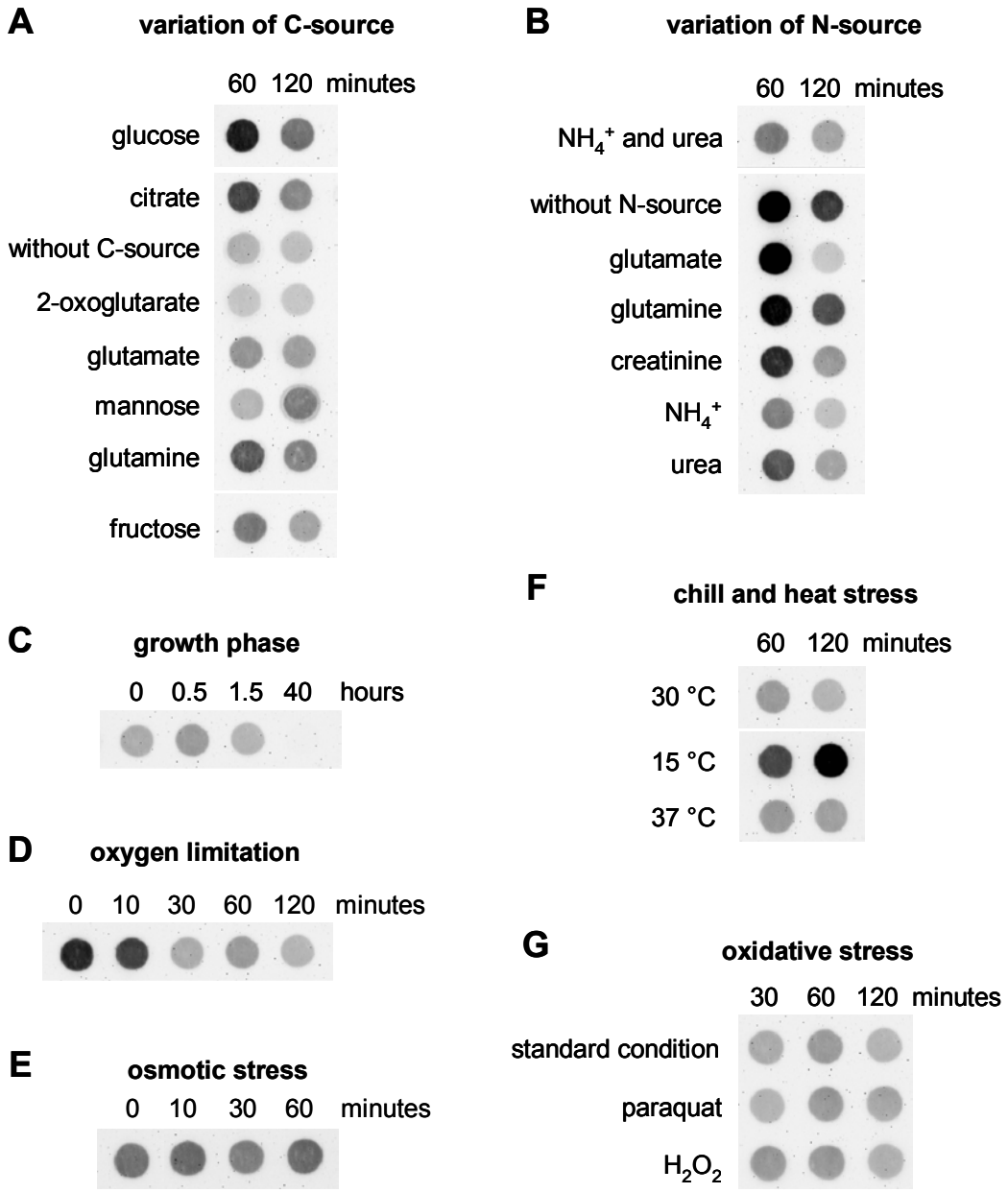

Figure 26: The effect of various conditions on *gdh* transcription. RNA dot blot hybridization was used to analyze *gdh* transcription in the *C. glutamicum* wild type strain ATCC13032 cultivated under various conditions. For this purpose, the cells were first cultivated in standard CgC medium to an optical density of 4.5 (600 nm). Then, *C. glutamicum* was exposed to various conditions as described in the following and *gdh* transcription was analyzed after the given periods of time. A: CgC medium containing the given carbon sources. B: CgC medium containing the nitrogen sources. C: in CgC medium until the stationary phase was reached. D: in a sealed falcon tube without oxygen supply. E: addition of sodium chloride to a final concentration of 1 M. F: in CgC medium under the given temperatures. G: in CgC medium (standard) and after the addition of 100 µM paraquat (superoxide stress) or 58 µM H_2O_2 (peroxide stress).

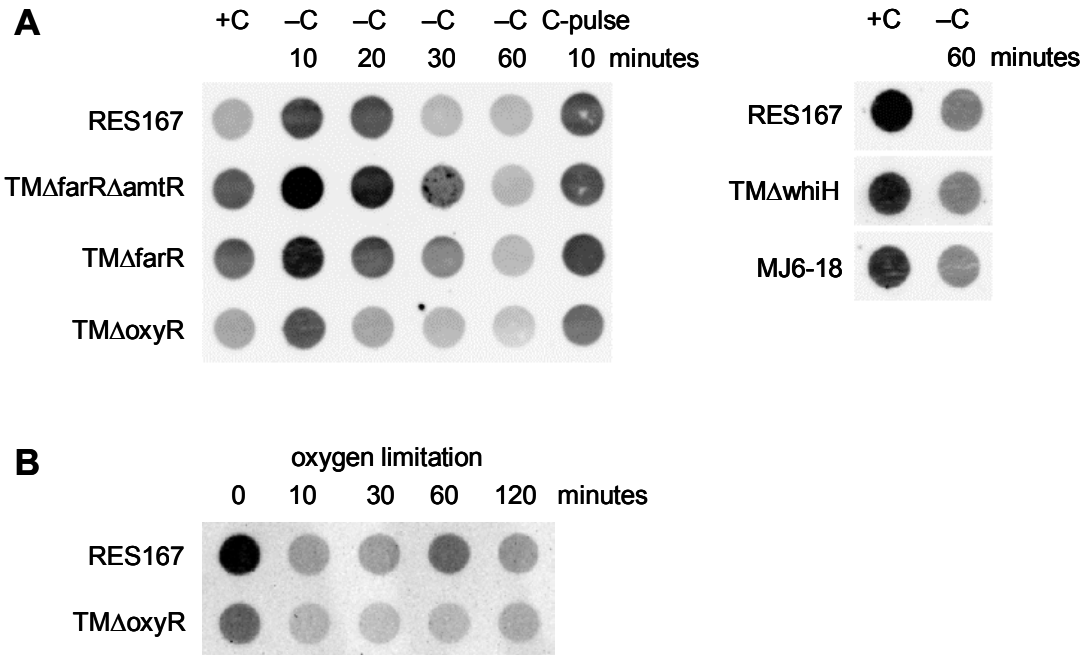

Figure 27: Transcription of *gdh* in response to carbon limitation and oxygen limitation. A: C. glutamicum strains were cultivated in CgC medium containing 2.5 % glucose (+C), then in medium without any carbon source (-C), and after an excess of glucose was added to the carbon-starved cells (C-pulse). Samples were taken after the given periods of time and were used for an RNA dot blot hybridization experiment using *gdh* as probe. B: RES167 and TMΔoxyR were cultivated in CgC medium in a standard 500 mL shaking flask. Then, the cultures were transferred to falcon tube, which were sealed to limit oxygen supply. Transcription of gdh was analyzed by RNA dot blot hybridization before (0 minutes) and 10, 30, 60, and 120 minutes after oxygen limitation was imposed.

(figure 26G), as well as osmotic stress (figure 26E) did not affect *gdh* transcription. Conclusively, an astonishingly broad range of stress conditions could be identified that affect *gdh* transcription.

It was investigated whether AmtR, FarR, WhiH, and OxyR are involved in *gdh* regulation in response to carbon starvation. For this purpose, the *C. glutamicum* strain RES167 as well as the deletion strains MJ8-16 (Δ*amtR*), TMΔfarR, TMΔwhiH, TMΔoxyR, and TMΔfarRΔamtR were cultivated in standard medium containing 2.5 % glucose. Then, the cells were transferred to medium without any carbon source. After 60 minutes of carbon starvation, an excess of glucose was added. Transcription of *gdh* was analyzed by RNA dot blot hybridization. In all investigated deletion strains, transcriptional regulation of *gdh* in response to carbon starvation

was not affected (figure 27A). Thus, a putative role of the regulators in carbon-dependent regulation of *gdh* transcription could not been demonstrated.

To investigate, if OxyR regulates *gdh* transcription in response to oxygen limitation, the respective deletion strain TMΔoxyR as well as RES167 were tested. Total RNA was isolated before (0 minutes) and 10, 30, 60, and 120 minutes after exposition to oxygen limitation. Transcription of *gdh* was analyzed by RNA dot blot hybridization. The repression of *gdh* under nitrogen limitation was not affected by a deletion of *oxyR* (figure 27B). Thus, OxyR does not regulate *gdh* transcription in response to oxygen limitation.

3.2. The impact of GDH on the nitrogen control network

Glutamate dehydrogenase is essential for nitrogen control by the GlnD/GlnK/AmtR signal cascade in *C. glutamicum*. Deletion of *gdh* leads to a loss of transcriptional repression by AmtR (L. Nolden, personal communication). It is unclear whether this effect is caused by the loss of putative protein interactions between GDH and any member of the GlnD/GlnK/AmtR signal cascade or if the absence of GDH causes changes in the concentration of a metabolite, which serves as the indicator for the nitrogen status of the cell (metabolic effect).

3.2.1. Expression of the *gdh* gene of *E. coli* in the *gdh* deletion strain of *C. glutamicum*

To investigate whether GDH activity or the presence of the GDH for a putative protein interaction predominantly affects nitrogen regulation in *C. glutamicum*, the influence of a non-*C. glutamicum* glutamate dehydrogenase was tested. Both, GDH from *C. glutamicum* and GDH from *E. coli* catalyze the NAPDH-dependent condensation of ammonium and 2-oxoglutarate forming glutamate. In sequence alignments, they share 53 % identical amino acids. Expression of *gdh* from *C.*

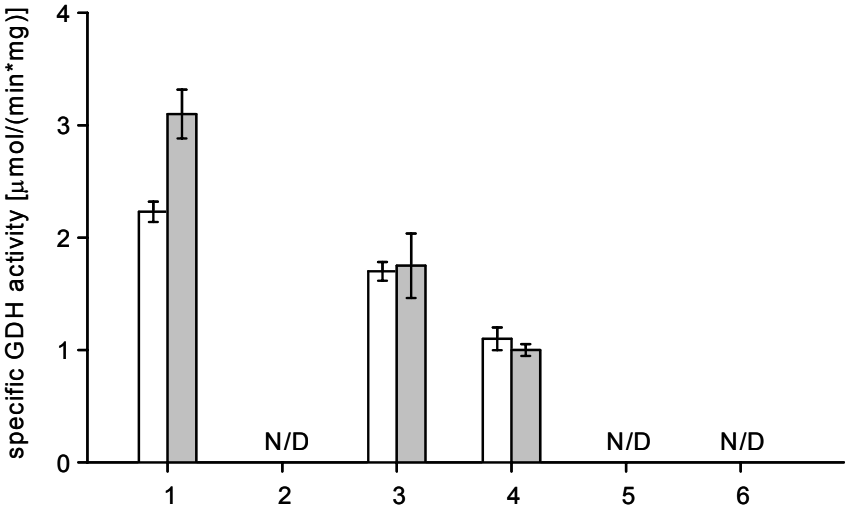

Figure 28: Specific GDH activity. Specific GDH activities of the *C. glutamicum* wild type strain ATCC 13032 (1), the *gdh* deletion strain LNΔGDH (2), LNΔGDH transformed with pZgdh harbouring *gdh* from *C. glutamicum* (3), LNΔGDH transformed with $pZgdh_{EC}$ harbouring *gdh* from *E. coli* (4), LNΔGDH transformed with pZgdh-K92L harbouring *gdh* from *C. glutamicum* with a point mutation (5), and LNΔGDH containing the control vector pZ8-1 (6). The strains were cultivated under nitrogen surplus (white bars) and under nitrogen starvation for 30 minutes (grey bars). N/D: no GDH activity was detectable.

glutamicum in a *gdh* deletion strain of *C. glutamicum* should complement both, a metabolic effect and a putative protein interaction. In contrast, glutamate dehydrogenase from *E. coli* heterologously expressed in a *gdh* deletion strain of *C. glutamicum* should only be able to complement a metabolic effect by its enzymatic activity, but not a putative protein interaction. The *gdh* genes of *C. glutamicum* and *E. coli*, respectively, were cloned into the plasmid pZ8-1 and were then transformed into the *gdh* deletion strain LNΔGDH of *C. glutamicum*. The resulting strains, LNΔGDH pzgdh and LNΔGDH $pZgdh_{EC}$, as well as the *C. glutamicum* wild type ATCC13032 and the *gdh* deletion strain LNΔGDH were cultivated under nitrogen surplus and nitrogen starvation. GDH activity was measured in these strains. Both, expression of *gdh* from *C. glutamicum* and *gdh* from *E. coli* restored GDH activity in the *gdh* deletion strain. GDH activities were almost on the level of the *C. glutamicum* wild type (figure 28). Additionally, total RNA was isolated from these strains cultivated under nitrogen surplus, under starvation, and after an excess of ammonium was added to the nitrogen starved cells. The samples were analysed by

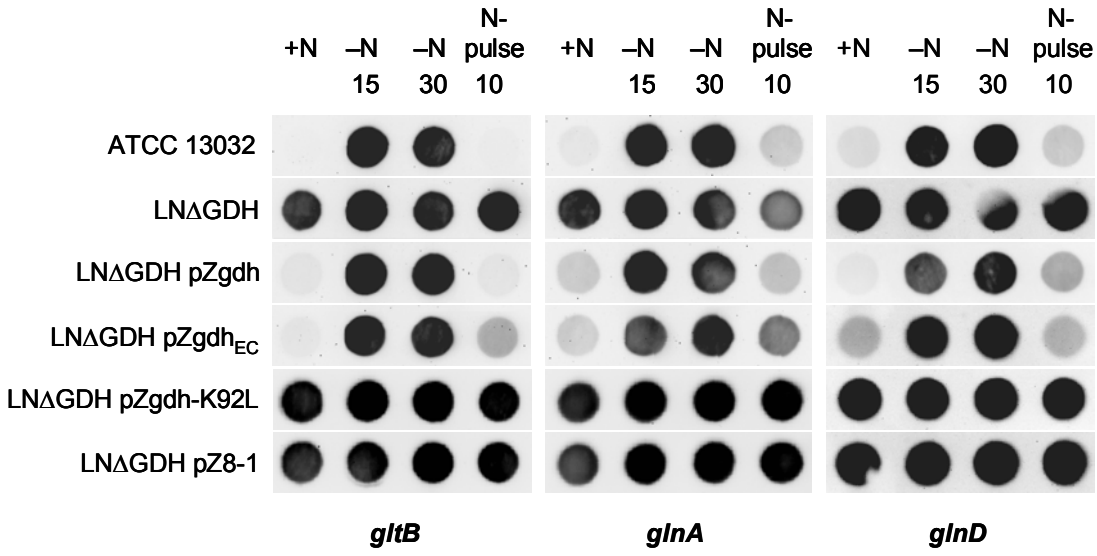

Figure 29: Analysis of the nitrogen-dependency of the transcription of *gltB*, *glnA*, and *glnD*. The *C. glutamicum* strains ATCC 13032 (wild type), LNΔGDH (*gdh* deletion strain), LNΔGDH pZgdh (LNΔGDH expressing plasmid-coded *gdh* from *C. glutamicum*), LNΔGDH $pZgdh_{EC}$ (LNΔGDH expressing plasmid-coded *gdh* from *E. coli*), LNΔGDH pZgdh-K92L (LNΔGDH expressing plasmid-coded *gdh* from *C. glutamicum* with a point mutation), and LNΔGDH pZ8-1 (LNΔGDH containing the control vector) were cultivated under nitrogen surplus (+N), under nitrogen starvation for 15 and 30 minutes (-N), and for 10 minutes after an excess of ammonium was added to the nitrogen-starved cells (N-pulse). Total RNA was isolated and analyzed by RNA dot blot hybridization using the *gltB* gene, the *glnA* gene, and the *glnD* gene as probe.

RNA dot blot hybridization using the AmtR-regulated genes *gltB*, *glnA*, and *glnD* as probe. The loss of nitrogen-dependent transcription control in the *gdh* deletion strain was complemented by both, *gdh* from *C. glutamicum* and *gdh* from *E. coli* (figure 29). Thus, GDH activity seems to be essential for nitrogen control and not the presence of GDH from *C. glutamicum* for putative protein interactions.

3.2.2. Expression of an enzymatically inactive glutamate dehydrogenase in the *gdh* deletion strain

To support this result, an enzymatically inactive glutamate dehydrogenase protein was constructed. An enzymatically inactive mutant of GDH from *C. glutamicum* with a single amino acid exchange in the active site is not able to complement the loss of GDH activity in the *gdh* deletion strain, but should still be able to perform a putative protein interaction.

Lysine 92 in the active centre of *C. glutamicum* GDH was chosen as a target for site-directed mutagenesis. It has been demonstrated for GDH from *Clostridium symbiosum* that an alteration of this residue to leucine leads to a loss of catalytic activity of GDH from *C. symbiosum*, whereas the conformation of this protein is unaffected, which could be shown by crystal structure analyses (Stilmann *et al*., 1999). Using site-directed mutagenesis, the expression vector pZgdh-K92L was constructed, which harbors the *gdh* gene from *C. glutamicum* containing a point

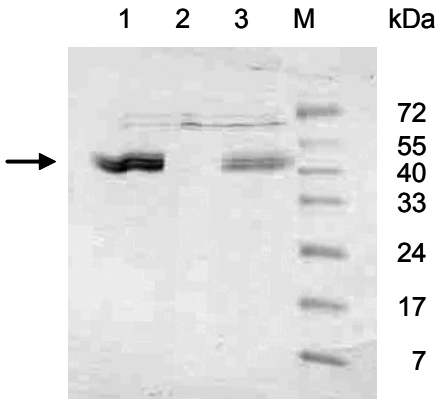

Figure 30: Western blot using antibodies for GDH. 1: Cell extract of the *C. glutamicum* wild type ATCC13032. 2: Cell extract of the *gdh* deletion strain LNΔGDH. 3: Cell extract of LNΔGDH pZgdh-K92L, which is the *gdh* deletion strain transformed with an expression vector harbouring *gdh* from *C. glutamicum* with a point mutation. M: molecular weight marker. The arrow indicates the presence of GDH protein.

mutation that leads to an exchange of lysine 92 to leucine. This plasmid was transformed into the *gdh* deletion strain of *C. glutamicum*. In the resulting strain, no GDH activity was detectable (figure 28). To verify the presence of the inactive GDH in this strain, antibodies for GDH were produced using purified His-tagged GDH from *C. glutamicum*. By Western blotting using these antibodies, the presence of GDH could be verified (figure 30). Thus, this strain harbours an enzymatically inactive mutant of GDH from *C. glutamicum*. The strain was cultivated under nitrogen surplus, nitrogen starvation, and after an excess of ammonium was added to the nitrogen-starved cells. Total RNA was isolated and analysed by RNA dot blot hybridization using the AmtR-regulated genes *gltB*, *glnA*, and *glnD* as probe. The loss of nitrogen-dependent transcription control in the *gdh* deletion strain could not be complemented by the enzymatically inactive mutant of GDH from *C. glutamicum* (figure 29), which was present in this strain as demonstrated by Western blotting (figure 30). Consequently, the physical presence of GDH from *C. glutamicum* for a putative protein interaction is not sufficient to complement this effect. It is GDH activity itself, which is essential for the nitrogen control by the GlnD/GlnK/AmtR signal cascade. Thus, the effect caused by the deletion of *gdh* is a metabolic effect, i.e. it is the result of changes in the concentration of one or more metabolites which serve(s) as indicator(s) for the nitrogen status of *C. glutamicum.*

3.2.3. Influence of a deletion of *gdh* on intracellular metabolite pools

Glutamate dehydrogenase directly influences the concentrations of 2-oxoglutarate, ammonium, and glutamate. Indirectly, also glutamine concentrations might be affected. Consequently, at least one of these metabolites might be the indicator for the nitrogen status and its internal concentration might change upon deletion of *gdh* resulting in a loss of nitrogen control. To investigate this, the *C. glutamicum* wild type ATCC 13032 and the *gdh* deletion strain LNΔGDH were cultivated under nitrogen surplus and under nitrogen starvation for 30 minutes. The internal concentrations of 2-oxoglutarate, ammonium, glutamate, and glutamine were measured by HPLC and gas chromatography, respectively. The results are given in figure 31.

The intracellular concentration of glutamate was constantly on a very high level between 70 mM and 150 mM in both strains and under both conditions of nitrogen

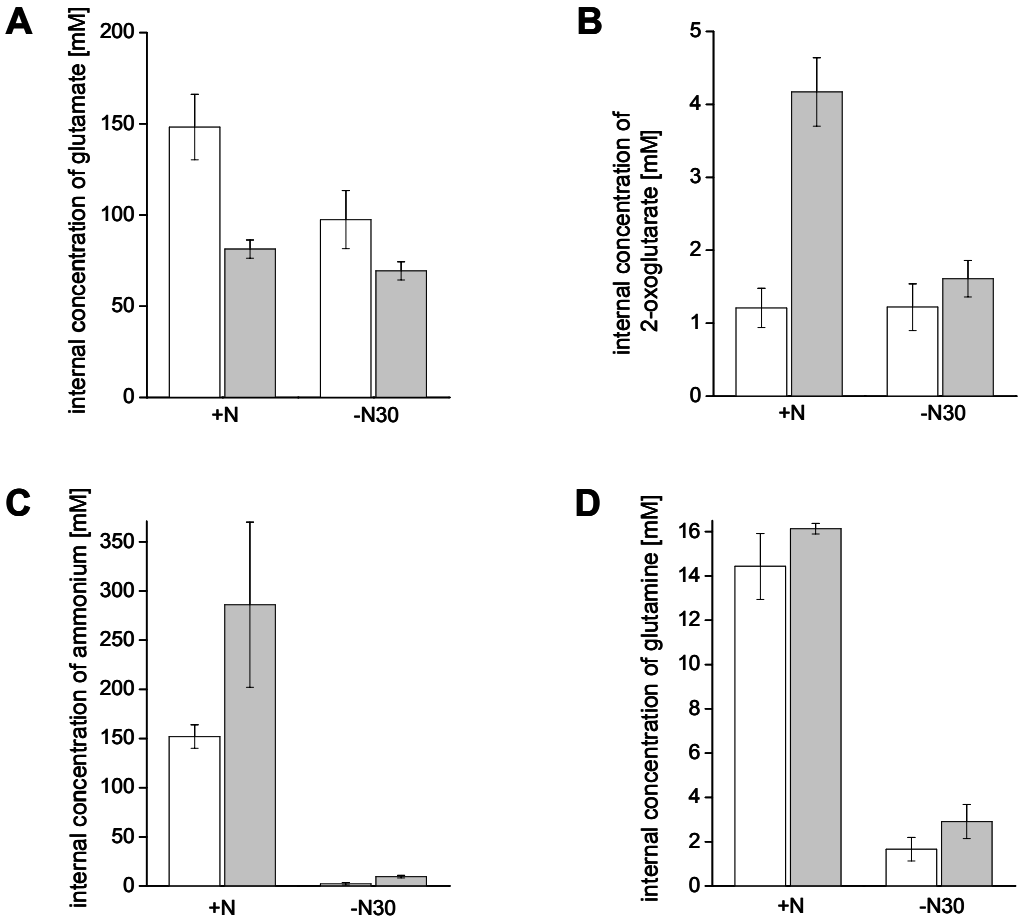

Figure 31: Internal concentrations of glutamate, 2-oxoglutarate, ammonium, and glutamine. The *C. glutamicum* wild type strain ATCC 13032 (white bars) and the *gdh* deletion strain LNΔGDH (grey bars) were cultivated under nitrogen surplus (+N), and under nitrogen starvation for 30 minutes (-N30). The internal concentrations of glutamate (A) and 2-oxoglutarate (B) were measured by gas chromatography, the internal concentrations of ammonium (C) and glutamine (D) were measured by HPLC.

supply (figure 31A). Consequently, glutamate cannot indicate the nitrogen status of the cell. As the concentration of glutamate is more or less constant, also the concentrations of metabolites derived from glutamate by biosynthesis should be constant (except glutamine, which is directly influenced by the availability of ammonium). Thus, these metabolites can be excluded as well. In the wild type strain ATCC 13032, the internal concentration of 2-oxoglutarate was constantly at 1.2 mM under nitrogen surplus as well as under nitrogen starvation (figure 31B). Consequently, neither 2-oxoglutarate nor any other metabolite of central carbon metabolism connected to 2-oxoglutarate indicated the nitrogen status in the wild type strain under the tested conditions. In contrast, the internal concentrations of

ammonium and glutamine were on high levels under nitrogen surplus (152 mM ammonium and 14.4 mM glutamine) and were significantly diminished under nitrogen starvation (2 mM ammonium and 1.7 mM glutamine) (figure 31CD). Thus, the internal concentrations of ammonium and glutamine correlated with the nitrogen supply, i.e. the availability of ammonium in the surrounding medium. Consequently, ammonium or glutamine or any metabolite derived from glutamine indicated the nitrogen status in the *C. glutamicum* wild type under the tested conditions.

However, neither the internal concentrations of ammonium nor the internal concentrations of glutamine were affected by a deletion of *gdh* (figure 31CD). In LNΔGDH, the internal concentrations of ammonium and glutamine were still on high levels under nitrogen surplus (286 mM ammonium and 16.1 mM glutamine) and were also diminished under nitrogen starvation (9 mM ammonium and 2.9 mM glutamine). Beside that, the internal concentrations of glutamate were not affected by a deletion of *gdh*, too (figure 31A). Thus, the loss of nitrogen control in the *gdh* deletion strain under nitrogen surplus was not mediated by ammonium, glutamine, glutamate, or any metabolite derived from ammonium, glutamine or glutamate by biosynthesis. However, a deletion of *gdh* caused a significant increase of internal 2-oxoglutarate under nitrogen surplus up to 4.2 mM compared to 1.2 mM in the wild type (figure 31B). Thus, the increase in the concentration of 2-oxoglutarate or any other metabolite of central carbon metabolism connected to 2-oxoglutarate is directly correlated to the loss of nitrogen control in the *gdh* deletion strain.

Conclusively, nitrogen control is affected by at least two metabolites. On the one hand, nitrogen control responded to the concentration of ammonium or glutamine or any metabolite derived from glutamine. On the other hand, an increase in the concentration of 2-oxoglutarate or any other metabolite of central carbon metabolism connected to 2-oxoglutarate seems to influences nitrogen control as it is directly correlated to the loss of repression by AmtR in the *gdh* deletion strain.

3.2.4. Influence of a deletion of *glnA* on intracellular metabolite pools

Beside 2-oxoglutarate, the nitrogen status is indicated either by ammonium or by glutamine or by any metabolite derived from glutamine by biosynthesis. To analyze which of these metabolites indicates the nitrogen status in particular, the *glnA* deletion strain LNΔGS was studied. This strain lacks glutamine synthetase, which

uses ammonium and glutamate to from glutamine. The *glnA* deletion strain LNΔGS was cultivated in medium containing ammonium and glutamine as nitrogen sources. Then, LNΔGS was cultivated in medium without any nitrogen source for 30 minutes. After that, either ammonium or glutamine or both, ammonium and glutamine, were added to the nitrogen-starved cells, which were then cultivated for another 30 minutes. Transcription of the *gltB* gene, which is under the control of AmtR, was analyzed by RNA dot blot hybridization. In addition, the internal concentrations of glutamine, ammonium, 2-oxoglutarate, and glutamate were measured by HPLC and GC, respectively. The results are given in figure 32.

The internal concentrations of ammonium correlated with the transcription level of *gltB* under all tested conditions (figure 32AB). Transcription of *gltB* was repressed under high internal concentrations of ammonium (+gln+NH_4^+: 604 mM; gln-NH_4^+-pulse: 478 mM; NH_4^+-pulse: 450 mM), and activated under low internal concentrations of ammonium (-N: 24 mM; gln-pulse: 26 mM). In contrast, the internal concentration of glutamine was not correlated to the transcription level of *gltB*, thus, was not decisive for nitrogen control (figure 32AC). After the addition of ammonium to a culture of nitrogen-starved cells (NH_4^+-pulse), the glutamine pool was almost unaltered compared to nitrogen starvation (-N: 6.8 mM glutamine; NH_4^+-pulse: 10.3 mM glutamine), nevertheless, transcription of *gltB* was repressed. Additionally, *gltB* was still transcribed after the addition of glutamine to a culture of nitrogen-starved cells even though the internal concentration of glutamine increased significantly (81 mM). Internal 2-oxoglutarate, which can also induce transcription in high concentrations, was on a low level (1.05 mM) after the glutamine pulse, thus, did not cause this effect (figure 32D). Beside that, glutamate can also be excluded as its internal concentration was unaltered under all tested conditions (figure 32E). Consequently, only the concentration of ammonium was correlated with the transcription level of *gltB*, whereas 2-oxoglutarate, glutamate, glutamine, and, consequently, all metabolites derived from 2-oxoglutarate, glutamate, and glutamine by biosynthesis could be excluded to mediate this effect.

To investigate if ammonium itself indicated the nitrogen status, it was analyzed if ammonium is assimilated only by GDH and GS in *C. glutamicum*, thus, can directly affect only metabolites involved in the reaction catalyzed by GDH and GS, namely 2-oxoglutarate, glutamate, and glutamine. As described below (section 3.3.3.),

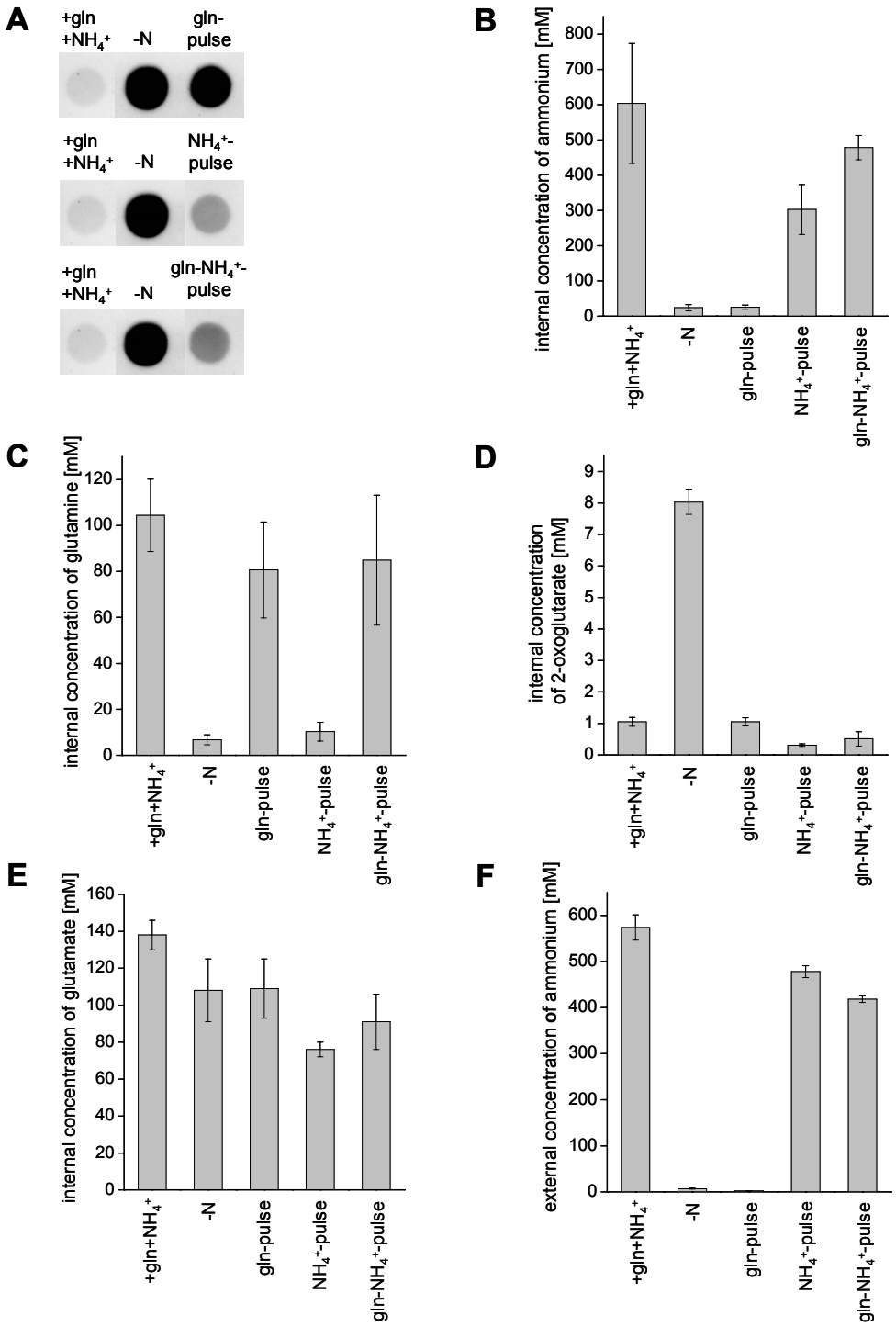

Figure 32: Transcription of *gdh* and internal concentrations of ammonium, glutamine, 2-oxoglutarate, and glutamate. The *glnA* deletion strain LNΔGS was cultivated in medium containing ammonium and glutamine as nitrogen sources (+gln+NH4+). Then, the cells were cultivated in medium without any nitrogen source for 30 minutes (-N). After that, either ammonium (NH4+-pulse) or glutamine (gln-pulse) or ammonium and glutamine (gln-NH4+-pulse) were added to the nitrogen-starved cells, which were then cultivated for another 30 minutes. Total RNA was isolated and analyzed by RNA dot blot hybridization using *gltB* as probe (A). The internal concentrations of ammonium (B), glutamine (C), 2-oxoglutarate (D), and glutamate (E) as well as the external concentration of ammonium (F) were measured by HPLC and GC, respectively.

analysis of a mutant strain lacking GDH and GS revealed the presence of a third enzyme for ammonium assimilation in *C. glutamicum*, which is unknown so far. However, assimilation of ammonium *via* this pathway was very slow, thus, the concentrations of the involved metabolites can be assumed to change relatively slowly in response to changes in the availability of ammonium. Because of that, these metabolites are not suitable to trigger the relatively fast response of the GlnD/GlnK/AmtR signal cascade. Thus, it was most probably ammonium itself that triggered nitrogen control under the tested conditions. However, it is not clear if the internal or the external concentration of ammonium was sensed by *C. glutamicum*, as both concentrations correlated with the transcription of *gltB* (figure 32B and 32F).

3.3. Putative toxicity of ammonium for *C. glutamicum*

Ammonium is suspected of being toxic for bacteria due to the formation of a putative energy-wasting transmembrane cycle. According to this theory, ammonium would first be transported into the cell by the use of energy and then it would diffuse passively back out of the cell resulting in a detrimental waste of energy (Castorph *et al*., 1984; Kleiner, 1985). However, this has never been demonstrated in bacteria. Because of that, a putative toxicity of ammonium for *C. glutamicum* was investigated.

3.3.1. Diffusion of ammonia across the cell envelope of *C. glutamicum*

The ability of ammonia to diffuse passively across the cell membrane is an essential requirement for the formation of a putative futile cycle. Rapid diffusion of ammonia across cell membranes has already been demonstrated for different bacteria, e.g. *Synechococcus* R-2, *Rhodobacter spheroides*, and *Bacillus firmus* (Gibson *et al*., 1987a; 1987b). However, *C. glutamicum* has a more complex cell envelope with an additional permeability barrier, the mycolic acid layer (Puech *et al*., 2001). Therefore, the ability of ammonia to diffuse across the cell envelope of *C. glutamicum* was investigated. For this purpose, the *C. glutamicum* strain JS-1 was used. In JS-1, the *amtA* and the *amtB* gene coding for ammonium transporters are deleted, thus, no ammonium transporters are present in this strain. JS-1 was cultivated in CgC medium supplemented with casamino acids. Then, the cells were washed with a pre-warmed isoosmolar solution of 330 mM sodium chloride, and the internal concentrations of ammonium of unwashed and washed cells were measured by HPLC in order to investigate if internal ammonium can be washed out. Prior to washing, the intracellular concentration of ammonium was 11.4 mM (± 4.2 mM). This concentration was significantly diminished by one washing step (1.0 ± 1.2 mM). However, the drop of internal ammonium could also be a result of rapid assimilation of ammonium instead of diffusion out of the cell. Therefore, it was investigated if the amount of ammonium that was lost by washing of the cells is present in the washing buffer after the washing step. For this purpose, the intracellular and extracellular amounts of ammonium per cell pellet weight present in a pellet of unwashed cells were determined. After that, the cell pellet was resuspended in pre-warmed isoosmolar solution of 330 mM sodium chloride and

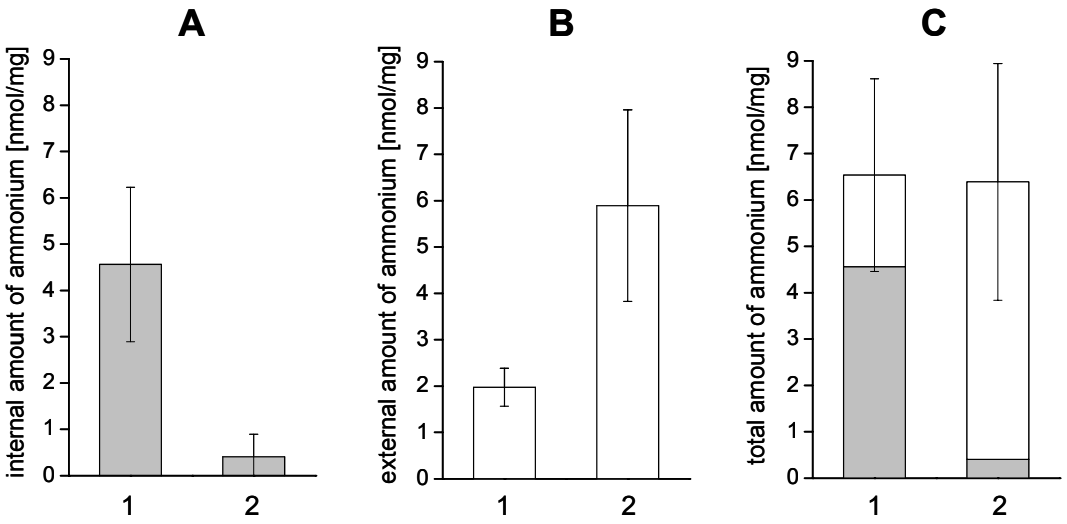

Figure 33: Internal and external amounts of ammonium before and after washing of the cells. The *amtAB* deletion strain JS-1 was cultivated in medium with casamino acids and cells were pelleted by centrifugation. The intracellular (grey bars) and extracellular (white bars) amounts of ammonium per cell pellet weight were determined in a cell pellet of unwashed cells (1) and after the cell pellet was resuspended in pre-warmed isoosmolar solution of 330 mM sodium chloride (2). A: internal amounts of ammonium per cell pellet weight. B: external amount of ammonium per cell pellet weight. C: total amount of internal (grey bars) and external (white bars) ammonium per cell pellet weight.

again the intracellular and extracellular amounts of ammonium per cell pellet weight were determined. The intracellular amount of ammonium per cell pellet weight was diminished by resuspension of the pellet in washing buffer (figure 33A), whereas the extracellular amount of ammonium per mg cell pellet weight raised significantly (figure 33B) as expected if the drop of internal ammonium concentrations during washing of the cell was caused by diffusion of ammonia out of the cell. As shown in, figure 33C, the total amount of ammonium per cell pellet weight did not change during resuspension of the cell pellet, thus, ammonium assimilation was negligible. It was the localization of ammonium that changed from intracellular to extracellular during the washing step. Thus, the cell envelope of *C. glutamicum* was obviously not a permeability barrier for ammonia and rapid diffusion of ammonia across the cell membrane occurred.

3.3.2. Growth of *C. glutamicum* under high concentrations of ammonium

To investigate putative ammonium toxicity, growth of *C. glutamicum* in the presence of high concentrations of ammonium was studied. The *C. glutamicum* strains ATCC13032, MJ6-18, and TMΔgdhΔglnA were investigated. ATCC 13032 is a *C. glutamicum* wild type strain, MJ6-18 is an *amtR* deletion strain lacking the global nitrogen regulator AmtR (Jakoby *et al.*, 2000), and TMΔgdhΔglnA, which was generated by allelic replacement as part of this work, lacks the *gdh* gene and the *glnA* gene, coding for the two ammonium assimilating enzymes of *C. glutamicum*.

Cultures of these strains were supplemented with raising concentrations of ammonium (0.5 M, 1 M, and 2 M) and growth was analyzed by following the optical density at 600 nm for 7 hours. TMΔgdhΔglnA was additionally supplemented with 100 mM glutamine to facilitate growth. As shown in figure 34, higher concentrations of ammonium caused a decrease in growth in all tested *C. glutamicum* strains.

To investigate if the retardation of growth is a specific effect caused by ammonium in particular, the concentration of ammonium was kept constantly at 0.5 M, and

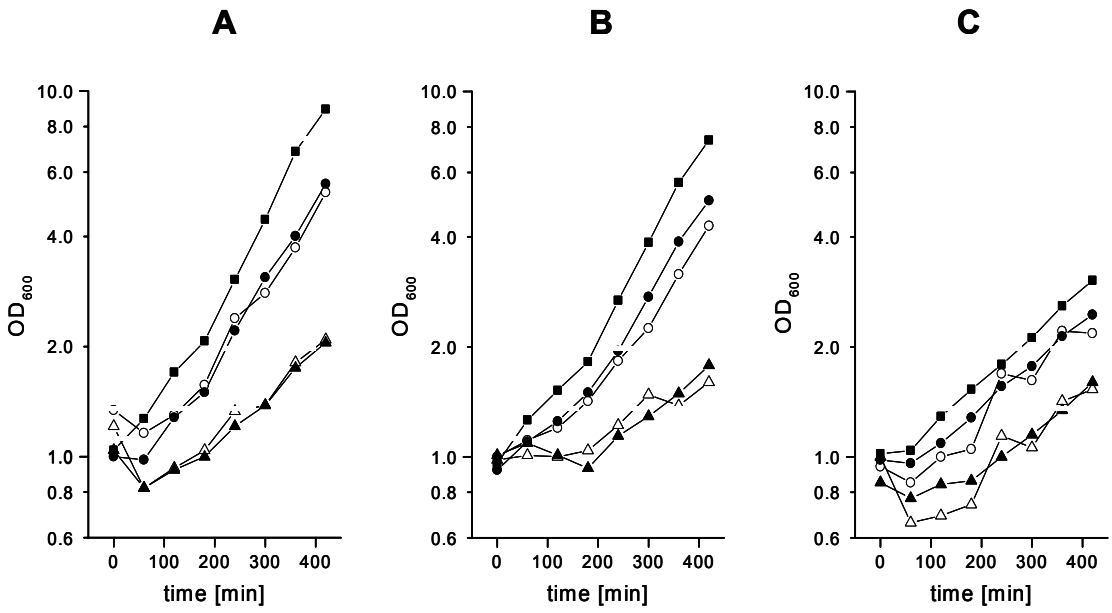

Figure 34: Growth of *C. glutamicum* strains under high ammonium concentrations. The *C. glutamicum* wild type ATCC13032 (A), the *amtR* deletion strain MJ6-18 (B), and TMΔgdhΔglnA, double deletion strain of *gdh* and *glnA* (C), were cultivated in CgC medium containing various concentrations of ammonium and Na^+ in form of ammonium sulphate and sodium sulphate, respectively. TMΔgdhΔglnA was additionally supplemented with 100 mM glutamine to facilitate growth. Black squares: 0.5 M ammonium. Black circles: 1 M ammonium. Black triangles: 2 M ammonium. Open circle: 0.5 M ammonium and 0.5 M Na^+. Open triangles: 0.5 M ammonium and 1.5 M Na^+.

raising amounts of sodium sulphate were added. Addition of sodium ions instead of ammonium caused an almost identical impairment of growth (figure 34). Thus, the observed retardation of growth was not caused specifically by ammonium, but is most probaly a general effect caused by the higher ionic strength or osmolarity of the medium. Thus, a specific toxicity of ammonium for *C. glutamicum* could not be observed.

3.3.3. Analysis of the presence of a putative futile cycle

The presence of ammonium transporters is an essential requirement for the formation of a putative futile cycle. Therefore, the expression levels of *amtA* and *amtB* were analyzed by RNA dot blot hybridization in ATCC 13032, MJ6-18, and TMΔgdhΔglnA cultivated under the conditions described above. In ATCC 13032, *amtA* and *amtB* were not expressed (figure 35), which might explain the absence of specific ammonium toxicity. However, *amtA* and *amtB* were expressed in MJ6-18 and TMΔgdhΔglnA under all tested conditions (figure 35). For MJ6-18, this is in accordance to previously described observations (Jakoby *et al*., 2000). In addition, B. Walter could demonstrate by uptake measurements of the ammonium analog [^{14}C]methylammonium that the ammonium transporters were active in both strains under the tested conditions (personal communication). Thus, all requirements for the formation of a putative futile cycle should be fulfilled. Nevertheless, a specific retardation of growth by ammonium could not be observed as described above.

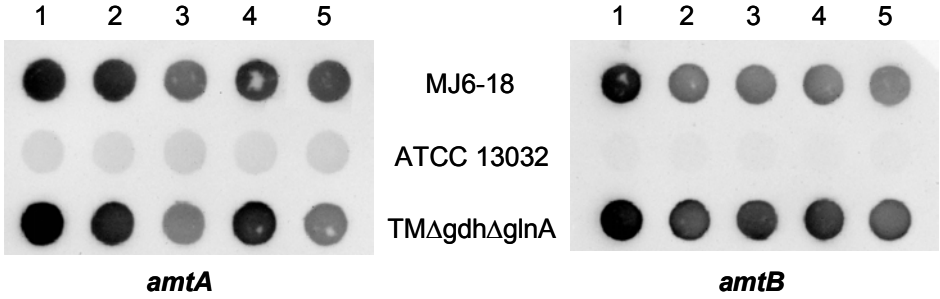

Figure 35: Expression of *amtA* and *amtB*. Using RNA dot blot hybridization, the expression of *amtA* and *amtB* were analyzed in the *C. glutamicum* wild type ATCC 13032, the *amtR* deletion strain MJ6-18, and a double deletion strain of *gdh* and *glnA* (TMΔgdhΔglnA), respectively, in response to the addition of $(NH_4)_2SO_4$ and Na_2SO_4, respectively. The strains were cultivated in CgC medium containing 0.5 M ammonium (1), 1 M ammonium (2), 2 M ammonium (3), 0.5 M ammonium and 0.5 M Na^+ (4), and 0.5 M ammonium and 1.5 M Na^+ (5), respectively. TMΔgdhΔglnA was additionally supplemented with 100 mM glutamine to facilitate growth.

However, in case of MJ6-18, one could postulate that ammonium might be assimilated by GDH and GS immediately after it has entered the cell and therefore can not diffuse out of the cell again to cause a putative futile cycle. Nevertheless, this should not happen in case of TMΔgdhΔglnA, as both assimilation systems are absent in this strain. To support this, ammonium assimilation by TMΔgdhΔglnA was studied. Surprisingly, TMΔgdhΔglnA was able to grow on medium with ammonium as the exclusive nitrogen source (figure 36). Thus, a third enzyme for ammonium assimilation must be present in *C. glutamicum*, which is unknown. However, TMΔgdhΔglnA grew only very slowly under these conditions. Thus, the putative new assimilation system should have only a very low activity, and ammonium assimilation in the TMΔgdhΔglnA strain should not be fast enough to prevent a putative futile cycle. Nevertheless, TMΔgdhΔglnA showed no specific growth retardation due to high concentrations of ammonium as described above. Thus, no indications for the presence of a energy-wasting transmembrane cycle of ammonium could be observed even in the presents of AmtA and AmtB and in the absence of GDH and GS.

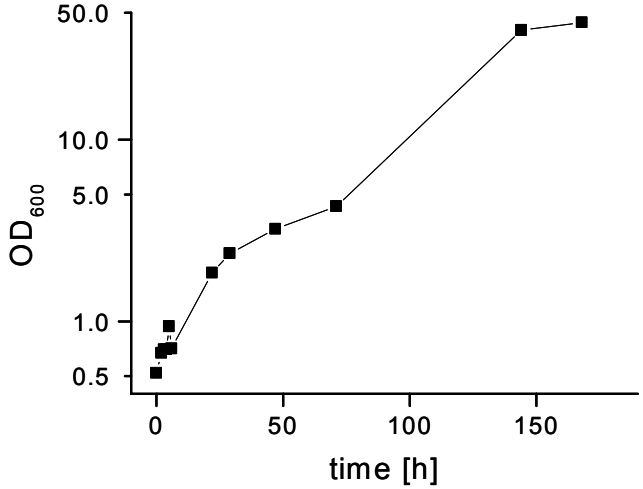

Figure 36: Growth of the double deletion strain of *gdh* and *glnA*. The double deletion strain TMΔgdhΔglnA was cultivated in medium containing ammonium as the exclusive nitrogen source for 180 hours. Growth was analyzed by following the optical density at 600 nm.

4. Discussion

Nitrogen control in *C. glutamicum* was investigated mainly in the last years. Several compounds of nitrogen metabolism, transport, and regulation are now well-characterized (Burkovski, 2003a; 2003b; 2005). Among those factors, glutamate dehydrogenase seems to play an important but less investigated role in nitrogen control of *C. glutamicum*. In this work, regulation of glutamate dehydrogenase and its impact on nitrogen control of *C. glutamicum* were investigated.

4.1. Regulation of glutamate dehydrogenase

Glutamate dehydrogenase assimilates ammonium under nitrogen surplus, whereas the glutamine synthetase/glutamate synthase pathway is downregulated under these conditions. However, as GDH has only a low affinity to ammonium, assimilation *via* GDH is not sufficient under nitrogen limitation. Consequently, the GS/GOGAT system with a high affinity to ammonium is upregulated under nitrogen limitation to ensure ammonium assimilation, whereas expression of GDH is either downregulated or remains constant under nitrogen limitation in most bacteria (Brenchley *et al*., 1975; Schwacha *et* al., 1993; Merrick and Edwards, 1995; Camarena *et al*., 1998). In accordance to this, GDH from *C. glutamicum* was first reported to be unaffected by nitrogen supply. Tesch *et al*. (1999) could not observe a significant change in GDH activity of *C. glutamicum* in response to changes in nitrogen supply. This observation was supported by transcriptome analyses of *C. glutamicum* cultivated under nitrogen excess and nitrogen limitation, where *gdh* transcription was observed to be unaffected (Beckers, 2004; Silberbach, 2004). In contrast to this, L. Nolden observed a significant increase in *gdh* transcription as well as GDH activity under nitrogen limitation (personal communication), which is remarkable, since an upregulation of GDH under nitrogen limitation has never been described before in bacteria. Because of these controversial observations, the regulation of *gdh* expression in response to nitrogen supply was reinvestigated as part of this work. The results obtained here clearly demonstrate that glutamate dehydrogenase is under nitrogen control. Nitrogen limitation caused a significant increase of the level of *gdh* mRNA, GDH protein, and GDH activity in *C. glutamicum*. Thus, expression of glutamate dehydrogenase is indeed upregulated

under nitrogen limitation in *C. glutamicum*. However, the reason for the discrepancy to the observations made by Tesch *et al*. (1999), Beckers (2004), and Silberbach (2004) is still unclear.

The underlying regulatory mechanism for the induction of GDH under nitrogen limitation was unknown as well. Because of that, the main aim of this work was the analysis of the nitrogen-dependent regulation of glutamate dehydrogenase in *C. glutamicum*.

In a first approach, it was demonstrated that nitrogen-dependent regulation of glutamate dehydrogenase occurs only on the level of expression. Regulation of GDH activity by posttranslational modifications could not be observed. This was demonstrated by creating a genetically engineered strain of *C. glutamicum*, where transcription of *gdh* was constant and nitrogen-independent. In this strain, GDH activity was not nitrogen-regulated anymore. Thus, GDH activity is directly correlated with the transcription level of *gdh* and a nitrogen-dependent regulation of GDH activity by posttranslational modifications is not present. This observation is in accordance with the fact that regulation of bacterial GDHs by posttranslational modifications is unknown (Minabres *et al*., 2000).

In addition, it could be demonstrated that a nitrogen-dependent regulation of the degradation rate of *gdh* mRNA is not present. The transcription rate of *gdh* is induced under nitrogen limitation, whereas the degradation rate of *gdh* mRNA is constant. Thus, glutamate dehydrogenase is regulated only on the level of transcription under the investigated conditions.

The part of the *gdh* promoter region that is responsible for nitrogen-dependent control was identified by reporter genes assays. By this approach, the 550 bp DNA sequence upstream of the *gdh* gene, which harbours the transcription start and all basic elements of the core promoter of *gdh* (Börmann *et al*., 1992), was found to be sufficient for a nitrogen-dependent expression. Thus, this 550 bp fragment of the *gdh* promoter region harbours the regulatory element for nitrogen-dependent transcription control, e.g. a binding site for a putative transcriptional regulator.

This part of the *gdh* promoter region was used to isolate putative transcriptional regulators of *gdh* by DNA affinity purification with magnetic beads. Four partially overlapping 200 bp DNA fragments were used as target DNAs, which span the 550

bp fragment of the *gdh* promoter. Purified proteins were identified by peptide mass fingerprinting. All isolated proteins were DNA-binding proteins as expected. Among these were DNA- and RNA-polymerase subunits and a helicase. These proteins bound to all four target DNAs. Thus, binding was unspecifically as one would expect for these proteins. In addition, four transcriptional regulators were isolated, which bound only to distinct parts of the *gdh* promoter. Thus, binding of these proteins was sequence-specific, which is typical for transcriptional regulators (Wagner, 2000). One of them is AmtR, the global transcriptional regulator of nitrogen control in *C. glutamicum*. The others have not been characterized in *C. glutamicum* yet, but by sequence alignments, they were found to be similar to the transcriptional regulators FarR from *E. coli*, WhiH from *S. coelicolor*, and OxyR from *M. leprae*, respectively. None of them has been described as a regulator of *gdh* transcription yet.

AmtR is the master regulator of nitrogen control in *C. glutamicum* and it represses the transcription of several genes of nitrogen metabolism, transport, and regulation under nitrogen limitation (Beckers, 2004). Nevertheless, binding of AmtR to the *gdh* promoter is astonishing, since AmtR does not seem to be responsible for nitrogen control of *gdh* transcription. It could be demonstrated that a deletion of *amtR* does not affect *gdh* transcription (L. Nolden, personal communication). Nevertheless, binding of AmtR to the *gdh* promoter could be clearly demonstrated in this work. The sequence-specific affinity of AmtR to distinct parts of the *gdh* promoter, which was observed by DNA affinity purification with magnetic beads, could be verified by gel shift assays. In addition, two distinct 25 bp binding sites of AmtR could be identified within the *gdh* promoter by gel shift assays. As expected, the sequences of these binding sites are homologous to the known consensus binding motif of AmtR from *C. glutamicum* (Beckers, 2004). One binding site is located 62 bp upstream of the start of transcription of *gdh* and the other 87 bp downstream of the start of transcription of *gdh*, which is a typically arrangement for AmtR. So far, the exact locations of AmtR binding sites compared to the start of transcription have been described for *amtA* (Jakoby *et al*., 2000) and *gltB* (Beckers *et al*., 2001; 2005). In both cases, two AmtR binding sites are present in the respective promoter regions, and in accordance to *gdh*, one is located upstream of the start of transcription, whereas the second binding site is located either downstream of the start of transcription (*gltB*) or exactly at the start of transcription (*amtA*). In addition, it could

be demonstrated in this work that four AmtR units (four AmtR monomers or four AmtR oligomers) can bind to the *gdh* promoter region, i.e. two AmtR units per binding site. This binding behaviour is also in accordance with previous observations. The two binding sites of the *gltB* promoter region can also bind four AmtR units (Beckers *et al*., 2001), whereas the *amtA* promoter region binds three AmtR units (Jakoby *et al*., 2000). Beside that, it could be demonstrated in this work that one of the two AmtR binding sites of the *gdh* promoter region has a significantly higher affinity to AmtR than the other binding site. This could be revealed by competition assays, and is in accordance to the estimated binding affinities of AmtR to the *gdh* promoter region. The affinities of two AmtR binding sites within one promoter region have not been investigated before for AmtR of *C. glutamicum*. However, the results obtained here are in accordance to general models of transcription control. The high affinity binding site of the gdh promoter region is the one located 87 bp downstream of the start of transcription, which is a typical location for a binding site of a transcriptional repressor (Wagner, 2000). The presence of a second low affinity binding site 150 bp upstream of the high affinity binding site is also a typical feature of transcription control. Such additional low affinity binding sites can cause higher local concentrations of the transcription factor around the high affinity binding site and, thereby, direct the transcription factor to the high affinity site making transcription control more efficient (Dröge and Müller-Hill, 2001). Thus, binding of AmtR to the *gdh* promoter could be clearly demonstrated and the sequences, locations, and affinities of the respective binding sites are consistent with previously investigated target genes of AmtR and general models of transcription control. Thus, these *in vitro* studies did not provide reasons why AmtR should not affect *gdh* transcription. Nevertheless, a deletion of *amtR* does not affect *gdh* transcription and has no effect on nitrogen-control. The reasons for this discrepancy are still unknown. One can speculate that transcription of *gdh* is regulated by more than one transcription factor and that a deletion of *amtR* can be compensated by another regulator with redundant function. However, this has not been proven yet.

The second putative transcription factor that could be isolated by magnetic DNA affinity purification using the *gdh* promoter region as target DNA has not been characterized in *C. glutamicum* yet, but it is similar to the transcriptional regulator

FarR from *E. coli*. The function of FarR from *E. coli*, which is a HutC/FarR-type regulator of the GntR family, has been described controversially as a fatty acyl responsive regulator of TCA cycle genes (Quail *et al*., 1994) and as a regulator of genes coding for a 2-*O*-α-mannosyl-D-glycerate transport and metabolism system (Sampaio *et al*., 2004). In principle, HutC/FarR-type regulators of the GntR family regulate genes of the central metabolism (Rigali *et al*., 2002) and are modulated in their activity by binding of small effector molecules (Aravind *et al*., 2003). During the DNA affinity purification with magnetic beads described here, FarR from *C. glutamicum* exhibited an interesting binding behaviour. It was isolated only from a total protein extract of *C. glutamicum* cultivated under nitrogen excess, but not from a total protein extract of *C. glutamicum* cultivated under nitrogen limitation. Thus, binding of FarR from *C. glutamicum* was somehow nitrogen-dependent. The capacity of FarR to bind specifically to distinct parts of the *gdh* promoter as demonstrated by magnetic DNA affinity purification was verified by gel shift assays. A distinct 25 bp binding site of FarR from *C. glutamicum* could be identified within the *gdh* promoter. This binding site harbours a palindromic sequence, which was assumed to be the FarR binding motif. Palindromic sequences are a typical feature of binding sites of transcription factors (Wagner, 2000). In addition, the sequence of the FarR binding site is homologous to the consensus binding motif of the HutC/FarR-type regulators of the GntR family (Rigali *et al*., 2002). It is located 172 bp upstream of the start of transcription of *gdh*. Typically, binding sites of transcriptional activators are located upstream of the core promoter, whereas this is uncommon for transcriptional repressors (Wagner, 2000). However, FarR of *C. glutamicum* was found to repress transcription. This was demonstrated by reporter gene assays of an *E. coli* strain harbouring a plasid-coded fusion of the *gdh* promoter region of *C. glutamicum* and a reporter gene. Heterologous expression of FarR from *C. glutamicum* in this *E. coli* strain caused a significant decrease of the expression of the reporter gene. Conclusively, specific binding of FarR to a distinct binding site within the *gdh* promoter region as well as a principle capacity of FarR to repress transcription could be demonstrated. Surprisingly, a deletion of *farR* from *C. glutamicum* has no effect on *gdh* transcription. Possibly, a deletion of *farR* can be compensated by another transcription factor with redundant function, or FarR

regulates *gdh* transcription only in response to certain conditions which have not been tested yet.

The third transcription factor that could be isolated by DNA affinity purification with magnetic beads is similar to WhiH from *S. coelicolor*, which is also a member of the GntR-family of transcriptional regulators. WhiH from *S. coelicolor* regulates transcription during the late phase of sporulation, however, the corresponding target genes are unkown (Ryding *et al*., 1998). During the DNA affinity purification with magnetic beads, WhiH from *C. glutamicum* bound specific to distinct parts of the *gdh* promoter. Until now, this could not be verified by gel shift assays. Again, a single deletion of the corresponding gene, *whiH*, had no effect on *gdh* transcription, which might have the same reasons as described for AmtR and FarR.

Another transcription factor that could be isolated by DNA affinity purification with magnetic beads is similar to OxyR from *M. leprae*, which is a LysR-type transcriptional regulator. In many organisms, OxyR-like regulators control transcription in response to oxidative stress. A distinct disulfide bound of OxyR is oxidized under peroxide stress, which triggers regulation of transcription of several genes of scavenging enzymes as well as of protection and repair systems (Christman *et al*., 1989; Storz *et al*., 1990; Mostertz *et al*., 2004). OxyR has not been described as a regulator of glutamate dehydrogenase yet. The specific binding of OxyR from *C. glutamicum* to a distinct part of the *gdh* promoter region, which was observed by DNA affinity purification with magnetic beads, could not be verified by gel shift assays yet. As observed for *amtR*, *farR*, and *whiH*, a single deletion of *oxyR* had no effect on *gdh* transcription.

Thus, four transcriptional regulators that bind specifically to the *gdh* promoter region could be identified. Surprisingly, none of these transcriptional regulators is responsible for nitrogen-dependent control of *gdh* transcription. Neither dot blot hybridization experiments nor quantitative real time PCR studies revealed any difference in *gdh* transcription between the *C. glutamicum* wild type and the single deletion strains of *amtR*, *farR*, *whiH*, and *oxyR*, respectively. Nitrogen-dependent regulation of *gdh* transcription was still observable in these mutant strains. For AmtR, this result is in accordance to previous observations (L. Nolden, personal communication). To investigate a putative functional redundancy of AmtR, FarR,

WhiH, and OxyR, multiple deletion strains were analyzed. None of the multiple deletions affected nitrogen-dependent *gdh* transcription. Even a quadruple deletion of all four regulators had no effect on transcription of *gdh*. Thus, a functional redundancy among the regulators could not be observed under the tested conditions. These results clearly show that AmtR, FarR, WhiH, and OxyR are not essential for transcription control of *gdh* in response to nitrogen starvation. Their deletion can either be compensated by other regulators or these transcription factors affect *gdh* transcription only under conditions that have not been tested yet. Consequently, another regulatory mechanism must be present in *C. glutamicum* which regulates *gdh* transcription in response to nitrogen supply. Using the approach of magnetic DNA affinity purification, a relevant transcriptional regulator could not be isolated. A possible explanation for this is that the assumed relevant transcriptional regulator did not bind under the conditions of the magnetic DNA affinity purification. For example, some transcriptional regulators need certain ligands or other interacting proteins to be able to bind to DNA. These might have been not present or not in the correct concentration during the purification procedure. In addition, for some regulators protein modifications are important. However, modifications like phosphorylation are known to be relatively unstable *in vitro*.

It is also possible, that nitrogen-dependent control of *gdh* transcription is not performed by a transcriptional regulator but by a different regulatory mechanism. This idea is supported by the fact that transcription of *gdh* starts 284 bp upstream of the first codon of the *gdh* gene. Thus, the mRNA of *gdh* possesses a 284 bp leader mRNA, which is relatively large for *C. glutamicum*. Normally, leader mRNAs that are larger than 150 bp exhibit a regulatory function in *C. glutamicum* (M. Pátek, personal communication). One possibility is translation-dependent attenuation. Attenuation describes the control of transcription by regulated termination of mRNA synthesis. The decision between termination and readthrough is triggered by the translation of a leader peptide from the growing mRNA chain. This leader peptide is encoded by an open reading frame on the leader mRNA and contains a cluster of certain amino acids (Wagner, 2000). Seven putative open reading frames could be identified within the leader mRNA of *gdh*, but none of them contains a significant accumulation of a certain amino acid. As such an accumulation is essential for

translation-dependent attenuation, *gdh* transcription is most likely not regulated by this mechanism. Thus, the role of the 284 bp leader mRNA of *gdh* is still unknown.
Beside that, transcription control can be achieved by several other mechanisms, e.g. by alternative σ factors, stringent control, translation-independent attenuation, or regulated antitermination (Wagner, 2000). However, these regulatory mechanisms have not been investigated in this work, but should be continued in future work. Thus, the regulatory mechanism that controls *gdh* transcription in response to nitrogen starvation is still unknown.

AmtR, FarR, OxyR, and WhiH do not regulate *gdh* transcription in response to nitrogen starvation, however, they might regulate *gdh* transcription under conditions which have not been tested so far, i.e. they respond to other stress conditions than nitrogen starvation. In this work, various approaches were used to identify conditions that trigger regulation of *gdh* transcription by AmtR, FarR, WhiH, and OxyR.
To get an idea about the function of FarR and WhiH *in vivo*, DNA microarrays were used to identify putative target genes of FarR and WhiH. In the *farR* deletion strain, the expression of several genes of arginine biosynthesis was induced compared to the wild type, namely *argBCDFJ*, *carB*, *glnA*, and *argR*. However, several other experiments did not support a putative role of FarR as a regulator of arginine biosynthesis. An increase of internal concentration of arginine could not be observed in the *farR* deletion strain. Beside that, FarR does not regulate transcription of *gdh* in response to the addition of arginine or the arginine precursors citrulline and ornithine. Using gel shift assays, binding of FarR to the promoter regions of *argC*, *argG*, and *argR*, respectively, could not be demonstrated yet (E. Hänßler, personal communication). Thus, FarR is most likely not a repressor of arginine biosynthesis genes and the induced expression of these genes in the *farR* deletion strain observed by DNA microarray experiments was most probably a secondary effect caused by metabolic perturbations.
DNA microarray analysis of the *whiH* deletion strain vs. the wild type did not revealed any putative target genes of WhiH. The fact that a differential expression of putative target genes of FarR and WhiH could not be observed by DNA microarray

analyses supports the idea that FarR and WhiH were not active under the tested conditions.

Using a bioinformatical approach, the *dtsR2* gene could be identified as a putative target gene of FarR. In this approach, the FarR binding motif of the *gdh* promoter was used to identify other putative binding sites of FarR within the genome of *C. glutamicum*. For one of the resulting putative binding sites, binding of FarR could be verified by competition gel shift assays. This FarR binding site is located 174 bp upstream of *dtsR2*. Thus, *dtsR2* is another putative target gene of FarR beside *gdh*. The *dtsR2* gene codes for DtsR2, which is a homolog of the detergent sensitive rescuer protein DtsR1. DtsR1 and DtsR2 are involved in fatty acid biosynthesis and

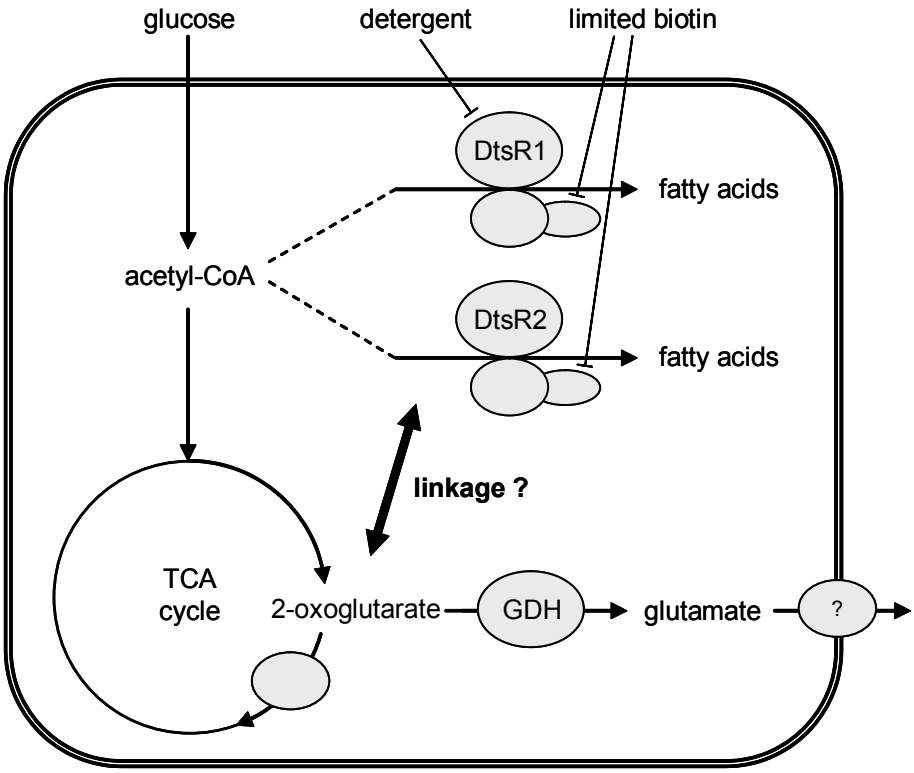

Figure 37: Overproduction of glutamate by *C. glutamicum*. Overproduction of glutamate is induced under biotin limitation or in the presence of detergents. Under both conditions, the level of a detergent sensitive rescue protein (DtsR1) is decreased. DtsR1 and its homolog DtsR2 are counterparts of biotin-binding acyl-CoA carboxylase (AccBC) This protein complex is involved in fatty acid biosynthesis in *C. glutamicum*. A decreased level of DtsR1 causes a decrease of the activity of 2-oxoglutarate dehydrogenase (ODHC) by a still unknown regulatory mechanism. A decrease of ODHC activity induces a drastic metabolic flux change towards glutamate production by glutamate dehydrogenase (GDH). Accumulated glutamate is then exported most probably by a specific transporter, which is still unknown. (Kinura, 2002)

act as counterparts of biotin-binding acyl-CoA carboxylase (AccBC) (Kimura, 2002). This protein complex catalyzes the first step of fatty acid biosynthesis of *C. glutamicum* (figure 37). Deletion of *dtsR1* causes a strict fatty acid auxotrophy (Kimura *et al*., 1997), whereas deletion of *dtsR2* causes only an altered fatty acid composition (Kimura, 2002). Whereas the function of DtsR2 is less clear, the role of DtsR1 has been further studied, DtsR1 was isolated by its ability to inhibit an overproduction of glutamate (Kimura *et al*., 1996). Overproduction of glutamate can be induced by biotin limitation or by the addition of detergents (figure 37) (Shiio *et al*., 1962; Takinami *et al*., 1965; Duperray *et al*., 1992). In both cases, the level of DtsR1 decreases (Kimura *et al*., 1999), which causes changes of the fatty acid composition of *C. glutamicum* as well as a decrease of the activity of 2-oxoglutarate dehydrogenase (ODHC) by a still unknown regulatory mechanism. A decrease of ODHC activity induces a drastic metabolic flux change towards glutamate production by GDH (Kawahara *et al*., 1997). Accumulated glutamate is then exported most probably by a specific transporter, which is still unknown (Hoischen *et al*., 1990; Gutmann *et al*., 1992; Krämer, 1994). This effect can be complemented by an overexpression of *dtsR1* (Kimura *et al*., 1996). Thus, the level of DtsR1 plays an important role in the triggering mechanism of glutamate overproduction. However, the role of DtsR2 for glutamate production is less clear. Beside that, the regulatory mechanism that provides the linkage between the DtsR proteins and the metabolic flux change towards the production of glutamate is unknown (figure 37). As FarR binds to the promoter regions of *gdh* and *dtsR2*, one can speculate about a putative role of FarR in this process. This idea is supported by the fact that FarR from *E. coli* has been described as a fatty acyl responsive regulator of TCA cycle genes. Referred to this, FarR from *E. coli* represses transcription of genes coding for subunits of 2-oxoglutarate dehydrogenase, pyruvate dehydrogenase, and citrate synthase. Repression is released in the presence of long chain fatty acids or their CoA thioesters, which bind to FarR from *E. coli* as effector molecules (Quail *et al*., 1994). However, a recent publication about FarR from *E. coli* is in contradiction to this and describes FarR from *E. coli* as a regulator of genes coding for a 2-*O*-α-mannosyl-D-glycerate transport and metabolism system (Sampaio *et al*., 2004).

However, FarR does not seem to be specifically influenced by fatty acids. As part of this work, a diverse range of metabolites were tested with respect to their ability to influence binding of FarR from *C. glutamicum* to the *gdh* promoter region. Most of the tested substances had no effect on FarR from *C. glutamicum*. Only the fatty acid salts sodium myristate and sodium palmitate, respectively, inhibited binding of FarR to the *gdh* promoter region. However, further experiments revealed that this effect was most probably not the result of a specific interaction of myristate and palmitate with a putative ligand binding domain of FarR. These substances most probably just denatured FarR in a detergent-like manner. This was demonstrated by analysis of substances similar to myristate and palmitate. Sodium dodecylsulfate (SDS), cetyl trimethyl ammonium bromide (CTAB), and sodium oleate also inhibited binding of FarR to the *gdh* promoter region. Especially for CTAB, this result is remarkable, since this molecule is positively charged in contrast to myristate and palmitate, which are negatively charged. Thus, inhibition by sodium myristate and sodium palmitate was most probably unspecific. In addition, sodium myristate and sodium palmitate influence FarR only in high concentrations, which are not in the physiological range. In contrast, the application of sodium palmitate in the physiological range of concentrations had no effect on FarR. Thus, the role of FarR remains unclear.

As described previously, AmtR, FarR, WhiH, and OxyR might regulate *gdh* transcription in response to stress conditions other than nitrogen starvation. However, other stress conditions that affect *gdh* transcription have not been described before. As part of this work, a broad range of stress conditions could be identified, which influence *gdh* transcription in *C. glutamicum*. It could be demonstrated that variation of the carbon source and the nitrogen source, carbon starvation, oxygen limitation, chill stress, and the growth phase affects *gdh* transcription in *C. glutamicum*. In contrast, heat stress, oxidative stress, and osmotic stress had no influence on *gdh* transcription. However, analysis of the deletion strains of *amtR*, *farR*, *whiH*, and *oxyR* revealed that the corresponding regulators are not involved in regulation of *gdh* transcription in response to carbon starvation. Beside that, OxyR does not regulate *gdh* transcription in response to oxygen limitation. Nevertheless, several other stress conditions could be identified that

influence *gdh* transcription as described above, and the role of AmtR, FarR, WhiH, and OxyR with regard to those conditions can be tested in the future. Conclusively, transcription control of *gdh* seems to be very complex, since *gdh* is regulated in response to a broad range of stress conditions. This is in accordance to the results of the isolation of putative transcriptional regulators by magnetic DNA affinity purification. Four transcriptional regulators could be identified that bind to the *gdh* promoter indicating that *gdh* transcription control is a complex process.

Complex regulatory networks for the control of glutamate dehydrogenase expression are also present in other bacteria. In *B. subtilis*, expression of the *rocG* gene, coding for a NADH-dependent glutamate dehydrogenase, is under the control of several regulatory systems. The transcription factors RocR, AhrC, and CcpA, respectively, regulate *rocG* transcription in response to various conditions (Calogero *et al*., 1994; Belitzky *et al*., 2004). In addition, expression of *rocG* from *B*. *subtilis* depends on the σ_{54} factor as well as on an enhancer element located 1.5 kb downstream of the *rocG* gene (Belitsky *et al*., 1999; 2004). In *E. coli*, at least two transcriptional regulators influence transcription of *gdhA*, coding for a NADPH-dependent glutamate dehydrogenase. The transcription factor Nac represses transcription of *gdhA* in *E. coli* under nitrogen limitation, whereas another still unknown transcription factor activates *gdhA* transcription under the same conditions. These contrary regulations finally result in an unaltered expression of *gdhA* from *E. coli* under nitrogen limitation (Camarena *et al*., 1998). Thus, the observation that transcription control of *gdh* from *C. glutamicum* is complex and most probably regulated by several transcription factors, is in accordance to the situation in other bacteria.

4.2. The role of GDH in the nitrogen regulation network of *C. glutamicum*

In the second part of this work, the role of glutamate dehydrogenase in the nitrogen regulation network of *C. glutamicum* was investigated. It has been observed previously, that glutamate dehydrogenase is essential for a functional nitrogen control in *C. glutamicum*. A deletion of *gdh*, coding for glutamate dehydrogenase, leads to a loss of nitrogen-dependent transcription control by the GlnD/GlnK/AmtR signal cascade resulting in a constitutive expression of genes that are nitrogen-

regulated in the wild type (L. Nolden, personal communication). However, the underlying mechanism of this effect was unknown. As part of this work, it could be demonstrated that GDH activity and not the GDH protein itself is essential for nitrogen control. This is supported by two observations. First, GDH from *E. coli* heterologously expressed in the *gdh* deletion strain of *C. glutamicum* was able to restore nitrogen control. This non-*C. glutamicum* GDH was most probably not able to perform a specific protein interaction. Thus, it was the enzymatic activity of GDH from *E. coli* that complemented the loss of nitrogen control in the *gdh* deletion strain of *C. glutamicum*. Second, an enzymatically inactive GDH from *C. glutamicum* did not restore nitrogen control in the *gdh* deletion strain. This inactive GDH was generated by the single amino acid exchange of lysine 92 in the active centre of GDH by a leucine residue, which resulted in loss of enzymatic activity. It has been demonstrated for GDH from *Clostridium symbiosum* by analyses of crystal structures that an alteration of this conserved amino acid does not change the conformation of this protein (Stilmann *et al*., 1999). Referred to this, GDH from *C. glutamicum* carrying this single point mutation should still able to perform a putative protein interaction when expressed in the *gdh* deletion strain, but it is not able to restore GDH activity. As this enzymatically inactive GDH was not able to complement the loss of nitrogen control in the *gdh* deletion strain, it is the GDH activity, which is essential for a functional nitrogen control by the GlnD/GlnK/AmtR signal cascade. Thus, the effect caused by the deletion of *gdh* is a metabolic effect, i.e. the lack of GDH activity causes changes in the concentration of one or more metabolites that serve as indicator(s) for the nitrogen status in *C. glutamicum* and thereby cause the loss of nitrogen control.

To identify the metabolites that indicate the nitrogen status in *C. glutamicum*, internal concentration of ammonium, 2-oxoglutarate, glutamate, and glutamine were measured in the *C. glutamicum* wild type, the *gdh* deletion strain, and a *glnA* deletion strain under various nitrogen conditions. By this approach, it could be demonstrated that at least two metabolites trigger nitrogen control. One of them is most probably ammonium. In high concentrations, ammonium indicated nitrogen surplus in *C. glutamicum* resulting in repression of transcription by AmtR. Under nitrogen limitation, low ammonium concentrations caused derepression of transcription by AmtR and the respective target genes were expressed. This was

demonstrated using a *glnA* deletion strain, where changes in the concentrations of ammonium were sufficient to regulate nitrogen control, whereas glutamate, glutamine, and 2-oxoglutarate could be excluded to mediate this effect. Nevertheless, it could not be completely excluded, that a metabolite involved in the third yet unknown ammonium assimilation pathway indicates the nitrogen status. However, assimilation of ammonium *via* this pathway is very slow, thus, the concentrations of the involved metabolites can be assumed to change relatively slowly in response to changes in the availability of ammonium. Because of that, these metabolites are not suitable to trigger the relatively fast response of the GlnD/GlnK/AmtR signal cascade. Hence, it is most probably ammonium itself that indicates the nitrogen status of *C. glutamicum*. Until now, it is not clear whether the intracellular concentration or the extracellular concentration of ammonium is sensed by *C. glutamicum*, as both correlated with nitrogen control by AmtR under the tested conditions.

The second metabolite that triggers transcription control by AmtR is most probably 2-oxoglutarate or any other metabolite of the central carbon metabolism connected to 2-oxoglutarate. If 2-oxoglutarate was present in high concentrations in the cytoplasm (approximately 4.2 mM), repression of transcription by AmtR was released. This occurred even under high concentrations of ammonium, which normally indicate nitrogen surplus. Thus, a high 2-oxoglutarate pool can antagonize the status of nitrogen surplus and trigger a nitrogen-starvation-like response by the GlnD/GlnK/AmtR signal cascade even in the presence of ammonium. Under low internal concentrations (≤ 1.2 mM), 2-oxoglutarate had no effect on nitrogen control under the tested conditions.

In contrast, the internal concentrations of glutamine and glutamate do obviously not affect nitrogen control by the GlnD/GlnK/AmtR signal cascade. This result is in accordance with previously published data (Nolden *et al*., 2001b). However, it still cannot be excluded completely that glutamine is an effector of nitrogen regulation in *C. glutamicum*. For example, regulation of GS activity by adenylylation through ATase works independently of the GlnD/GlnK/AmtR signal cascade in an unknown way (Burkovski, 2003b).

Conclusively, nitrogen control of *C. glutamicum* is affected by at least two signals, which are most probably ammonium and 2-oxoglutarate. Ammonium indicates the

nitrogen status of *C. glutamicum*. In addition, accumulation of 2-oxoglutarate can antagonize the status of nitrogen surplus resulting in a nitrogen-starvation-like response.

The loss of nitrogen control in the *gdh* deletion strain, which is a metabolic effect, was directly correlated to the internal concentration of 2-oxoglutarate. Due to the lack of 2-oxoglutarate consuming GDH, 2-oxoglutarate was accumulated under nitrogen surplus in the *gdh* deletion strain. This seems to trigger the expression of AmtR-regulated genes, which are normally repressed in the wild type under these conditions. Consequently, the loss of nitrogen control by the GlnD/GlnK/AmtR signal cascade was most probably caused by an accumulation of 2-oxoglutarate under nitrogen surplus due to the lack of 2-oxoglutarate-consuming GDH.

Comparison of the nitrogen control of *C. glutamicum* and that of the model organism *E. coli* revealed several substantial differences, but also some similarities. One of the two metabolites that influence nitrogen-dependent regulation in *E. coli* is glutamine (Jiang *et al*., 1998a). In contrast, the availability of nitrogen in *C. glutamicum* is indicated most probably by ammonium and not by glutamine. In *E. coli*, internal glutamine is sensed by UTase (Jiang *et al*., 1998a), whereas the UTase homolog in *C. glutamicum*, GlnD, is probably not a primary sensor of the nitrogen status (Nolden *et al*., 2001b). In a recent publication, a putative role of the ammonium transporter AmtB of *E. coli* as a sensor for external ammonium was discussed (Javelle *et al*., 2004). However, in *C. glutamicum*, this possibility can be excluded, as a double deletion of *amtA* and *amtB*, coding for the two ammonium transporter of *C. glutamicum*, had no effect on nitrogen control of *C. glutamicum* (J. Strösser, personal communication). Thus, the first signal as well as the corresponding sensor for the availability of nitrogen in *C. glutamicum* differs substantially from that of *E. coli*.

The second metabolite that influences the nitrogen regulation network of *C. glutamicum* is most probably 2-oxoglutarate. This is in accordance to *E. coli*, where internal 2-oxoglutarate also affects nitrogen control in response to the carbon or energy status of the cell (Jiang *et al*., 1998a; 1998b; Arcondeguy *et al*., 2001). In *C. glutamicum* as well as in *E. coli*, an accumulation of 2-oxoglutarate antagonizes the status of nitrogen surplus and causes a nitrogen starvation-like response even

under good nitrogen supply. The internal concentrations of 2-oxoglutarate in *C. glutamicum* and *E. coli* are more or less in the same range. In *C. glutamicum*, the internal concentration ranges from 0.3 mM to 8 mM, whereas, between 0.1 mM and 0.9 mM 2-oxoglutarate are present in *E. coli* (Senior, 1975). In *E. coli* as well as in several other bacteria, internal 2-oxoglutarate is sensed by PII proteins, which are integral components of the nitrogen control networks (Ninfa *et al*., 2005). A PII-type protein, GlnK, is also present in *C. glutamicum* (Nolden *et al*., 2001b). However, it could not be demonstrated yet that GlnK of *C. glutamicum* is a sensor of internal 2-oxoglutarate.

4.3. Investigations of a putative toxicity of ammonium for *C. glutamicum*

In the third part of this work, a putative toxicity of ammonium for *C. glutamicum* was investigated. In contrast to the situation in plants (Britto *et al*., 2001; Kronzucker *et al*., 2001; Britto *et al*., 2002) and animal cells (Martinelle *et al*., 1993), a specific toxicity of ammonium for *C. glutamicum* could not be observed. Rising concentrations of ammonium caused a decrease in growth of *C. glutamicum* However, this was not caused specifically by ammonium but by the rising ionic strength or osmolarity of the medium. Thus, ammonium is not specifically toxic for *C. glutamicum* even in molar concentrations. This makes sense from the physiological point of view, since ammonium is the preferred nitrogen source of *C. glutamicum*. In addition, *C. glutamicum* even produces ammonium when it is forced to grow on glutamate as sole carbon and nitrogen source (A. Burkovski, personal communication).

As a reason for putative ammonium toxicity, the formation of a putative futile transmembrane cycle of ammonium was discussed. According to the model of a futile ammonium cycle, ammonium would first be transported into the cell by the use of energy and then it would diffuse passively back out of the cell resulting in a detrimental waste of energy (Castorph *et al*., 1984; Kleiner, 1985). However, no indications for the presence of a putative futile transmembrane cycle of ammonium in *C. glutamicum* could be observed in this work. It could be demonstrated that rapid diffusion of ammonia across the cell membrane most probably occurs in *C. glutamicum*. This is in accordance to other bacteria, e.g. *Synechococcus* R-2,

Rhodobacter spheroides, and *Bacillus firmus* (Gibson *et al*., 1987a; 1987b). In addition, B. Walter demonstrated that the ammonium transporters AmtA and AmtB are active in the *amtR* deletion strain and the double deletion strain of *gdh* and *glnA* of *C. glutamicum* under the tested conditions (personal communication). Thus, all requirements for the formation of a putative futile cycle should have been fulfilled in these strains under the tested conditions. In the double deletion strain of *gdh* and *glnA*, the situation is even more extreme. The main ammonium assimilation systems, GDH and GS, are absent, while a third still unknown assimilation system has only a very low activity. Thus, ammonium assimilation in this strain should not be fast enough to prevent a loss of ammonium by diffusion immediately after it has entered the cell by active transport. Nevertheless, in all tested strains, ammonium had no detrimental effect on growth. Thus, putative futile transmembrane cycling of ammonium does not occur in the studied *C. glutamicum* strains or its putative negative effect is negligible.

This result is remarkable, since such a putative detrimental effect of ammonium cycling was always discussed as a reason for the strict regulation of the ammonium transporters. In addition, the absence of a detrimental effect suggests that uptake of ammonium by transporters is energy-independent. However, the mode of transport by AmtA and AmtB is still under discussion. It was first described as an energy-dependent transport of charged ammonium (Kleiner, 1993, Siewe *et al*., 1996; Meier-Wagner *et al*., 2001). Later, these transporters were described as gas channels that simply facilitate passive diffusion of uncharged ammonia across the cell membrane (Soupene *et al*., 1998, 2002; Khademi *et al*., 2004; Zheng *et al*., 2004; Javelle *et al*., 2005). In accordance, the results obtained here support an energy-independent uptake by AmtA and AmtB in *C. glutamicum*.

4.4. Summary

The regulation of glutamate dehydrogenase in *C. glutamicum* was investigated. Under nitrogen limitation, glutamate dehydrogenase is upregulated on the level of transcription. Using reporter gene assays, the part of the *gdh* promoter region that is responsible for this regulation was identified. DNA fragments spanning this part of the *gdh* promoter region were used to isolate putative transcriptional regulators of *gdh* by DNA affinity purification with magnetic beads. Four transcriptional regulators could be isolated: AmtR, the master regulator of nitrogen control in *C. glutamicum*, and FarR, WhiH, and OxyR, which have not been characterized in *C. glutamicum* yet but are homologous to transcriptional regulators of other bacteria. For AmtR and FarR, binding was verified by gel shift assays and the corresponding binding sites were mapped. In addition, the principle capacity of FarR to repress *gdh*-promoter-driven transcription was demonstrated by reporter gene assays in *E. coli*.

Surprisingly, none of the four regulators is responsible for nitrogen control of *gdh* transcription. Neither single deletions nor a quadruple deletion of *amtR*, *farR*, *whiH*, and *oxyR* in *C. glutamicum* had any effect on nitrogen-dependent transcription of *gdh*. Consequently, the presence of another transcriptional regulator or any other regulatory mechanism for the nitrogen control of *gdh* transcription can be postulated. Nevertheless, translation-dependent attenuation could be excluded as the respective regulatory mechanism.

The four transcriptional regulators AmtR, FarR, WhiH, and OxyR do not regulate *gdh* transcription in response to nitrogen starvation, nevertheless, they might affect *gdh* transcription in response to other stress conditions. A broad range of stress conditions were identified that influence *gdh* transcription. Beside that, a putative role of FarR in the regulation of fatty acid biosynthesis and/or glutamate overproduction was suggested, since an additional FarR binding site could be identified within the promoter region of the *dtsR2* gene, which is presumed to be involved in these processes.

Conclusively, regulation of *gdh* transcription was found to be a complex process, which responds to various stress conditions and includes several regulators.

In the second part of this work, the reason for the loss of nitrogen control in a *gdh* deletion strain of *C. glutamicum* was investigated. It was demonstrated that this

effect is caused by the loss of GDH activity and not by the absence of the GDH protein itself. Nitrogen control was restored by a heterologous expression of GDH from *E. coli* in the *gdh* deletion strain of *C. glutamicum*, but not by expression of an enzymatically inactive mutant of GDH from *C. glutamicum* Thus, the loss of nitrogen control is a metabolic effect, i.e. the lack of GDH activity causes changes in the concentration of a metabolite that influences nitrogen control. In this work, it could be demonstrated that at least two metabolites influence nitrogen control in *C. glutamicum*. These are most probably ammonium and 2-oxoglutarate. The loss of nitrogen control in the *gdh* deletion strain is directly correlated to an accumulation of 2-oxoglutarate under nitrogen surplus due to the lack of 2-oxoglutarate-consuming GDH. A high 2-oxoglutarate pool seems to antagonizes the nitrogen status and triggers a nitrogen starvation-like response even under nitrogen surplus.

In the third part of this work, it was demonstrated that ammonium is not toxic for *C. glutamicum* and the formation of a putative futile transmembrane cycle of ammonium was not observed.

5. References

Abe, S., Takayama, K., Kinoshita, S. (1967). Taxonomical studies on glutamic acid producing bacteria. J. Gen. Microbiol. 13: 279-301.

Antonopoulos, D. A., Aminov, R. I., Duncan, P. A., White, B. A. & Mackie, R. I. (2003). Characterization of the gene encoding glutamate dehydrogenase (*gdhA*) from the ruminal bacterium *Ruminococcus flavefaciens* FD-1. Arch. Microbiol. 179: 184-190.

Aravind, L. & Anatharaman, V. (2003). HutC/FarR-like bacterial transcription factors of the GntR family contain a small molecule-binding domain of the chorismate lyase fold. FEMS Microbiol. Lett. 222: 17-23.

Arcondeguy, T., Jack, R. & Merrick, M. (2001). PII signal transduction proteins, pivotal players in microbal nitrogen control. Microbiol. Mol. Biol. Rev. 65: 80-105.

Atkinson, M. R. & Ninfa, A. J. (1998). Role of the GlnK signal transduction protein in the regulation of nitrogen assimilation in *Escherichia coli*. Mol. Microbiol. 29:431-447.

Atkinson, M. R. & Ninfa, A. J. (1999). Characterization of the GlnK protein of *Escherichia coli*. Mol. Microbiol. 32: 301-313.

Atkinson, M. R., Blauwkamp, T. A. & Ninfa, A. J. (2002). Context-dependent functions of the PII and GlnK signal transduction proteins in *Escherichia coli*. J. Bacteriol. 184: 5364-5375.

Baker, P. J., Britton, K. L., Engel, P. C., Farrants, G. W., Lilley, K. S., Rice, D. W. & Stillman T. J. (1992). Subunit assembly and active site location in the structure of glutamate dehydrogenase. Proteins. 12: 75-86.

Barker, H. A. (1981). Amino acid degradation by anaerobic bacteria. Annu. Rev. Biochem. 50: 23-40.

Beckers, G., Nolden, L. & Burkovski, A. (2001). Glutamate synthase of C*orynebacterium glutamicum* is not essential for glutamate synthesis and is regulated by the nitrogen status. Microbiology 147: 2961-2970.

Beckers, G. (2004). AmtR – ein globaler Repressor der Stickstoff-Kontrolle in *Corynebacterium glutamicum*. Dissertation an der Mathematisch-Naturwissenschaftlichen Fakultät der Universität zu Köln.

Beckers, G., Bendt, A. K., Krämer, R. & Burkovski, A. (2004). Molecular identification of the urea uptake system and transcriptional analysis of urea transporter- and urease-encoding genes in *Corynebacterium glutamicum*. J. Bacteriol. 186(22): 7645-7652.

Beckers, G., Strösser, J., Hildebrandt, U., Kalinowski, J., Farwick, M., Krämer, R. & Burkovski, A. (2005). Regulation of AmtR-controlled gene expression in *Corynebacterium glutamicum*: mechanism and characterization of the AmtR regulon. Mol. Microbiol.

Belitsky, B. R. & Sonenshein, A. L. (1999). An enhancer element located downstream of the major glutamate dehydrogenase gene of *Bacillus subtilis*. Proc. Natl. Acad. Sci. USA. 96: 10290-10295.

Belitsky, B. R., Kim, H. J. & Sonenshein, A. L. (2004). CcpA-dependent regulation of *Bacillus subtilis* glutamate dehydrogenase gene expression. J. Bacteriol. 186: 3392-3398.

Bendt, A. K., Becker, G., Silberbach, M., Wittman, A. & Burkovski R. (2004). Utilization of creatinine as an alternative nitrogen source in *Corynebacterium glutamicum*. Arch. Microbiol. 181: 443-450.

Börmann E. R., Eikmanns, B. J. & Sahm, H. (1992). Molecular analysis of the *Corynebacterium glutamicum gdh* gene encoding glutamate dehydrogenase. Mol. Microbiol. 6: 317-326.

Bradford, M. A. (1976). A rapid and sensitive method fort he quantification of microgram quantities of protein utilizing the principle of protein-dye binding. Anal. Biochem. 72: 248-254.

Brenchley, J. E., Baker, C. A. & Patil, L. G. (1975). Regulation of the ammonia assimilatory enzymes in *Salmonella typhimurium*. J. Bacteriol. 124(1): 182-189.

Britto, D. T., Siddiqi, M. Y., Glass, A. D. & Kronzucker, H. J. (2001). Futile transmembrane NH_4^+ cycling: a cellular hypothesis to explain ammonium toxicity in plants. Proc. Natl. Acad. Sci. USA. 98:4255-4258.

Britto, D. T. & Kronzucker, H. J. (2002). NH_4^+ toxicity in higher plants: a critical review. J. Plant Physiol. 159: 567-584.

Burkovski, A., Weil, B. & Krämer, R. (1996). Characterization of a secondary uptake system for L-glutamate in *Corynebacterium glutamicum*. FEMS Microbiol. Lett. 136: 169-173.

Burkovski, A. (2003a). I do it my way: Regulation of ammonium uptake and ammonium assimilation in *Corynebacterium glutamicum*. Arch. Microbiol. 179: 83-88.

Burkovski, A. (2003b). Ammonium assimilation and nitrogen control in *Corynebacterium glutamicum* and its relatives: an example for new regulatory mechanisms in actinomycetes. FEMS Microbiol. Rev. 27: 617-628.

Burkovski, A. (2005). Nitrogen metabolism and its regulation. In: Bott, M. & Eggeling L. (eds.) Handbook of *Corynebacterium glutamicum*. CRC Press LLC, Boca Raton, FL.

Calogero, S., Gardan, R., Glaser, P., Schweizer, J., Rapoport, G. & Debarbouille, M. (1994). RocR, a novel regulatory protein controlling arginine utilization in *Bacillus subtilis*, belongs to the NtrC/NifA family of transcriptional activators. J. Bacteriol. 176: 1234-1241.

Camarena, L., Poggio, S., Garcia, N. & Osorio, A. (1998). Transcriptional repression of *gdhA* in *Escherichia coli* is mediated by the Nac protein. FEMS. Microbiol. Lett. 167: 51-56.

Castorph, H. & Kleiner, D. (1984). Some properties of a *Klebsiella pneumoniae* ammonium transport negative mutant (Amt). Arch. Microbiol. 139: 245-247.

Christman, M. F., Storz, G. & Ames, B. N. (1989). OxyR, a positive regulator of hydrogen peroxide-inducible genes in *Escherichia coli* and *Salmonella typhimurium*, is homologous to a family of bacterial regulatory proteins. Proc. Natl. Acad. Sci. USA 86: 3484-3488.

Chun, J., Kang, S.-O., Hah, Y. C. & Goodfellow, M. (1996). Phylogeny of mycolic acid-containing actinomycetes. J. Indust. Microbiol. 17: 205-213.

Cremer, J., Eggeling, L. & Sahm, H. (1990). Cloning of the *dapA dapB* cluster of the lysine-secreting bacterium *Corynebaterium glutamicum*. Mol. Gen. Genet. 220: 478-480.

Dominguez, H., Rollin, C., Guyonvarch, A., Guerquin-Kern, J.-L., Cocaign-Bousquet, M. & Lindley, N. D. (1998). Carbon-flux distribution in the central metabolic pathways of *Corynebacterium glutamicum* during growth on fructose. Eur. J. Biochem 254: 96-102.

Dondrup, M., Goesmann, A., Bartels, D., Kalinowski, J., Krause, L., Linke, B., Rupp, O., Sczyrba, A., Pühler, A. & Meyer, F. (2003). EMMA: a platform for consistent storage and efficient analysis of microarray data. J. Biotechnol. 106: 135-146.

Dröge, P. & Müller-Hill, B. (2001). High local concentrations at promoters: strategies in prokaryotic and eukaryotic cells. Bio Éssays. 23: 179-183.

Duperray, F., Jezequel, D., Ghazi, A., Letellier, L. & Shechter, E. (1992). Excretion of glutamate from *Corynebacterium glutamicum* triggered by amine surfactants. Biochim. Biophys. Acta. 1103: 250-258.

Eikmanns, B. J., Thum-Schmitz, N., Eggeling, L., Ludtke, K. U. & Sahm, H. (1994). Nucleotide sequence, expression and transcriptional analysis of the *Corynebacterium glutamicum gltA* gene encoding citrate synthase. Microbiology 140: 1817-1828.

Erdmann, A., Weil, B. & Krämer, R. (1994). Lysine secretion by *Corynebacterium glutamicum* wild-type: regulation of secretion activity. Appl. Microbiol. Biotechnol. 42: 604-610.

Fisher, S. H. (1999). Regulation of nitrogen metabolism in *Bacillus subtilis*: vive la différence!. Mol. Microbiol. 32: 223-232.

Flores, E. & Herrero, A. (2005). Nitrogen assimilation and nitrogen control in cyanobacteria. Biochem. Soc. Trans. 33: 164-167.

Forchhammer, K., Hedler, A., Strobel, H. & Weiss, V. (1999). Heterotrimerization of PII-like signalling proteins: implications for PII-mediated signal transduction systems. Mol. Microbiol. 33: 338-349.

Grant, S. N. G., Jessee, J., Bloom, F. R. & Hanahan, D. (1990). Different plasmid rescue from transgenic mouse DNAs into *Escherichia coli* methylation-restriction mutants. Proc. Natl. Acad. Sci. USA 87: 4645-4649.

Gutmann, M., Hoischen, C. & Krämer, R. (1992). Carrier-mediated glutamate secretion by *Corynebacterium glutamicum* under biotin limitation. Biochim. Biophys. Acta. 1112: 115-123.

Hermann T. (2003). Industrial production of amino acids by coryneform bacteria. J. Biotechnol 104: 155-172

Hoischen, C. & Krämer, R. (1990). Membrane alteration is necessary but not sufficient for effective glutamate secretion in *Corynebacterium glutamicum*. J. Bacteriol. 172: 3409-3416.

Horton, R. M., Hunt, H. D., Ho, S. N., Pullen, J .K. & Pease, L. R. (1989). Engineering hybrid genes without the use of restriction enzymes: gene splicing by overlap extension. Gene. 77: 61-68.

Hüser, A., Becker, A., Brune, I., Dondrup, M., Kalinowski, J., Plassmeier, J., Pühler, A., Wiegräbe, I. & Tauch, A. (2003). Development of a *Corynebacterium glutamicum* DNA microarray and validation by genome-wide expression profiling during growth with propionate as carbon source. J. Biotechnol., 106: 269-286.

Jahns, T., Zobel, A., Kleiner, D. & Kaltwasser, H. (1988). Evidence for carrier-mediated, energy dependent uptake of urea in some bacteria. Arch. Microbiol. 149: 377-383.

Jakoby, M., Tesch, M., Sahm, H., Krämer, R. & Burkovski, A. (1997). Isolation of the *Corynebacterium glutamicum glnA* gene encoding glutamine synthetase I. FEMS Microbiol. Lett. 154: 81-88.

Jakoby, M., Krämer, R. & Burkovski, A. (1999). Nitrogen regulation in *Corynebacterium glutamicum*: isolation of genes involved and biochemical characterization of corresponding proteins. FEMS Microbiol. Lett. 173: 303-310.

Jakoby, M., Nolden, L., Meier-Wagner, J., Krämer, R. & Burkovski, A. (2000). AmtR, a global repressor in the nitrogen regulation system of *Corynebacterium glutamicum*. Mol. Microbiol. 37: 964-977.

Javelle, A., Severi, E., Thornton, J. & Merrick, M. (2004). Ammonium sensing in *Escherichia coli*. Role of the ammonium transporter AmtB and AmtB-GlnK complex formation. J. Biol. Chem. 279: 8530-8538.

Javelle, A., Thomas, G., Marini, A.-M., Krämer, R. & Merrick, M. (2005). *In vivo* characterisation of the *E. coli* ammonium channel AmtB: evidence for the metabolic coupling of AmtB to glutamine synthetase. Biochem. J. 15: 215-222.

Jiang, P., Peliska, J. A. & Ninfa, A. J. (1998a). Enzymological characterization of the signal-transducing uridylyltransferase/uridylyl-removing enzyme (EC 2.7.7.59) of *Escherichia coli* and its interaction with the PII protein. Biochemistry 37: 12782-12794.

Jiang, P., Peliska, J. A. & Ninfa, A. J. (1998b). The regulation of *Escherichia coli* glutamine synthetase revisited: role of 2-ketoglutarate in the regulation of glutamine synthetase adenylylation state. Biochemistry 37: 12802-12810.

Jiang, P., Peliska, J. A. & Ninfa, A. J. (1998c). Reconstitution of the signal-transduction bicyclic cascade responsible for the regulation of Ntr gene transcription in *Escherichia coli*. Biochemistry 37: 12795-12801.

Kalinowski, J., Bathe, B., Bartels, D., Bischoff, N., Bott, M., Burkovski, A., Dusch, N., Eggeling, L., Eikmanns, B. J., Gaigalat, L., Goesmann, A., Hartmann, M., Huthmacher, K., Krämer, R., Linke, B., McHardy, A. C., Meyer, F., Möckel, B., Pfefferle, W., Pühler, A., Rey, D., Rückert, C., Rupp, O., Sahm, H., Wendisch, V. F., Wiegräbe, I. & Tauch, A. (2003). The complete *Corynebacterium glutamicum* ATCC 13032 genome sequence and its impact on the production of L-aspartate-derived amino acids and vitamins. J. Biotechnol. 104: 5-25.

Kamberov, E. S., Atkinson, M. R. & Ninfa, A. J. (1995). The *Escherichia coli* PII signal transduction protein is activated upon binding 2-ketoglutarate and ATP. J. Biol. Chem. 270: 17797-17807.

Kawahara, Y., Takahashi-Fuke, K., Shimizu, E., Nakamatsu, T. & Nakamori, S. (1997). Relationship between the glutamate production and the activity of 2-oxoglutarate dehydrogenase in *Brevibacterium lactofermentum*. Biosci. Biotechnol. Biochem. 61: 1109-1112.

Khademi, S. O'Connell III, J., Remis, J., Robles-Colmenares, Y., Miercke, L. J. W. & Stroud, R. M. (2004). Mechansim of ammonia transport by Amt/MEP/Rh: structure of AmtB at 1.35 Å. Sience 305: 1587-1594.

Kiefer, P., Heinzle, E., Zelder, O. & Wittmann, C. (2004). Comparative metabolic flux analysis of lysine-producing *Corynebacterium glutamicum* cultured on glucose or fructose. Appl. Environ. Microbiol. 70: 229-239.

Kimura, E., Abe, C., Kawahara, Y. & Nakamatsu, T. (1996). Molecular cloning of a novel gene, *dtsR*, which rescues the detergent sensitivity of a mutant derived from *Brevibacterium lactofermentum*. Biosci. Biotechnol. Biochem. 60: 1565-1570.

Kimura, E., Abe, C., Kawahara, Y., Nakamatsu, T. & Tokuda, H. (1997). A *dtsR* gene-disrupted mutant of *Brevibacterium lactofermentum* requires fatty acids for growth and efficiently produces L-glutamate in the presence of an excess of biotin. Biochem. Biophys. Res. Commun. 234: 157-161.

Kimura, E., Yagoshi, C., Kawahara,Y., Ohsumi, T. & Nakamatsu, T. (1999). Glutamate overproduction in *Corynebacterium glutamicum* triggered by a decrease in the level of a complex comprising DtsR and a biotin-containing subunit. Biosci. Biotech. Biochem. 63: 1274-1278.

Kimura, E. (2002). Triggering mechanism of L-glutamate overproduction by DtsR1 in coryneform bacteria. J. Biosci. Bioeng. 94: 545-551.

Kleiner, D. (1985). Bacterial ammonium transport. FEMS Microbiol. Rev. 32: 87-100.

Kleiner, D. (1993). NH_4^+ transport systems. In: Bakker, E. P. (ed) Alkali cation transport systems in prokaryotes. CRC press, Boca Raton, FL.

Kinoshita, S., Udaka, S. & Shimono, M. (1957). Amino acid fermentation. I. Production of L-glutamic acid by various microorganisms. J. Gen. Appl. Microbiol. 3: 193-205.

Krämer, R. & Lambert, C. (1990). Uptake of glutamate in *Corynebacterium glutamicum*. Eur. J. Biochem. 194: 937-944.

Krämer, R. (1994). Secretion of amino acids by bacteria: physiology and mechanism. FEMS Microbiol. Rev. 13: 75-79.

Krömer, J. O., Sorgenfrei, O., Klopprogge, K., Heinzle, E. & Wittmann, C. (2004). In-depth profiling of Lysine-producing *Corynebacterium glutamicum* by combined analysis of the transcriptome, metabolome and fluxome. J. Bacteriol. 186: 1769-1784.

Kronemeyer, W., Peekhaus, N., Krämer, R., Eggeling, L. & Sahm, H. (1995). Structure of the *gluABCD* cluster encoding the glutamate uptake system of *Corynebacterium glutamicum.* J. Bacteriol. 177: 1152-1158.

Kronzucker, H. J., Britto, D. T., Davenport, R. J. & Tester, M. (2001). Ammonium toxicity and the real cost of transport. Trends Plant Sci. 6: 335-337.

Leuchtenberger, W. (1996). Amino acids – technical production and use. In: Rehm, H. & Reed, G. (eds) Products of primary metabolism. Biotechnology, Volume 6. VCH Verlagsgesellschaft mbH, Weinheim/Germany.

Lindroth, P. & Mopper, K. (1979). High performance liquid chromatography determination of subpicomole amounts of amino acids by precolumn flourescence derivatization with *o*-phthaldialdehyde. Anal. Chem. 51: 1667-1674.

Martinelle, K. & Haggestrom, L. (1993). Mechanisms of ammonia and ammonium ion toxicity in animal cells: transport across cell membranes. J. Biotechnol. 30: 339-350.

Marx, A., Eikmanns, B., Sahm, H., de Graaf, A. A. & Eggeling, L. (1999). Response of the central metabolism in *Corynebaterium glutamicum* to the use of NADH-dependent glutamate dehydrogenase. Metabol. Eng. 1: 35-48.

Meier-Wagner, J., Nolden L., Jakoby, M., Siewe, R., Krämer, R. & Burkovski, A. (2001). Multiplicity of ammonium uptake systems in *Corynebacterium glutamicum*: Role of Amt and AmtB. Microbiology 147, 135-143.

Merrick, M. J. & Edwards, R. A. (1995). Nitrogen control in bacteria. Microbiol. Rev. 59: 604-622.

Millevoi, S., Pasquo, A., Chiaraluce, R., Consalvi, V., Giangiacomo, L., Britton, K. L., Stillman, T. J., Rice, D. W. & Engel, P. C. (1994). A monomeric mutant of *Clostridium symbiosum* glutamate dehydrogenase: comparison with a structured monomeric intermediate obtained during refolding. Protein Sci. 7: 966-974.

Minambres, B., Olivera, E. R., Jensen, R. A. & Luengo, J. M. (2000). A new class of glutamate dehydrogenases (GDH). J. Biol. Chem. 275: 39529-39542.

Muse, E. B. & Bender, R. A. (1998). The *nac* (nitrogen assimilation control) gene from *Escherichia coli*. J. Bacteriol. 180: 1166-1173.

Niebisch, A. & Bott, M. (2001). Molecular analysis of the cytochrome bc1-aa3 branch of the *Corynebacterium glutamicum* respiratory chain containing an unusual diheme cytochrome c1. Arch. Microbiol. 175: 282-294.

Ninfa, A. J., Jiang, P. (2005). PII signal transduction proteins: sensors of alpha-ketoglutarate that regulate nitrogen metabolism. Curr. Opin. Microbiol. 8: 168-173.

Nolden, L. (2001). Mechanismen der Stickstoffkontrolle in *Corynebacterium glutamicum*. Dissertation an der Mathematisch-Naturwissenschaftlichen Fakultät der Universität zu Köln.

Nolden, L., Farwick, M., Krämer, R. & Burkovski, A. (2001a). Glutamine synthetases of *Corynebacterium glutamicum*: transcriptional control and regulation of activity. FEMS Microbiol. Lett. 201: 91-98.

Nolden, L., Ngouto-Nkili, C.-E., Bendt, A. K., Krämer, R., Burkovski, A. (2001b). Sensing nitrogen limitation in *Corynebacterium glutamicum*: The role of *glnK* and *glnD*. Mol. Microbiol. 42: 1281-1295.

Pascual, C., Lawson, P. A., Farrow, J. A. E., Giminez, M. & Collins, M. D. (1995). Phylogenetic analysis of the genus *Corynebacterium* based on 16S rRNA gene sequences. Int. J. System. Bacteriol. 45: 724-728.

Pasquo, A., Britton, K. L., Stillman, T. J., Rice, D. W., Colfen, H., Harding, S. E., Scandurra, R. & Engel, P. C. (1996). Construction of a dimeric form of glutamate dehydrogenase from *Clostridium symbiosum* by site-directed mutagenesis. Biochim. Biophys. Acta. 1297: 149-158.

Patriaca, E. J., Rosirita, T. & Iaccarino, M. (2002). Key role of bacterial NH_4^+ metabolism in rhizobium-plant symbiosis. Microbiol. Mol. Biol. Rev. 66: 203-222.

Puech, V., Chami, M., Lemassu, A., Laneelle, M. A., Schiffler, B., Gounon, P., Bayan, N., Benz, R. & Daffe, M. (2001). Structure of the cell envelope of corynebacteria: inportance of the non-covalently bound lipids in the formation of the cell wall permeability barrier and fracture plane. Microbiology 147: 1365-1382.

Quail, M. A., Dempsey, C. E. & Guest, J. R. (1994). Identification of a fatty acyl regulator (FarR) in *Escherichia coli*. FEBS Lett. 356: 183-187.

Reitzer, L. (2003). Nitrogen assimilation and global regulation in *Escherichia coli*. Annu. Rev. Microbiol. 57: 155-176.

Ritchie, R. J. & Gibson, J. (1987a). Permeability of ammonia, methylamine and ethylamine in the cyanobacterium *Synechococcus* R-2 (*Anacystis nidulans*) PCC7942. J. Membr. Biol. 95: 131-142.

Ritchie, R. J. & Gibson, J. (1987b). Permeability of ammonia and amines in *Rhodobacter spheroides* and *Bacillus firmus*. Arch. Biochem. Biophys. 285: 322-341.

Rigali, S., Derouaux, A., Giannotta, F. & Dusart, J. (2002). Subdivision of the helix-turn-helix GntR family of bacterial regulators in the FadR, HutC, MocR and YtrA subfamilies. J. Biol. Chem. 227: 12507-12515.

Rönsch, H. (2000). Untersuchung zum Einfluss der Osmoregulation auf die Aminosäure-Produktion mit *Corynebacterium glutamicum*. Dissertation an der Mathematisch-Naturwissenschaftlichen Fakultät der Universität zu Köln.

Ryding, N. J., Kelemen, G. H., Whatling, C. A., Flardh, K., Buttner, M. J. & Chater, K.F. (1989). A developmentally regulated gene encoding a repressor-like protein is essential for sporulation in *Streptomyces coelicolor* A3(2). Mol. Microbiol. 29: 343-357.

Sambrook, J., Fritsch, E. F. & Maniatis, T. (1989). Molecular cloning: a laboratory manual, 2nd edition, Cold Spring Habor Laboratory Press, Cold Spring Harbor, N. Y.

Sampaio, M. M., Chevance, F., Dippel, R., Eppler, T., Schlegel, A., Boos, W., Lu, Y. J. & Rock, C. O. (2004). Phosphotransferase-mediated transport of the osmolyte 2-O-alpha-mannosyl-D-glycerate in *Escherichia coli* occurs by the product of the *mngA* (*hrsA*) gene and is regulated by the *mngR* (*farR*) gene product acting as repressor. J. Biol. Chem. 279: 5537-5548.

Schäfer, A., Tauch, A., Jäger, W., Kalinowski, J., Thierbach, G. & Pühler, A. (1994). Small mobilizable multi-purpose cloning vectors derived from the *Escherichia coli* plasmids pK18 and pK19: selection of defined deletions in the chromosome of *Corynebacterium glutamicum*. Gene 145:69-73.

Schulz, A. A., Collet, H. J. & Reid, S. J. (2001). Nitrogen and carbon regulation of glutamine synthetase and glutamate synthase in *Corynebacterium glutamicum* ATCC 13032. FEMS Microbiol. Lett. 205: 361-367.

Schwacha, A. & Bender, R. A. (1993). The product of the *Klebsiella aerogenes nac* (nitrogen assimilation control) gene is sufficient for activation of the *hut* operons and repression of the *gdh* operon. J. Bacteriol. 175: 2116-2124.

Senior, P. J. (1975). Regulation of nitrogen metabolism in *Escherichia coli* and *Klebsiella aerogenes*: studies with the continuous-culture technique. J. Bacteriol. 123: 407-418.

Shiio, I., Otsuka, S. & Takahashi, M. (1962). Effect of biotin on the bacterial formation of glutamic acid. I. Glutamate formation and cellular permeability of amino acids. J. Biochem. 51: 56-62.

Shiio, I. & Ozaki, H. (1970). Regulation of nicotinamide dinucleotide phosphate-specific glutamate dehydrogenase from *Brevibacterium flavum*, a glutamate-producing bacterium. J. Biochem. 68: 633-647.

Siewe, R. M., Weil, B. & Krämer, R. (1995). Glutamine uptake by a sodium dependent secondary transport system in *Corynebacterium glutamicum*. Arch. Microbiol. 164: 98-103

Siewe, R. M., Weil, B., Burkovski, A., Eikmanns, B. J., Eikmanns, M. & Krämer, R. (1996). Functional and genetic characterization of the (methyl)ammonium uptake carrier of *Corynebacterium glutamicum*. J. Biol. Chem. 271: 5398-5403.

Siewe, R. M., Weil, B., Burkovski, A., Eggeling, L., Krämer, R. & Jahns, T. (1998). Urea uptake and urease activity in *Corynebacterium glutamicum*. Arch. Microbiol. 169: 411-416.

Silberbach, M. (2004). Biochemische, biotechnologische und molekularbiologische Analyse eines Signaltransduktionsweges in *Corynebacterium glutamicum*. Dissertation an der Mathematisch-Naturwissenschaftlichen Fakultät der Universität zu Köln.

Soupene, E., He, L., Yan, D. & Kustu, S. (1998). Ammonium acquisition in enteric bacteria: physiological role of the ammonium/methylammonium transport B (AmtB) protein. Proc. Natl. Acad. Sci. USA 95: 7030-7034.

Soupene, E., Lee, H. & Kustu, S. (2002). Ammonium/methylammonium transport (Amt) proteins facilitate diffusion of NH_3 bidirectionally. Proc. Natl. Acad. Sci. USA 90: 3926-3931.

Stadtman, E. R. (1990). Discovery of glutamine synthetase cascade. Methods Enzymol. 182: 793-809.

Stillman, T. J., Migueis, A. M., Wang, X. G., Baker, P. J., Britton, K. L., Engel, P. C. & Rice, D. W. (1999). Insights into the mechanism of domain closure and substrate specificity of glutamate dehydrogenase from *Clostridium symbiosum*. J. Mol. Biol. 285: 875-885.

Storz, G., Tartaglia, L. A. & Ames, B. N. (1990). Transcriptional regulator of oxidative stress-inducible genes: direct activation by oxidation. Science. 248: 189-194.

Strösser, J., Lüdke, A., Schaffer, S., Krämer, R. & Burkovski, A. (2004). Regulation of GlnK activity: modification, membrane sequestration and proteolysis as regulatory principles in the network of nitrogen control in *Corynebacterium glutamicum*. Mol. Microbiol. 54: 132-147.

Takinami, K., Yoshii, H., Tsuji, H. & Okada, H. (1965). Biochemical effects of fatty acids and its derivatives on L-glutamic acid and the growth of *Brevibacterium lactofermentum*. Agric. Biol. Chem. 29: 351-359.

Tauch, A., Kirchner, O., Löffler, B., Götker, S., Pühler, A. & Kalinowski, J. (2002). Efficient electrotransformation of *Corynebacterium diphtheriae* with a minireplicon derived from the *Corynebacterium glutamicum* plasmid pGA1. Curr. Microbiol. 45: 362-367.

Tesch, M., Eikmanns, B., de Graaf, A. A. & Sahm, H. (1998). Ammonium assimilation in *Corynebacterium glutamicum* and a glutamate dehydrogenase-deficient mutant. Biotech. Lett. 20: 953-957.

Tesch, M., de Graaf, A. A. & Sahm, H. (1999). *In-vivo* fluxes in the ammonium assimilatory pathways in *Corynebacterium glutamicum* studied by ^{15}N nuclear magnetic resonance. Appl. Environ. Microbiol. 65: 1099-1109.

Trötschel, C., Kandirali, S., Diaz-Achirica, P., Meinhardt, A., Morbach, S., Krämer, R. & Burkovski, A. (2003). GltS, a sodium-coupled L-glutamate uptake system of *Corynebacterium glutamicum*: Identification of the corresponding gene and impact on L-glutamate production. Appl. Microbiol. Biotechnol. 60: 738-742.

van Heeswijk, W. C., Wen, D., Clancy, P., Jaggi, R., Ollis, D. L., Westerhoff, H. V. & Vasudevan, S. G. (2000). The *Escherichia coli* signal transducers PII (GlnB) and GlnK form heterotrimers *in vivo*: fine tuning the nitrogen signal cascade. Proc. Natl. Acad. Sci. USA 97: 3942-3947.

Viera, J. & Messing, J. (1982). The pUC plasmid, an M13mp7-derived system for insertion mutagenesis and sequencing with synthetic primers, Gene 19: 259-268.

Wagner, R. (2000). Transcription regulation in prokaryotes. Oxford University Press Inc., Oxford.

Wang, X. G., Dean, J. L., Engel, P. C., Baker, P. J., Britton, K.L., Stillman, T. J. & Rice D. W. (1994). The changed pattern of substrate specificity in the K89L mutant of glutamate dehydrogenase of *Clostridium symbiosum*. Biochem. Soc. Trans. 22: 320-323.

Wendisch VF, de Graaf AA, Sahm H, Eikmanns BJ. (2000). Quantitative determination of metabolic fluxes during co-utilization of two carbon sources: comparative analysis with *Corynebacterium glutamicum* during acetate and/or glucose. J. Bacteriol 182: 3088-3096.

Wray, L. V. Jr., Zalieckas, J. M. & Fisher, S. H. (2001). *Bacillus subtilis* glutamine synthetase controls gene expression through a protein-protein interaction with transcription factor TnrA. Cell. 107: 427-435.

Yanisch-Perron, C., Viera, J. & Messing, J. (1985). Improved M13 phage vectors and host strains:nucleotide sequence of the M13mp18 and pUC19 vectors. Gene 33: 103-119.

Zheng, L., Kostrewa, D., Bernèche, S., Winkler, F. K. & Li, X.-D. (2004). The mechanism of ammonia transport based on the crystal structure of AmtB of *Escherichia coli*. Proc. Natl. Acad. Sci. USA 101: 17090-17095.

Zittrich, S. & Krämer, R. (1994). Quantitative discrimination of carrier-mediated excretion of isoleucine from uptale and diffusion in *Corynebacterium glutamicum*. J. Bacteriol. 176: 6892-6899.

6. Appendix

6.1. Construction of *C. glutamicum* strains

TMΔfarR:

This *farR* deletion strain of *C. glutamicum* was derived from RES167 using the deletion vector pK18ΔfarR following the protocol of Schäfer *et al*. (1994).

TMΔwhiH:

This *whiH* deletion strain of *C. glutamicum* was derived from RES167 using the deletion vector pK18ΔwhiH following the protocol of Schäfer *et al*. (1994).

TMΔoxyR:

This *oxyR* deletion strain of *C. glutamicum* was derived from RES167 using the deletion vector pK18ΔoxyR following the protocol of Schäfer *et al*. (1994).

TMΔfarRΔamtR:

This double deletion strain of *C. glutamicum* lacking *farR* and *amtR* was derived from TMΔfarR using the deletion vector pK18ΔamtR following the protocol of Schäfer *et al*. (1994).

TMΔfarRΔamtRΔwhiH:

This triple deletion strain of *C. glutamicum* lacking *farR*, *amtR*, and *whiH* was derived from TMΔfarRΔamtR using the deletion vector pK18ΔwhiH following the protocol of Schäfer *et al*. (1994).

TMΔfarRΔamtRΔwhiHΔoxyR:

This quadruple deletion strain of *C. glutamicum* lacking *farR*, *amtR*, *whiH*, and *oxyR* was derived from TMΔfarRΔamtRΔwhiH using the deletion vector pK18ΔoxyR following the protocol of Schäfer *et al*. (1994).

TMΔgdhΔglnA:

This double deletion strain of *C. glutamicum* lacking *gdh* and *glnA* was derived from LNΔGDH using the deletion vector pK18ΔglnA following the protocol of Schäfer *et al*. (1994).

6.2. Construction of plasmids

pZgdh:

This plasmid is an expression vector of *gdh* from *C. glutamicum*. The full-length *gdh* gene of *C. glutamicum* was amplified by PCR. For subsequent cloning steps, *Eco*RI and *Sal*I restriction sites (shown in bold) were introduced in the primer sequences (5'-GCG CGC **GAA TTC** ATG ACA GTT GAT GAG CAG GTC-3' / 5'-GCG CGC **GTC GAC** TTA GAT GAC GCC CTG TGC C-3'). After restriction of the PCR product and the expression vector pZ8-1 (Degussa AG, Halle) with *Eco*RI and *Sal*I, the *gdh* gene was ligated to vector pZ8-1 leading to plasmid pZgdh. The cloned *gdh* gene was sequenced.

pZgdh$_{EC}$:

This plasmid is an expression vector of *gdh* from *E. coli*. The full-length *gdh* gene of *E. coli* was amplified by PCR. For subsequent cloning steps, *Eco*RI and *Bam*HI restriction sites (shown in bold) were introduced in the primer sequences (5'-GCG CGC **GAA TTC** ATG GAT CAG ACA TAT TCT CTG G-3' / 5'-GCG CGC **GGA TCC** TTA TCA CAC CCT GCG CCA G-3'). After restriction of the PCR product and the expression vector pZ8-1 (Degussa AG, Halle) with *Eco*RI and *Bam*HI, the *gdh* gene of *E. coli* was ligated to vector pZ8-1 leading to plasmid pZgdh$_{EC}$. For verification, the plasmid was transformed into the *gdh* deletion strain LNΔGDH and GDH-activity was measured. The cloned *gdh* gene was not sequenced.

pZgdh-K92L:

This plasmid is an expression vector for an enzymatic inactive mutant of GDH from *C. glutamicum* harbouring a single point mutation (K92L). The vector was derived from pZgdh by site-directed mutagenesis using the primers 5'-GCA CT TGG ACC ATA CCT GGG CGG CCT GCG CTT C-3' and 5'-GAA GCG CAG GCC GCC CAG GTA TGG TCC AAG TGC-3'. The mutated *gdh* gene was sequenced.

pQE30Xagdh:

This plasmid is an expression vector for GDH from *C. glutamicum* with a histag at its N-terminus. The full-length *gdh* gene of *C. glutamicum* was amplified by PCR. For subsequent cloning steps, *Sph*I and *Hin*dIII restriction sites (shown in bold) were introduced in the primer sequences (5'-GCG CGC **GCA TGC** ATG GAT CAG ACA TAT TCT CTG G-3' / 5'-GCG CGC **AAG CTT** TTA GAT GAC GCC CTG TGC C-3'). After restriction of the PCR product and the expression vector pQE30Xa (Qiagen, Hilden)

with *Sph*I and *Hin*dIII, the *gdh* gene was ligated to vector pQE30Xa leading to plasmid pQE30Xagdh. The cloned *gdh* gene was sequenced.

pJCgdhlacZ:

This plasmid harbours a fusion of the *gdh* promoter region of *C. glutamicum* and the *lacZ* gene coding for β-galactosidase and can be used for reporter gene assays. The vector pK18gdh-lacZ (Nolden, 2001) was restricted with *Eco*RI and *Pst*I, The resulting insert, which harbours the fusion of the *gdh* promoter region and the *lacZ* gene, was ligated to the *Eco*RI-*Pst*I-restricted vector pJC1 (Cremer *et al*., 1990) leading to pJCgdhlacZ.

pUCfarR:

This plasmid is an expression vector of *farR* from *C. glutamicum*. The full-length *farR* gene of *C. glutamicum* was amplified by PCR. For subsequent cloning steps, *Bam*HI restriction sites (shown in bold) were introduced in the primer sequences (5'-GCG CGC **GGA TCC** TTG CTT TTT ACT AGG CGC TCC-3' / 5'-GCG CGC **GGA TCC** CGT CAG AGA TCT TCG GAG-3'). After restriction of the PCR product and the expression vector pUC18 (Viera & Messing, 1982) with *Bam*HI, the *farR* gene was ligated to pUC18 leading to plasmid pUCfarR. The cloned *farR* gene was sequenced.

pUCwhiH:

This plasmid is an expression vector of *whiH* from *C. glutamicum*. The full-length *whiH* gene of *C. glutamicum* was amplified by PCR. For subsequent cloning steps, *Eco*RI restriction sites (shown in bold) were introduced in the primer sequences (5'-GCG CGC **GAA TTC** ATG ACC CCA GCA AAC GAA AG-3' / 5'-GCG CGC **GAA TTC** TTA GTT CAG CGT GCC CCA GC-3'). After restriction of the PCR product and the expression vector pUC18 (Viera & Messing, 1982) with *Eco*RI, the *whiH* gene was ligated to pUC18 leading to plasmid pUCwhiH. The cloned *whiH* gene was sequenced.

pUCoxyR:

This plasmid is an expression vector of *oxyR* from *C. glutamicum*. The full-length *oxyR* gene of *C. glutamicum* was amplified by PCR. For subsequent cloning steps, *Eco*RI restriction sites (shown in bold) were introduced in the primer sequences (5'-GCG CGC **GAA TTC** ATG AGC AAT AAA GAG TAC CGG-3' / 5'-GCG CGC **GAA TTC** CGT TAC TGC GCT ACC GCG -3'). After restriction of the PCR product and the expression vector

pUC18 (Viera & Messing, 1982) with *Eco*RI, the *oxyR* gene was ligated to pUC18 leading to plasmid pUCoxyR. The cloned *oxyR* gene was sequenced.

pK18ΔfarR:

This plasmid is a deletion vector for *farR* from *C. glutamicum*. The 800 bp sequence upstream of the *farR* gene of *C. glutamicum* was amplified by PCR (5'-TCA ATG ATT TCG TCC TTG TGG-3' / 5'-GTG GTT TTG GTG ACT GAA GC-3') and ligated to the vector pDrive (Qiagen, Hilden) by T/A-cloning. The resulting plasmid pDrive-ΔFarR-oben-neu was sequenced. The 800 bp sequence downstream of the *gdh* gene of *C. glutamicum* was amplified by PCR. For subsequent cloning steps, *Xba*I and *Xma*I restriction sites (shown in bold) were introduced in the primer sequences (5'-GCG CGC **TCT AGA** GAC GTG AAC CCA TTT TGG TG -3' / 5'-GCG CGC **CCC GGG** ACA CCA AGG TTG ACT G-3'). The PCR product and the vector pUC18 (Viera & Messing, 1982) were restricted with *Xba*I and *Xma*I and ligated to form the plasmid pUC18-ΔFarR-unten, which was sequenced. After that, the plasmid pDrive-ΔFarR-oben-neu was linearized by restriction with *Bam*HI and the plasmid pUC18-ΔFarR-unten was linearized with *Xba*I. Subsequently, both were treated the large Klenow fragment of DNA polymerase I for fill-in of 5' overhangs to form blunt ends and subsequently restricted with *Hin*dIII. The resulting 800 bp insert of pDrive-ΔFarR-oben-neu was ligated to the linearized vector pUC18-ΔFarR-unten leading to pUC-ΔFarR-gesamt. This plasmid as well as pK18mobsacB (Schäfer *et al*., 1994) were restricted with *Hin*dIII and *Xma*I, and the insert of pUC-ΔFarR-gesamt was ligated to pK18mobsacB leading to pK18ΔfarR.

pK18ΔwhiH:

This plasmid is a deletion vector for *whiH* from *C. glutamicum*. By SOE-PCR, a fusion of the 800 bp sequences upstream and downstream of the *whiH* gene of *C. glutamicum* was synthesized. For subsequent cloning steps, *Eco*RI restriction sites (shown in bold) were introduced in the outer primer sequences (5'-GCG CGC **GAA TTC** ACA GGT CTC AAA CTG GGC C-3' / 5'-CGC AGT GCG CGT ATC ACG GGT GCC TCT TTA ATG GGC C-3' / 5'-GGC CCA TTA AAG AGG CAC CCG TGA TAC GCG CAC TGC G-3' / 5'-GCG CGC **GAA TTC** GCA GCT GAA GCT GTG CGC G-3'). After restriction of the SOE-PCR product and the vector pK18mobsacB (Schäfer *et al*., 1994) with *Eco*RI, the SOE-PCR product was ligated to vector pK18mobsacB leading to plasmid pK18ΔwhiH, which was sequenced.

pK18ΔoxyR:

This plasmid is a deletion vector for *oxyR* from *C. glutamicum*. By SOE-PCR, a fusion of the 800 bp sequences upstream and downstream of the *oxyR* gene of *C. glutamicum* was synthesized. For subsequent cloning steps, *Eco*RI restriction sites (shown in bold) were introduced in the outer primer sequences (5'-GCG CGC **GAA TTC** GTT GTG CGC GAC ATG ATC G-3' / 5'-CTC TGG AAA ACC TCT AGA AAA ATG CCT ATA ACT ATA ACG GTG-3' / 5'-CAC CGT TAT AGT TAT AGG CAT TTT TCT AGA GGT TTT CCA GAG-3' / 5'-GCG CGC **GAA TTC** GCA GCT GAA GCT GTG CGC G-3'). After restriction of the SOE-PCR product and the vector pK18mobsacB (Schäfer *et al*., 1994) with *Eco*RI, the SOE-PCR product was ligated to vector pK18mobsacB leading to plasmid pK18ΔoxyR, which was sequenced.

6.3. Complete list of the results of the DNA microarray analyses

Table 8: A complete list of all genes which were found to be differentially expressed in the DNA microarray analyses of RES167 vs. TMΔfarR, RES167 vs. TMΔwhiH, and RES167 vs. TMΔfarRΔamtR. Genes were regarded as differentially expressed if the respective intensities resulted in ratios greater than 1.52 or smaller than -1.52. These regulation factors are given. A positive factor indicates a higher expression in the deletion strain, whereas a negative value indicates a higher expression in RES167.

No.	RES167 vs. TMΔfarR	vs. TMΔwhiH	vs. TMΔfarRΔamtR		Annotation
NCgl0008		1.56			Conserved hypothetical protein
NCgl0012			1.60	*gyrA*	DNA gyrase (topoisomerase II) A subunit
NCgl0032			-2.31		Conserved hypothetical protein
NCgl0033			-1.60	*ppiA*	Peptidyl-prolyl cis-trans isomerase
NCgl0034		-1.75	-1.96		Putative membrane protein
NCgl0042	-1.84			*pbpA*	Cell division protein FtsI/penicillin-binding protein 2
NCgl0044		-1.84		*ppp*	Serine/threonine protein phosphatase
NCgl0059	-1.60	-1.68	-1.52		Spore coat assembly protein
NCgl0061			1.63		4-oxalocrotonate tautomerase homolog
NCgl0074			3.52		Permeases of the major facilitator superfamily
NCgl0075			21.19	*codA*	Creatinine deaminase
NCgl0082			1.55	*ureR*	Transcriptional regulator, MarR family
NCgl0083			10.33	*ureA*	Urea amidohydrolase (urease) gamma subunit
NCgl0085			5.42	*ureC*	Urea amidohydrolase (urease) alpha subunit
NCgl0086			4.95	*ureE*	Urease accessory protein
NCgl0087			6.89	*ureF*	Urease accessory protein
NCgl0088			7.82	*ureG*	Urease accessory protein
NCgl0089			5.91	*ureD*	Urease accessory protein
NCgl0090			2.63		Predicted hydrolases or acyltransferases
NCgl0104	2.41				ATP/GTP-binding protein
NCgl0105			-1.99		Transcriptional regulator of sugar metabolism
NCgl0107			1.52	*sixA*	Phosphohistidine phosphatase SixA
NCgl0118			1.69		Predicted hydrolase (HAD superfamily)
NCgl0119			1.80		Carbonic anhydrases/acetyltransferases
NCgl0124	2.01		-1.62		Putative secreted or membrane protein

NCgl0134			-1.79		Uncharacterized protein conserved in bacteria
NCgl0135			-1.58		Putative ammonia monooxygenase
NCgl0146	1.90				Predicted methylated DNA methyltransferase
NCgl0156	2.24				Conserved hypothetical protein
NCgl0168	2.07				Predicted dehydrogenases and related proteins
NCgl0171	-1.57			*cspA*	Cold shock proteins
NCgl0172	-1.66		-1.80		Hypothetical memebrane protein
NCgl0173			1.70		Transcriptional regulator, ArsR-family
NCgl0176	-1.84	-1.96			Transcriptional regulators, LacI-family
NCgl0181			5.14	*gltB*	NADPH-dependent glutamate synthase
NCgl0182			27.31	*gltD*	NADPH-dependent glutamate synthase
NCgl0183			-2.15		Conserved hypothetical protein
NCgl0185			-1.55		Putative membrane protein
NCgl0186		1.57			pedicted short-chain alcohol dehydrogenases
NCgl0187	1.93	2.06	1.77		FAD/FMN-containing dehydrogenases
NCgl0188		1.55	2.09		Hypothetical protein
NCgl0191			2.54		Hypothetical protein
NCgl0206			1.64	*moaE*	Molybdopterin converting factor, large subunit
NCgl0207			1.61	*moaB*	Molybdopterin biosynthesis enzymes
NCgl0208			1.74	*moaC*	Molybdenum cofactor biosynthesis enzyme
NCgl0243	1.67				UDP-N-acetylmuramyl tripeptide synthase
NCgl0245		-1.79		*leuA*	Isopropylmalate/homocitrate/citramalate synthases
NCgl0247			-1.79	*lysC*	Aspartokinases
NCgl0248			-1.83	*asd*	Aspartate-semialdehyde dehydrogenase
NCgl0251			1.75	*katA*	Catalase
NCgl0274		-1.74	-2.20	*ponA*	Membrane carboxypeptidase
NCgl0275			-1.52	*whiB4*	Putative regulatory protein
NCgl0276			1.65		Conserved hypothetical protein
NCgl0293		1.62			Putative membrane protein
NCgl0303	-1.74			*cspA2*	Cold shock protein
NCgl0304			-1.81	*topA*	Topoisomerase IA
NCgl0308		1.73			Uncharacterized phage-associated protein
NCgl0312	-1.59				Beta-glucosidase-related glycosidases
NCgl0313			1.73	*adhE*	Zn-dependent alcohol dehydrogenases, class III
NCgl0314			1.73		Zn-dependent hydrolases, including glyoxylases
NCgl0318	-1.56		-2.02		Conserved hypothetical membrane protein
NCgl0325			-1.55	*rmlA1*	dTDP-glucose pyrophosphorylase
NCgl0328			-1.78		Nitroreductase
NCgl0338			-1.74	*ptpA2*	Protein-tyrosine-phosphatase
NCgl0339			-1.63		Secreted protein, carrying a eukaryotic domain
NCgl0351			-1.92	*udgA1*	Predicted UDP-glucose 6-dehydrogenase
NCgl0359	-1.91			*sdhCD*	Succinate dehydrogenase/fumarate reductase
NCgl0360	-2.43	-1.55		*sdhA*	Succinate dehydrogenase/fumarate reductase
NCgl0361	-1.92			*sdhB*	Succinate dehydrogenase/fumarate reductase
NCgl0362	-2.05				Conserved hypothetical membrane protein
NCgl0375		1.56	2.18	*ctpA*	Cation transport ATPase
NCgl0375		1.64	3.77	*ctpA*	Cation transport ATPase
NCgl0377			-1.97		Conserved secreted protein
NCgl0378		-1.60	-2.13		ABC-type hemin transport system
NCgl0379		-1.58	-1.65		ABC-type Fe^{3+}-siderophore transport system
NCgl0381	-1.89				Conserved secreted protein
NCgl0388		1.53		*fadD5*	Acyl-CoA synthetases
NCgl0390	1.71			*gpmA*	Phosphoglycerate mutase 1
NCgl0398	1.84			*proC*	Pyrroline-5-carboxylate reductase
NCgl0406	2.26				Putative membrane protein
NCgl0427			-1.66	*ccsB*	Transport system of cytochrome c biogenesis
NCgl0430			1.88		Predicted transcriptional regulators
NCgl0431			1.92		Putative secreted protein
NCgl0432			1.92		Hypothetical protein
NCgl0440			1.70		Putative serine protease (ClpP class)
NCgl0444			-2.33		Putative membrane protein
NCgl0445			-1.90	*pitA*	Phosphate/sulphate permeases
NCgl0448		1.52			Peptidase E

NCgl0450			-1.73	*menD*	2-Succinyl-6-hydroxy carboxylate synthase
NCgl0452			1.56		Predicted glycosyltransferases
NCgl0459		-2.52		*rplK*	Ribosomal protein L11
NCgl0460		-2.66		*rplA*	Ribosomal protein L1
NCgl0465			7.93		Cation transport ATPase
NCgl0468		-1.82		*rplJ*	Ribosomal protein L10
NCgl0469		-2.16		*rplL*	Ribosomal protein L7/L12
NCgl0475		1.67			Conserved hypothetical protein
NCgl0476	-1.55	-2.07		*rpsL*	Ribosomal protein S12
NCgl0477		-1.58		*rpsG*	Ribosomal protein S7
NCgl0478		-1.96		*fusA*	Translation elongation factors (GTPases)
NCgl0480		-1.94		*tuf*	GTPases - translation elongation factors
NCgl0486	-2.55	-2.66	-1.89	*rpsJ*	Ribosomal protein S10
NCgl0487	-2.00	-2.03	-2.20	*rplC*	Ribosomal protein L3
NCgl0489	-1.87	-2.12	-1.75	*rplW*	Ribosomal protein L23
NCgl0491		-2.27		*rpsS*	Ribosomal protein S19
NCgl0492	-1.52	-1.88		*rplV*	Ribosomal protein L22
NCgl0493		-2.04		*rpsC*	Ribosomal protein S3
NCgl0494	-1.69	-2.27		*rplP*	Ribosomal protein L16/L10E
NCgl0495		-2.27		*rpmC*	Ribosomal protein L29
NCgl0496		-2.17		*rpsQ*	Ribosomal protein S17
NCgl0499		-1.58		*rplN*	Ribosomal protein L14
NCgl0501		-1.67		*rplE*	Ribosomal protein L5
NCgl0503			1.61	*dkg*	Aldo/keto reductases
NCgl0508		-1.58			Secreted protein
NCgl0509		-1.70			Putative membrane protein
NCgl0510		-1.97			ABC-type cobalt transport system
NCgl0511		-1.67			ABC-type cobalt transport system
NCgl0512		-1.90	-1.96		Dehydrogenase/glutathione oxidoreductase
NCgl0513			-1.69		Putative secreted protein
NCgl0516		-1.90		*rplF*	Ribosomal protein L6P/L9E
NCgl0517	-1.53	-2.04		*rplR*	Ribosomal protein L18
NCgl0518		-1.73		*rpsE*	Ribosomal protein S5
NCgl0519		-1.64		*rpmD*	Ribosomal protein L30/L7E
NCgl0520		-1.62		*rplO*	Ribosomal protein L15
NCgl0531			1.71		Transcriptional regulator LcIR-family
NCgl0535	2.46				Uncharacterized protein conserved in bacteria
NCgl0536	-1.88	-2.49		*infA*	Translation initiation factor 1 (IF-1)
NCgl0537	-2.07	-2.38		*rpsM*	Ribosomal protein S13
NCgl0538		-1.96	-1.57	*rpsK*	Ribosomal protein S11
NCgl0539		-1.58		*rpsD*	Ribosomal protein S4 and related proteins
NCgl0541		-1.58		*rplQ*	Ribosomal protein L17
NCgl0556		-1.67		*rplM*	Ribosomal protein L13
NCgl0557		-2.03		*rpsI*	Ribosomal protein S9
NCgl0565		1.96	2.75		Predicted permease
NCgl0572		-2.02		*groES*	Co-chaperonin GroES (HSP10)
NCgl0575			2.26	*sigD*	RNA polymerase specialized sigma subunit
NCgl0578			-2.14	*guaB2*	IMP dehydrogenase/GMP reductase
NCgl0583		1.56			Conserved hypothetical protein
NCgl0588	1.93				Putative membrane protein
NCgl0592			-1.64		Putative secreted protein
NCgl0603			-1.57		Predicted sugar epimerases
NCgl0608			-1.53	*metI*	ABC-type metal ion transport system
NCgl0609			-1.57	*metN*	ABC-type metal ion transport system
NCgl0610	2.75	1.90	-1.82	*metQ*	ABC-type metal ion transport system
NCgl0618			-1.94		ABC-type $Fe3^{+}$-hydroxamate transport system
NCgl0622			-1.61		Uncharacterized protein conserved in bacteria
NCgl0625		2.65		*metY*	O-acetylhomoserine sulfhydrylase
NCgl0629	-2.89			*prpB2*	PEP phosphonomutase and related enzymes
NCgl0630		-3.51		*prpC2*	Citrate synthase
NCgl0635			-1.81		Siderophore-interacting protein
NCgl0639			-4.20	*Irp1*	ABC-type $Fe3^{+}$-hydroxamate transport system
NCgl0641			-1.96		Exonuclease III
NCgl0649		1.67			Putative membrane protein
NCgl0659		-2.19	-1.98	*pyc*	Pyruvate carboxylase
NCgl0661		2.00			Uncharacterized protein with SCP/PR1 domains
NCgl0666	-1.90	-1.86		*prpC1*	Citrate synthase

NCgl0670	1.57		1.52	*accBC*	Acetyl/propionyl-CoA carboxylase, alpha subunit
NCgl0671			1.78	*thtR*	Rhodanese-related sulfurtransferase
NCgl0673			1.65		Conserved hypothetical protein
NCgl0676			-1.86		Conserved hypothetical protein
NCgl0677			-2.20	*dtsR2*	Acetyl-CoA carboxylase subunit
NCgl0689	-3.36	-2.82	-1.72		predicted short-chain alcohol dehydrogenases)
NCgl0690	-1.73				Putative membrane protein
NCgl0694	-1.93	-2.10	-2.15		ABC-type sugar transport system
NCgl0695	-1.84	-2.08	-2.27		ABC-type sugar transport systems
NCgl0696	-1.57				Uncharacterized conserved protein
NCgl0697		-2.93			ABC-type sugar transport system
NCgl0698	-1.53		-1.54	*msiK2*	ABC-type sugar transport systems
NCgl0699			-1.53		Predicted membrane protein
NCgl0700	-2.04	-1.56	-2.93		Distinct helicase family with a unique C-terminus
NCgl0702			1.65		Conserved hypothetical protein
NCgl0715			1.68		Conserved hypothetical protein
NCgl0717		1.81			Putative secreted protein
NCgl0730			1.58	*aroA*	5-enolpyruvylshikimate-3-phosphate synthase
NCgl0734			1.83	*whiB1*	Transcription factor WhiB
NCgl0755	2.00		-1.58		Predicted glutamine amidotransferase
NCgl0765	1.53				Archaeal fructose-1,6-bisphosphatase
NCgl0766	1.74				Archaeal fructose-1,6-bisphosphatase
NCgl0768			-1.78	*ftsE*	Predicted ATPase involved in cell division
NCgl0769			-2.46	*ftsX*	Cell division protein
NCgl0776		-2.20	-9.94		ABC-type enterochelin transport system
NCgl0777			-7.07		ABC-type enterochelin transport system
NCgl0778			-5.60		ABC-type enterochelin transport system
NCgl0779			-4.60		ABC-type enterochelin transport system
NCgl0788			-1.52		Glutamine cyclotransferase
NCgl0790			-1.59		Permeases
NCgl0793			1.59		Conserved hypothetical protein
NCgl0794			-3.16	*serC*	Phosphoserine aminotransferase
NCgl0795		-1.84	-2.44	*gltA*	Citrate synthase
NCgl0801			-1.67		Putative secreted protein
NCgl0805	-1.52				Homoserine acetyltransferase
NCgl0807			-1.71		Hypothetical protein
NCgl0811			1.54	*cysQ*	Phosphoadenosine phosphosulfate phosphatase
NCgl0826		-1.63	-1.97	*purN*	phosphoribosylglycinamide formyltransferase
NCgl0831		-1.86		*rpsR*	Ribosomal protein S18
NCgl0832		-1.70		*rpsN*	Ribosomal protein S14
NCgl0833	-1.72	-1.91		*rpmG*	Ribosomal protein L33
NCgl0834		-1.71		*rpmB*	Ribosomal protein L28
NCgl0837		-1.98		*rpmE*	Ribosomal protein L31
NCgl0838		-2.00		*rpmF*	Ribosomal L32p protein family
NCgl0841		-1.53	-2.88		Trypsin-like serine proteases, typically periplasmic
NCgl0842			-1.78		Molybdopterin biosynthesis enzymes
NCgl0845			1.96		5-formyltetrahydrofolate cyclo-ligase
NCgl0853			2.03		Glycosidases
NCgl0857			-2.27	*metS*	Methionyl-tRNA synthetase
NCgl0878			1.86		Uncharacterized conserved protein
NCgl0879			2.07		Uncharacterized conserved protein
NCgl0885			-1.88	*cmt3*	Predicted esterase
NCgl0888		-1.76	-1.66	*menG*	Demethylmenaquinone methyltransferase
NCgl0893			18.64	*urtA*	Urea transport system
NCgl0894			7.66	*urtB*	Urea transport system
NCgl0895			19.42	*urtC*	Urea transport system
NCgl0896			9.19	*urtD*	Urea transport system
NCgl0897			10.65	*urtE*	Urea transport system
NCgl0898			3.02	*Pth2*	Peptidyl-tRNA hydrolase
NCgl0899	1.67	1.56			Predicted 2-nitropropane dioxygenase
NCgl0902		-1.71		*rplY*	Ribosomal protein L25 (general stress protein Ctc)
NCgl0903		1.95			Predicted lactoylglutathione lyase

NCgl0905			-2.56	*prsA*	Phosphoribosylpyrophosphate synthetase
NCgl0906			-2.01	*glmU*	N-acetylglucosamine-1-phosphate uridyltransferase
NCgl0908		1.59			Putative multicopper oxidases
NCgl0909		1.88			ABC-type multidrug transport system
NCgl0910		1.77			Putative membrane protein
NCgl0917			1.98		Hypothetical protein predicted by Glimmer/Critica
NCgl0925		1.55			ABC-type multidrug transport system
NCgl0933			-3.22	*porB*	Anion-specific porin precursor
NCgl0934		1.56			Membrane-bound lytic murein transglycosylase B
NCgl0935		1.76	1.59	*eno*	Enolase
NCgl0936		1.54	1.85		Septum formation initiator
NCgl0943		-1.65	-2.47		AraC-type DNA-binding domain-containing proteins
NCgl0950		-1.83	-1.70	*aroF*	3-deoxy-D-arabino-heptulosonate synthase
NCgl0954			-2.93	*glyA*	Glycine/serine hydroxymethyltransferase
NCgl0955			-1.62	*pabAB*	Anthranilate/para-aminobenzoate synthases
NCgl0957			2.19		Conserved hypothetical protein
NCgl0967		1.80		*fum*	Fumarase
NCgl0976	1.61			*glpX*	Fructose-1,6-bisphosphatase
NCgl0982			2.19	*lytB*	Penicillin tolerance protein
NCgl0985			-1.72		Putative secreted protein
NCgl1015			1.86		PEP phosphonomutase and related enzymes
NCgl1016			2.14		ATPase components of ABC transporter
NCgl1022			-2.00		Cysteine sulfinate desulfinase/cysteine desulfurase
NCgl1023			-2.15	*nadC*	Nicotinate-nucleotide pyrophosphorylase
NCgl1024			-2.74	*nadA*	Quinolinate synthase
NCgl1033	-1.76		-3.08		Predicted membrane protein
NCgl1034	-1.85	-1.68	-3.75		ABC-type cobalt transport system
NCgl1035	-1.58	-1.75	-2.94		ABC-type cobalt transport system
NCgl1036	-1.59	-1.80	-2.10		Adenylate kinase and related kinases
NCgl1053			-1.93		Predicted membrane GTPase
NCgl1061			1.72	*dapD*	Tetrahydrodipicolinate N-succinyltransferase
NCgl1064			1.53	*dapE*	Acetylornithine deacetylase
NCgl1066			1.52	*folP2*	Dihydropteroate synthase and related enzymes
NCgl1068	1.70				Conserved hypothetical protein
NCgl1069			1.71		Conserved hypothetical protein
NCgl1070			1.74	*rrmA*	SAM-dependent methyltransferases
NCgl1074			1.54		Predicted O-methyltransferase
NCgl1082			1.95		Conserved hypothetical secreted protein
NCgl1083	1.84	1.72	1.52		Putative secreted protein
NCgl1088			1.72	*lipT*	Carboxylesterase type B
NCgl1089			1.76		Conserved hypothetical protein
NCgl1090	2.59				Conserved hypothetical protein
NCgl1094	-1.62		-9.18	*metE*	Methionine synthase II (cobalamin-independent)
NCgl1095	2.39	2.58	3.11		Putative membrane protein
NCgl1096			1.54		Predicted flavoprotein involved in K^+ transport
NCgl1098			2.46		Predicted esterase
NCgl1099			4.63		Predicted hydrolases or acyltransferases (
NCgl1100			2.48		Non-ribosomal peptide synthetase
NCgl1104	-1.61			*cydA*	Cytochrome bd-type quinol oxidase, subunit 1
NCgl1109	1.66				Superfamily II DNA and RNA helicases
NCgl1127		1.61	2.14		cAMP-binding proteins - catabolite gene activator
NCgl1130			1.57		Uncharacterized protein conserved in bacteria
NCgl1131			-3.22		Predicted hydrolases or acyltransferases)
NCgl1132			-1.99	*argS*	Arginyl-tRNA synthetase
NCgl1133			-2.14	*lysA*	Diaminopimelate decarboxylase
NCgl1136		1.63		*hom*	Homoserine dehydrogenase
NCgl1137		1.54		*thrB*	Homoserine kinase
NCgl1139			3.11	*narI*	Nitrate reductase gamma subunit
NCgl1140			3.06	*narJ*	Nitrate reductase delta subunit
NCgl1141			2.98	*narH*	Nitrate reductase beta subunit

NCgl1142			1.81	*narG*	Nitrate reductase alpha subunit
NCgl1145		1.75			Membrane-associated phospholipid phosphatase
NCgl1158			-2.01	*atpI*	Hypothetical protein
NCgl1160			-1.67	*atpE*	F0F1-type ATP synthase
NCgl1161			-1.79	*atpF*	F0F1-type ATP synthase
NCgl1162			-2.04	*atpH*	F0F1-type ATP synthase
NCgl1163			-1.95	*atpA*	F0F1-type ATP synthase
NCgl1164			-2.31	*atpG*	F0F1-type ATP synthase
NCgl1165			-2.09	*atpD*	F0F1-type ATP synthase
NCgl1166			-1.52	*atpC*	F0F1-type ATP synthase
NCgl1167			-1.83		Conserved hypothetical protein
NCgl1174		1.70		*ssuC*	ABC-type nitrate/sulfonate/bicarbonate transporter
NCgl1192			-1.83		Predicted tRNA methyltransferase
NCgl1194		1.53			Permease of the major facilitator superfamily
NCgl1197		1.71			Conserved hypothetical protein
NCgl1200			-1.69		Siderophore-interacting protein
NCgl1201		1.59	1.82		Putative membrane protein
NCgl1202	1.59		1.89	*pfkA*	6-phosphofructokinase
NCgl1209			-1.80		ABC-type Fe^{3+}-hydroxamate transport system
NCgl1210			-3.03		Predicted Na^{+}-dependent transporter
NCgl1218	1.52	1.63			Predicted membrane protein
NCgl1221			-1.66	*yggB*	Small-conductance mechanosensitive channel
NCgl1222		-1.85	-2.25	*ilvB*	Thiamine pyrophosphate-requiring enzymes
NCgl1223		-1.71	-1.69	*ilvN*	Acetolactate synthase, small (regulatory) subunit
NCgl1235	1.62		-6.08	*serA*	Phosphoglycerate dehydrogenase
NCgl1242	1.74				SAM-dependent methyltransferases
NCgl1252			-1.65		Conserved hypothetical protein
NCgl1253			-2.21	*thiC*	Thiamine biosynthesis protein ThiC
NCgl1255			-2.60	*glgP1*	Glucan phosphorylase
NCgl1262	1.80	-1.65	-3.51	*leuC*	3-isopropylmalate dehydratase large subunit
NCgl1263	1.89		-2.92	*leuD*	3-isopropylmalate dehydratase small subunit
NCgl1277			-1.52		ABC-type amino acid transport system
NCgl1286			1.60		Hypothetical protein predicted by Glimmer/Critica
NCgl1288	-2.31	-1.52	-1.52		Putative secreted protein
NCgl1289	-1.56				Putative secreted protein
NCgl1290	-1.60				Hypothetical protein predicted by Glimmer/Critica
NCgl1291	-1.62	-1.70			Putative secreted protein
NCgl1300	2.46				Permease of the major facilitator superfamily
NCgl1305	-1.64			*ptsG*	Phosphotransferase system IIC components
NCgl1324	-1.67	-1.71		*infC*	Translation initiation factor 3 (IF-3)
NCgl1326	-1.58			*rplT*	Ribosomal protein L20
NCgl1331	3.42			*ugpB*	ABC-type sugar transport system
NCgl1337			-1.58		Secreted hydrolase, GDSL lipolytic enzyme
NCgl1340	2.83			*argC*	Acetylglutamate semialdehyde dehydrogenase
NCgl1341	3.57		-1.75	*argJ*	N-Acetylglutamate synthase
NCgl1342	4.19		-1.62	*argB*	Acetylglutamate kinase
NCgl1343	3.58			*argD*	Ornithine/acetylornithine aminotransferase
NCgl1344	2.69		-1.61	*argF*	Ornithine carbamoyltransferase
NCgl1345	1.80			*argR*	Arginine repressor
NCgl1346		-1.67	-1.72	*argG*	Argininosuccinate synthase
NCgl1347			-1.97	*argH*	Argininosuccinate lyase
NCgl1371	-1.55				16S rRNA uridine-516 pseudouridylate synthase
NCgl1372	-1.59	-1.60	-1.52	*cmk*	Cytidylate kinase
NCgl1373	-1.88	-1.62	-1.60		Predicted GTPases
NCgl1375	2.82				Transcriptional regulator
NCgl1385		1.58			FOG: FHA domain
NCgl1396	2.27			*gnd*	6-phosphogluconate dehydrogenase
NCgl1399		1.52			ABC-type multidrug transport system
NCgl1408			-1.70	*thiM*	Hydroxyethylthiazole kinase, sugar kinase family
NCgl1421	1.58				Conserved hypothetical protein

NCgl1422	-1.73				Putative membrane-associated GTPase
NCgl1425			1.76		Protein affecting phage T7 exclusion
NCgl1433			-1.58	*tatC*	Sec-independent protein secretion pathway
NCgl1444	1.62		1.69		Plasmid maintenance system antidote protein
NCgl1446			-1.64	*aspA*	Aspartate ammonia-lyase
NCgl1450		1.77		*metH*	Methionine synthase I, cobalamin-binding domain
NCgl1461			-1.65	*pyrD*	Dihydroorotate dehydrogenase
NCgl1466	3.14				Phospholipid-binding protein
NCgl1472		-1.54	-1.76	*mcmA*	Methylmalonyl-CoA mutase
NCgl1474			1.85		Conserved hypothetical protein
NCgl1475	1.68				Membrane protease subunits
NCgl1484	2.88				GMP synthase - Glutamine amidotransferase
NCgl1485		1.58	2.27		Predicted diphosphate-sugar epimerases
NCgl1488		2.08	1.95	*pacL*	Cation transport ATPase
NCgl1490			1.96		Putative membrane protein
NCgl1500			-1.81	*nifS2*	Selenocysteine lyase
NCgl1501			-1.79	*sufC*	Transport system involved in Fe-S cluster assembly
NCgl1502			-2.32	*sufD*	Transport system involved in Fe-S cluster assembly
NCgl1503	-1.68	-1.57	-2.31	*sufB*	Transport system involved in Fe-S cluster assembly
NCgl1504	-1.62		-2.39		Predicted transcriptional regulator
NCgl1508			1.59	*ctaA*	Protein required for cytochrome oxidase assembly
NCgl1519			17.44		Glycine/D-amino acid oxidases (deaminating)
NCgl1520			23.83	*ocd*	Predicted ornithine cyclodeaminase
NCgl1521			19.25	*amt*	Ammonium transporter
NCgl1525			2.10	*pgk*	3-phosphoglycerate kinase
NCgl1526			1.54	*gap*	Glyceraldehyde-3-phosphate dehydrogenase
NCgl1544			-1.73	*gmk*	Guanylate kinase
NCgl1546		-1.69		*pyrF*	Orotidine-5'-phosphate decarboxylase
NCgl1547	1.53	-1.57		*carB*	Carbamoylphosphate synthase large subunit
NCgl1556		-1.59	-1.82	*nusB*	Transcription termination factor
NCgl1557		-1.55	-1.70	*efp*	Translation elongation factor P
NCgl1559			-1.86	*aroB*	3-dehydroquinate synthetase
NCgl1565			1.52		ABC-type $Fe3^{+}$-hydroxamate transport system
NCgl1567		-2.66	-2.20	*aroE3*	Shikimate 5-dehydrogenase
NCgl1568		-1.54	-1.85		Predicted periplasmic solute-binding protein
NCgl1570			-1.76	*alaS*	Alanyl-tRNA synthetase
NCgl1574			-2.00		Predicted metalloprotease
NCgl1576			-1.65		Predicted membrane protein
NCgl1577			-1.64		Conserved hypothetical protein
NCgl1579	2.03				Conserved hypothetical protein
NCgl1583			-1.81	*sdaA*	L-Serine deaminase
NCgl1588			-1.87		Putative secreted protein
NCgl1589		1.53	-3.48		Putative membrane protein
NCgl1593		-1.76		*secF*	Preprotein translocase subunit SecF
NCgl1594		-1.78	-1.68	*secD*	Preprotein translocase subunit SecD
NCgl1600			-2.80	*tesB2*	Acyl-CoA thioesterase
NCgl1601			-2.97		Putative membrane protein
NCgl1602			-1.78		Putative membrane protein
NCgl1609			-2.44		Uncharacterized protein conserved in bacteria
NCgl1610		1.56			Putative Cu resistance protein
NCgl1611		-1.95	-1.60		Hypothetical protein predicted by Glimmer/Critica
NCgl1612	-1.80	-2.12	-2.03		Hypothetical protein predicted by Glimmer/Critica
NCgl1616		-2.08	-1.91		Putative secreted protein
NCgl1623		-2.25	-2.46		ABC-type multidrug transport system
NCgl1631	1.80		-1.58		Hypothetical protein predicted by Glimmer/Critica
NCgl1632			-1.73		Hypothetical protein predicted by Glimmer/Critica
NCgl1656	-1.65	-1.66	-1.54		Putative secreted protein
NCgl1665			-1.56		Hypothetical protein
NCgl1672	1.89				Putative membrane protein

NCgl1676			2.63		Hypothetical protein predicted by Glimmer/Critica
NCgl1737	1.60				Putative membrane protein
NCgl1756	1.85				Putative secreted protein
NCgl1821			1.72	*ribD*	Pyrimidine reductase, riboflavin biosynthesis
NCgl1837			-1.83		Predicted membrane protein
NCgl1847			-1.56		Conserved hypothetical protein
NCgl1855			1.66	*lexA*	SOS-response transcriptional repressors
NCgl1859			1.95		Transcriptional regulators of sugar metabolism
NCgl1860			2.24	*pfkB*	Fructose-1-phosphate kinase
NCgl1861			2.29	*ptsF*	Phosphotransferase system
NCgl1862			2.01	*ptsH*	Phosphotransferase system, HPr-related proteins
NCgl1866			-2.11		Conserved hypothetical protein
NCgl1873			1.68		Putative membrane protein
NCgl1875		-3.16	3.55	*gluA*	Glutamate transporter
NCgl1876		-2.99	3.80	*gluB*	Glutamate transporter
NCgl1877		-3.24	3.15	*gluC*	Glutamate transporter
NCgl1878		-1.95	3.10	*gluD*	Glutamate transporter
NCgl1886	2.75				Phage shock protein A
NCgl1898			1.53	*dapB*	Dihydrodipicolinate reductase
NCgl1901		-1.78		*rpsO*	Ribosomal protein S15P/S13E
NCgl1905	1.99			*pptA*	Phosphopantetheinyl transferase
NCgl1907			-1.75	*dinF*	Na^+-driven multidrug efflux pump
NCgl1912			-1.74	*nusA*	Transcription elongation factor
NCgl1915		-3.58	3.24		ABC-type oligopeptide transport system
NCgl1916		-2.67			ABC-type dipeptide/oligopeptide/nickel transporter
NCgl1917		-3.98			ABC-type dipeptide/oligopeptide/nickel transporter
NCgl1918		-2.86	3.88		ABC-type transport systems
NCgl1919			-1.54	*proS*	Prolyl-tRNA synthetase
NCgl1921	2.73				Mg-chelatase subunit ChlD
NCgl1923	2.31			*cobA*	Uroporphyrinogen-III methylase
NCgl1926			-2.87	*mqo*	Predicted dehydrogenase
NCgl1934	3.09				Response regulator
NCgl1941		1.56			Putative membrane protein
NCgl1945	1.65				Putative membrane protein
NCgl1960	-1.63	-1.85		*rplS*	Ribosomal protein L19
NCgl1961			-1.76	*thiE*	Thiamine monophosphate synthase
NCgl1962			-1.92	*thiO*	Glycine/D-amino acid oxidases (deaminating)
NCgl1963			-1.74	*thiS*	Sulfur transfer protein of thiamine biosynthesis
NCgl1964	-1.54		-2.02	*thiG*	Uncharacterized enzyme of thiazole biosynthesis
NCgl1973		1.98	1.57		Putative secreted protein
NCgl1974			1.55	*rimM*	RimM protein, required for 16S rRNA processing
NCgl1976	-1.56	-1.77		*rpsP*	Ribosomal protein S16
NCgl1981			1.90	*glnD*	GlnB-like adenylyltransferase
NCgl1982			6.71	*glnK*	Nitrogen regulatory protein PII
NCgl1983			14.17	*amtB*	Ammonium transporter
NCgl1995	1.77				Predicted metal-binding
NCgl2006	2.29		1.80	*glgP2*	Glucan phosphorylase
NCgl2008		1.53	1.67	*pyk*	Pyruvate kinase
NCgl2020			-1.74	*hisC*	Histidinol-phosphate/aromatic aminotransferase
NCgl2023	-1.69	-1.77			Putative membrane protein
NCgl2024			-3.20		Putative secreted protein
NCgl2027			-1.69		SAM-dependent methyltransferases
NCgl2033	1.56		1.53		ABC-type cobalamin/Fe^{3+}-siderophores transporter
NCgl2034			2.76		Predicted transcriptional regulators
NCgl2047			-2.56		Putative secreted protein
NCgl2048		1.53	-1.54		Methionine synthase II (cobalamin-independent)
NCgl2049			-1.62	*dnaE1*	DNA polymerase III alpha subunit
NCgl2053		1.52			predicted short-chain alcohol dehydrogenases
NCgl2059		-1.52			Putative secreted protein

NCgl2064	1.71			*dinP*	Nucleotidyltransferase/DNA polymerase
NCgl2068		-1.66		*ileS*	Isoleucyl-tRNA synthetase
NCgl2070		1.52			Cell division initiation protein
NCgl2086	1.69			*mraW*	Predicted methyltransferase
NCgl2090			1.61		Acetyltransferases
NCgl2098		-1.65	-2.03	*aroG*	3-deoxy-D-arabino-heptulosonate synthase
NCgl2100			-1.58		Putative membrane protein
NCgl2101			-1.65	*cmt4*	Predicted esterase
NCgl2107			-1.57		Cell wall-associated hydrolases
NCgl2108	-1.89		-1.89		Cell wall-associated hydrolases
NCgl2109			-1.56	*qcrB*	Cytochrome b subunit of the bc complex
NCgl2110			-1.64	*qcrA1*	Rieske Fe-S protein
NCgl2112	-1.57			*ctaE*	Heme/copper-type cytochrome/quinol oxidase
NCgl2114			-2.06		Putative membrane protein
NCgl2115			-1.64	*ctaC*	Heme/copper-type cytochrome/quinol oxidases
NCgl2128			-1.93	*lipA*	Lipoate synthase
NCgl2130		1.70	2.09		Predicted permease
NCgl2133	1.63		2.45	*glnA*	Glutamine synthetase
NCgl2137	2.55				methylene tetrahydromethanopterin reductase
NCgl2139			-2.08	*thrC*	Threonine synthase
NCgl2145			-1.55		Hypothetical protein predicted by Glimmer/Critica
NCgl2146	-1.58	-2.12	-3.08	*hmuO*	Heme oxygenase
NCgl2157			1.63		Uncharacterized conserved protein
NCgl2158			1.91	*pgp2*	Predicted phosphatases
NCgl2167		1.66	1.81	*aceE*	Pyruvate dehydrogenase complex
NCgl2168		-2.01			ABC-type uncharacterized transport system
NCgl2169		-2.14			ABC-type uncharacterized transport system
NCgl2170		-2.36			ABC-type uncharacterized transport system
NCgl2174		1.55		*acpM*	Acyl carrier protein
NCgl2175		1.63		*nagD*	Predicted sugar phosphatases
NCgl2177			1.93		Conserved hypothetical protein
NCgl2191			-1.52	*glmS*	Glucosamine 6-phosphate synthetase
NCgl2196	2.07				Hypothetical protein predicted by Glimmer/Critica
NCgl2199			2.12		Predicted transcriptional regulators
NCgl2200			1.69	*fur*	Fe^{2+}/Zn^{2+} uptake regulation proteins
NCgl2208		-1.59		*phoH2*	Phosphate starvation-inducible protein PhoH
NCgl2213			1.56		Putative secreted protein
NCgl2214			1.55		Conserved hypothetical protein
NCgl2230			-2.08	*ectP*	Choline-glycine betaine transporter
NCgl2243			1.97	*rbsK2*	Sugar kinases, ribokinase family
NCgl2247	-2.60	-2.52		*aceB*	Malate synthase
NCgl2248		-3.99		*aceA*	Isocitrate lyase
NCgl2252	1.53	1.56	2.32		Hypothetical protein predicted by Glimmer/Critica
NCgl2260			1.61		Conserved hypothetical protein
NCgl2261		-1.64		*rpsT*	Ribosomal protein S20
NCgl2272			1.73	*proA*	Gamma-glutamyl phosphate reductase
NCgl2276			-1.79		Xanthine/uracil permeases
NCgl2280		-1.52		*rplU*	Ribosomal protein L21
NCgl2290			1.53		Conserved hypothetical protein
NCgl2296		1.61	1.98		Predicted Rossmann fold nucleotide-binding protein
NCgl2297	1.72	2.22	2.08	*mdh*	Malate/lactate dehydrogenases
NCgl2301	-1.57			*vanB*	vanillate demethylase
NCgl2302	-1.56	-1.65	-2.23	*vanK*	probalbe protocatechuate transporter
NCgl2305			1.66		Conserved hypothetical protein
NCgl2313			2.88	*pcaB1*	Adenylosuccinate lyase
NCgl2319		-1.65	4.16	*catA1*	Protocatechuate 3,4-dioxygenase beta subunit
NCgl2327	1.52			*clpP2*	Protease subunit of ATP-dependent Clp proteases
NCgl2329		-1.72	-2.12	*tig*	FKBP-type peptidyl-prolyl cis-trans isomerase
NCgl2333			-2.19		Conserved hypothetical protein
NCgl2336			-1.54		Putative membrane protein
NCgl2349	1.66	1.55			Uncharacterized protein conserved in bacteria
NCgl2350	2.34	1.60			ABC-type transport system

NCgl2351	1.64	1.69			ABC-type transport system
NCgl2352	1.65	1.99			ABC-type transport system
NCgl2357			1.79		Uncharacterized membrane-associated protein
NCgl2358		1.60	1.68		Probalbe short-chain dehydrogenase
NCgl2373		-1.71			ABC-type sugar transport system
NCgl2376	-1.93				Conserved hypothetical protein
NCgl2377	-2.10			*msiK1*	ABC-type sugar transport systems
NCgl2399		1.53		*gntV*	Gluconate kinase
NCgl2439			2.90	*ftn*	Ferritin-like protein
NCgl2444		1.53		*nrdI*	Protein involved in ribonucleotide reduction
NCgl2445			-1.91	*nrdH*	Glutaredoxin and related proteins
NCgl2447			2.41		Uncharacterized protein conserved in bacteria
NCgl2448			1.70		Conserved hypothetical protein
NCgl2450		1.81	-2.22		Uncharacterized protein of propionate catabolism
NCgl2451		1.92	-2.22		Uncharacterized conserved protein
NCgl2452			-1.72		Putative secreted protein
NCgl2457			1.74		-
NCgl2463		1.89			Na^+/H^+-dicarboxylate symporters
NCgl2470			1.80	*murA2*	UDP-N-acetylglucosamine enolpyruvyl transferase
NCgl2471			1.53	*pduO*	Uncharacterized conserved protein
NCgl2473	2.05		1.65	*cysK*	Cysteine synthase
NCgl2476		-1.99	1.74	*sucD*	Succinyl-CoA synthetase, alpha subunit
NCgl2477			1.55	*sucC*	Succinyl-CoA synthetase, beta subunit
NCgl2485	-1.57			*pstC*	ABC-type phosphate transport system
NCgl2487			1.74		Acetyltransferases
NCgl2495			-1.87	*purF*	Glutamine phosphoribose amidotransferase
NCgl2497			-2.06		Acyl-CoA hydrolase
NCgl2499			-2.37	*purL*	Phosphoribosylformylglycinamidine synthase
NCgl2500			-2.20	*purQ*	Phosphoribosylformylglycinamidine synthase
NCgl2508			-1.53	*purC*	Phosphoribosylaminosuccinoamide synthase
NCgl2517		-1.55	-2.10	*cgtS3*	Signal transduction histidine kinase
NCgl2530		1.56			Predicted hydrolases of the HAD superfamily
NCgl2534			1.82		Conserved hypothetical protein
NCgl2535			1.60	*otsA*	Trehalose-6-phosphate synthase
NCgl2536			-1.64		Putative membrane protein
NCgl2537	1.75			*otsB*	Trehalose-6-phosphatase
NCgl2562		-1.68			ABC-type dipeptide transport system
NCgl2574			-1.69		Putative secreted protein
NCgl2577	1.71		1.54		Putative secreted protein
NCgl2578			2.10	*xylC*	Benzaldehyde dehydrogenase
NCgl2579			-1.81	*cynT*	Carbonic anhydrase
NCgl2582	1.66	2.21	2.04	*butA*	L-2,3-butanediol dehydrogenase/acetoin reductase
NCgl2584			-2.64		Uncharacterized enzyme of polysacc, biosynthesis
NCgl2597			1.56		Putative membrane protein
NCgl2621		-1.93		*groEL*	Chaperonin GroEL (HSP60 family)
NCgl2645			1.57	*xthA*	Exonuclease III
NCgl2654			-1.65		ABC-type amino acid transporter
NCgl2656		-2.24		*ackA*	Acetate kinase
NCgl2657	-2.30	-2.04		*pta*	Phosphotransacetylase
NCgl2658			1.69	*fpr1*	NADPH-dependent glutamate synthase
NCgl2665		-1.76			-
NCgl2666			-1.53		Transposase and inactivated derivatives
NCgl2669			-1.67	*purA*	Adenylosuccinate synthase
NCgl2672	1.82				Predicted membrane protein
NCgl2673			1.67	*fda*	Fructose/tagatose bisphosphate aldolase
NCgl2692			1.62		Uncharacterized protein conserved in bacteria
NCgl2699			2.22	*hspR*	Predicted transcriptional regulators
NCgl2700			2.59	*dnaJ*	DnaJ-class molecular chaperone
NCgl2701			2.35	*grpE*	Molecular chaperone GrpE (heat shock protein)
NCgl2702			1.68	*dnaK*	Molecular chaperone
NCgl2709			5.44	*adhA*	Zn-dependent alcohol dehydrogenases
NCgl2713	1.85	2.56		*cysZ*	Predicted permeases

NCgl2714	1.94	2.72		*cysY*	Uncharacterized conserved protein
NCgl2715	2.56	2.81		*cysN*	GTPases - Sulfate adenylate transferase subunit 1
NCgl2716	3.01	3.93	2.48	*cysD*	3'-phosphoadenosine 5'-phosphosulfate synthetase
NCgl2717	3.35	5.04	3.16	*cysH*	3'-phosphoadenosine 5'-phosphosulfate synthetase
NCgl2718	3.88	4.69	3.24	*cysI*	Sulfite reductase
NCgl2719	1.94	2.71	2.62	*cydJ*	Ferrodoxin reductase
NCgl2730			1.77		Acetylornithine deacetylase
NCgl2737			2.18		Membrane protease subunit
NCgl2739			1.87	*tagA1*	3-methyladenine DNA glycosylase
NCgl2747		-1.72	-2.49		Aspartate/tyrosine/aromatic aminotransferase
NCgl2752		-1.68	-2.53		Putative secreted protein
NCgl2753			-1.57		Uncharacterized vancomycin resistance protein
NCgl2765	2.88		2.20	*pck*	Phosphoenolpyruvate carboxykinase (GTP)
NCgl2770		-1.69			Predicted integral membrane protein
NCgl2775			-1.53		Putative secreted protein
NCgl2776			-1.90		Putative secreted protein
NCgl2779			-1.88	*cmt2*	Predicted esterase
NCgl2782			-1.61		Membrane-associated phospholipid phosphatase
NCgl2783			-1.91		Predicted glycosyltransferases
NCgl2784		1.81	1.77		Putative secreted protein
NCgl2785		1.78			Membrane-associated phospholipid phosphatase
NCgl2787	-9.32	-2.90	1.88		Predicted flavoprotein involved in K^+ transport
NCgl2789			-3.05	*psp5*	Putative secreted protein
NCgl2791			-1.52		Predicted hydrolases of the HAD superfamily
NCgl2792			-1.58		1-acyl-sn-glycerol-3-phosphate acyltransferase
NCgl2794	-9.75		-8.68		Transcriptional regulators
NCgl2795	-1.73		-1.94		Conserved hypothetical protein
NCgl2809		1.73	2.86		Pyruvate kinase
NCgl2810	2.47	2.46	3.19	*ldh*	Malate/lactate dehydrogenases
NCgl2813		1.56	2.57		Predicted flavoprotein
NCgl2814			1.61		Transcriptional regulators
NCgl2817	1.91			*lldA*	L-lactate dehydrogenase
NCgl2820			2.28		Hypothetical protein predicted by Glimmer
NCgl2834			-1.67	*cgtR11*	Response regulator
NCgl2842	1.98	1.83	1.77	*uspA3*	Universal stress protein
NCgl2843			1.60		Alkanal monooxygenase
NCgl2848		1.67	1.66		Phage shock protein A
NCgl2849			1.76		Hypothetical protein predicted by Glimmer
NCgl2854			1.76		Uncharacterized membrane protein
NCgl2858		1.83			Uncharacterized protein conserved in bacteria
NCgl2859		1.67	1.72		Cation transport ATPase
NCgl2860		2.34	2.72		Copper chaperone
NCgl2864			-1.67		Putative secreted protein
NCgl2875	-1.64		-1.59		Copper chaperone
NCgl2876			4.11		Permease of the major facilitator superfamily
NCgl2877			7.41		Predicted transcriptional regulators
NCgl2879		-1.77		*rplI*	Ribosomal protein L9
NCgl2880		-1.56		*ssb*	Single-stranded DNA-binding protein
NCgl2881		-1.73		*rpsF*	Ribosomal protein S6
NCgl2886	1.72		2.58		Bacterial regulatory protein, MarR family
NCgl2887	2.46		1.66		Universal stress protein
NCgl2894			-2.39		Myo-inositol-1-phosphate synthase
NCgl2897			6.88	*dps*	DNA-binding ferritin-like protein
NCgl2902			1.68		NADPH:quinone reductase
NCgl2915			-1.52	*leuS*	Leucyl-tRNA synthetase
NCgl2924		-1.64	-2.05		Na^+/H^+-dicarboxylate symporters
NCgl2940			-1.71		Uncharacterized conserved protein
NCgl2943	2.31				Predicted diphosphate-sugar epimerases
NCgl2948			-1.64		Sec-independent protein secretion pathway

Danksagung

Diese Arbeit wurde am Institut für Biochemie der Universität zu Köln im Rahmen der *International Max Planck Research School* des Max-Planck-Instituts für Züchtungsforschung in Köln durchgeführt.

Mein besonderer Dank gilt Herrn Prof. Dr. Andreas Burkovski für die Überlassung des interessanten Arbeitsthemas, die kontinuierlich gute Betreuung, seine stete Diskussionsbereitschaft und die viele Tipps und Tricks für die praktische Arbeit.

Herrn Prof. Dr. Reinhard Krämer danke ich für die Möglichkeit diese Arbeit durchzuführen und seine große fachliche Unterstützung.

Herrn Prof. Dr. George Coupland vom Max-Planck-Institut für Züchtungsforschung in Köln danke ich für die fachlichen Diskussionen.

Herrn Dr. Jörn Kalinowski und Jens Plassmeier von der Universität Bielefeld danke ich für die Bereitstellung der DNA-*Microarrays* und die Unterstützung bei der Durchführung der damit verbundenen Experimente.

Herrn Prof. Dr. H. Bothe und Bettina Berger von der Universität zu Köln danke ich für die Möglichkeit zur Durchführung von *real-time*-PCR-Experimenten.

Bei allen meinen Kollegen aus der Arbeitsgruppe Krämer bedanke ich mich für die schöne Zeit, die ausgesprochen gute Arbeitsatmosphäre und die große Hilfe bei der Durchführung vieler Experimente. Besonders danke ich Astrid für ihre Unterstützung bei den Ammoniummessungen sowie Andreas und Maike für das Korrekturlesen der Arbeit.

Ich danke Lucie für ihre Unterstützung und das Korrekturlesen der Arbeit.

Meinen Eltern danke ich für die große Unterstützung während meines gesamten Studiums.

Lebenslauf

Tim Müller
Hanns-Maria-Lux-Str. 46
56077 Koblenz

Angaben zur Person

Geburtsdatum:	09.01.1976
Geburtsort:	Koblenz
Staatsangehörigkeit:	deutsch

Schulbildung und Zivildienst

1982 – 1985	Grundschule Asterstein, Koblenz
1985 – 1995	Gymnasium auf dem Asterstein, Koblenz Abschluss: Allgemeine Hochschulreife
1995 – 1996	Zivildienst, Rhein-Mosel-Werkstatt für Behinderte gem. GmbH, Koblenz

Hochschulbildung

1996 – 1998	Studium der Chemie, Johannes Gutenberg-Universität Mainz, Vordiplom in Chemie
1998 – 1999	Studium der Chemie, Westfälische Wilhelms-Universität Münster
1999 – 2000	Forschungsaufenthalt, *Institute of Inorganic Chemistry*, *University of Auckland*, Neuseeland
2000 – 2002	Studium der Chemie, Westfälische Wilhelms-Universität Münster, Diplomarbeit in Biochemie, Abschluss: Diplom-Chemiker
2002 - 2005	Promotion in Biochemie, Universität zu Köln

Köln, 05.10.2005

Erklärung

Ich versichere, dass ich die von mir vorgelegte Dissertation selbständig angefertigt, die benutzten Quellen und Hilfsmittel vollständig angegeben und die Stellen der Arbeit - einschließlich Tabellen, Karten und Abbildungen -, die anderen Werken im Wortlaut oder dem Sinn nach entnommen sind, in jedem Einzelfall als Entlehnung kenntlich gemacht habe; dass diese Dissertation noch keiner anderen Fakultät oder Universität zur Prüfung vorgelegen hat; dass sie - abgesehen von unten angegebenen Teilpublikationen - noch nicht veröffentlicht worden ist sowie, dass ich eine solche Veröffentlichung vor Abschluss des Promotionsverfahrens nicht vornehmen werde. Die Bestimmungen dieser Promotionsordnung sind mir bekannt. Die von mir vorgelegte Dissertation ist von Prof. Dr. A. Burkovski betreut worden.

Keine Teilpublikationen.

Köln, 05.10.2005